University of Stavanger

FACULTY OF SCIENCE AND TECHNOLOGY

MASTER'S THESIS

Study programme/specialisation: Petroleum Technology/Natural Gas	Spring Semester, 2020 Open
Author: Linda Monsen	
Programme coordinator: Mohsen Assadi Supervisor(s): Mohsen Assadi, Homam Nikpey Somehsaraei	
Title of master's thesis: Emission Free North Sea: A Study of Alternative Solutions for Power Generation on Offshore Installations	
Credits: 30	
Keywords: Power Generation, Gas Turbines, CO_2-Emissions, Electrification, Floating Wind Turbines, Combined Cycle, HAT Cycle, Fuel Cells, Energy Efficiency Measures, Hydrogen, CCS	Number of pages: 146 + supplemental material/other: 2 Stavanger, June 15th 2020 date/year

Preface

This thesis has been done as a final assignment for my master's degree in Petroleum Technology with specialization in Natural Gas. My big passion is energy efficiency and smarter energy solutions, as I believe these factors to be important to both satisfy the growing energy demand *and* the rising climate challenges the world is facing.

In that regard, I would like to thank my supervisor Professor Mohsen Assadi for letting me form my own thesis, whilst still providing relevant input and expanding my horizon to include several technologies and solutions. I am amazed by all the knowledge you carry, and your ability to pass it forward. I would also like to thank Homam Nikpey Somehsaraei for your comments and inputs, and for reaching out to people on my behalf.

To my dear Alexander. Thank you for listening and letting me think out loud. Thank you for reading every single word. Thank you for supporting me through all the ups and downs this semester. Finally, thank you for taking care of the little monkey of a toddler running around the house, climbing everywhere in search for new sources of food. Not being able to work at the university this semester has been nothing but rewarding, as five-minute breaks with the two of you have enabled me to focus yet again, when the theory becomes a bit too heavy. Without you, this thesis would not have been the final end-product it is today.

Abstract

As a contribution to the 2°C goal of the Paris Agreement, The Norwegian Oil and Gas Association aims to reduce their GHG emissions to 40% of the 2005 level by 2030 and to have zero emissions by 2050. Gas turbines producing electricity and mechanical work on offshore installations was accountable for 66.7% of the petroleum industry's GHG emissions in Norway in 2018, due to their low efficiency and high CO_2-emission factor.

This thesis has reviewed nine different alternatives to the conventional simple cycle gas turbine for power generation on offshore installations, with a goal in mind to find a more sustainable alternative for energy production, which will contribute to a substantial CO_2-emission reduction at an affordable cost. The 2018 energy requirements for Greater Ekofisk Area has been chosen as a basis for energy calculations.

Partial electrification would contribute to the highest guaranteed CO_2-emission reduction of 20.8%, however at the highest cost of 2 995 NOK/ton CO_2 reduced. Combined cycle, HAT cycle and fuel cells would all increase the efficiency of the power generation and contribute to a CO_2-emission reduction of approximately 7%. Energy Efficiency Measures involving optimization of equipment to reduce energy loss and limiting operative time on injection pumps have already contributed to a CO_2-emission reduction of 5.5% for the insignificant abatement cost of 0.73 NOK/ton CO_2 reduced. Producing hydrogen through SMR and combusting a fuel blend of NG/H_2 in gas turbines would increase the final CO_2-emission level by 7.6%. Pre-combustion capture of CO_2 from the SMR process would however decrease the CO_2-emissions with 15.1% for an abatement cost of 584 NOK/ton CO_2 reduced. The cost does not include transportation and final storage of CO_2. Carbon capture from fuel cells by oxy-fuel combustion would reduce CO_2-emissions with 20.8%. The technology for a medium ranged, compact fuel cell, capable of operating on natural gas is however still under development.

Finally, floating wind turbines supplying the offshore installations with electricity stands out as the most suitable alternative, with potential of decreasing CO_2-emissions with 20.8% for an abatement cost of 1 156NOK/ton CO_2 reduced.

Abbreviations

AC	Alternating Current
AHAT	Advanced Humid Air Turbine
bbl	Barrel of oil
BEC	Bare Erected Cost
C&OC	Contingencies & Owners Cost
CAPEX	Capital Expenditure
CC	Carbon Capture
CCS	Carbon Capture and Storage
CH_4	Methane
CHEOP	Clean Highly Efficient Offshore Power
CHEOP-CC	Clean Highly Efficient Offshore Power with Carbon Capture
CO	Carbon Monoxide
CO_2	Carbon Dioxide
COP	Conference of Parties
DC	Direct Current
EOR	Enhanced oil recovery
EPC	Engineering Procurement and Construction
EvGT	Evaporative Gas Turbine
FWT	Floating Wind Turbines

GEA	Greater Ekofisk Area
GHG	Green House Gases
GT	Gas Turbine
H_2	Hydrogen
H_2O	Water
HAT	Humid Air Turbine
HRSG	Heat Recovery Steam Generator
HVDC	High Voltage Direct Current
IC	Indirect Cost
LCC	Line Commutate Converter
LCOE	Levelized cost of energy
N_2	Nitrogen
NCS	Norwegian Continental Shelf
NG	Natural Gas
NOK	Norwegian Kroner
NO_x	Nitrogen Oxides
NPD	Norwegian Petroleum Directorate
OPEX	Operational Expenditure
OTSG	Once Through heat recovery Steam Generator
PDO	Plan for Development and Operation

PEM	Proton Exchange Membrane
PEMFC	Proton Exchange Membrane Fuel Cell
PFS	Power from Shore
ppm	Parts per million
PSA	Pressure Swing Adsorption
PWM	Pulse Width Modulation
S/C	Steam to carbon ratio
SAC	Single Annular Combustor
SMR	Steam Methane Reforming
SOFC	Solid Oxide Fuel Cell
TDPC	Total Plant Direct Cost
TIC	Total Installation Cost
TLP	Tension Leg Platform
TOC	Total Overnight Cost
TRL	Technology Readiness Level
UNFCCC	United Nations Framework Convention against Climate Change
VSC	Voltage Source Converter
WGS	Water Gas Shift
WHRU	Waste Heat Recovery Unit
WLE	Wet Low Emission

Nomenclature

$\dot{m}$	Mass flow	MW	Megawatt
£	British Pound	MWh	Megawatt hour
A	Area	n/g	Net to gross ratio
c_p	Specific heat at constant pressure	Nm^3	Normal cubic meter
c_v	Specific heat at constant volume	ϕ	Humidity
E	Free Electrolysis Voltage	P	Power
ɣ	Ratio of specific heat	P	Pressure
Gt	Giga ton	Q	Power density
GWh	Gigawatt hour	Q_{in}	Heat input
h	specific enthalpy	Q_{out}	Heat output
Hz	Hertz	R	Resistance
I	Current	S_{eff}	Fraction of stored CO_2 relative to pore volume
KE	Kinetic Energy	Sm^3	Standard cubic meter
kW	Kilowatt	T	Temperature
kWh	Kilowatt hour	TJ	Terajoule
LHV	Lower heating value	TWh	Terawatt hour
M_{CO2}	Tonnes of CO_2	U	Cell voltage
MPa	Mega Pascal	U	Wind speed

V	Voltage	η_{el}	Electrical efficiency
Vb	Bulk volume	η_{th}	Thermal efficiency
W	Work	η_{tot}	Total efficiency
ΔG	Gibbs Free Energy change	μW	Microwatt
ΔH	Enthalpy change	π_c	Pressure ratio P_2/P_1
ΔS	Entropy change	ρ	Density
$\eta_{ch.con}$	Chain conversion efficiency		

Table of Contents

List of Figures

List of Tables

1 Introduction

The atmosphere is crucial for all life on Earth. As sunlight warm up the Earth's surface, some of its energy reflects and radiates back to space as infrared radiation, or heat. Water vapour (H_2O), carbon dioxide (CO_2), methane (CH_4), nitrous oxide and ozone are gases present in the atmosphere, which absorbs this heat, keeping the Earth warm and habitable. Gases with this ability are known as Green House Gases (GHGs) [1].

Since the beginning of the industrial revolution, the temperature of the Earth's surface has been increasing rapidly, due to an increased amount of GHGs in the atmosphere. The main cause is the burning of fossil fuels, as it produces CO_2, which is the most significant GHG due to its large amount. The concentration of CO_2 in the atmosphere has increased from roughly 280 parts per million (ppm) at the beginning of the industrial revolution, to 406 ppm by the middle of 2018 [2]. To avoid further increase in temperature, emission of GHG, specifically CO_2, would have to be reduced.

1.1 Climate Control

The United Nations Framework Convention against Climate Change (UNFCCC) is an international environmental agreement, adopted and signed in 1992 by 156 countries, pledging to stabilize emissions of GHG on a 1990-level to avoid dangerous anthropogenic interference with the Earth's climate system. The agreement was set to force in 1994, and from that year, the Conference of Parties (COP) has had annual meetings [3]. The Parties have since then adopted the Kyoto Protocol in 1997 and the Paris Agreement in 2015. The Kyoto Protocol commits industrialized countries to limit and reduce emissions of GHG to a specific target, individualized for each party [4]. The Paris Agreements main goal is to limit average global temperature rise to below 2°C (preferably 1,5°C) above pre-industrial levels [5].

1.1.1 Norway's Environmental Commitment

Norway is an oil and gas nation with a strong climate policy, two factors that rarely goes hand in hand. Still the Norwegian Oil and Gas Association support the UNFCCC and strives to deliver the lowest possible emissions from fossil fuel production, to both meet the growing energy demand and the escalating climate challenges. The Norwegian Oil and Gas

Association aims to reduce their GHG emission to 40% of the 2005 level by 2030, and to have zero emission by 2050 [6].

The first measure was taken in 1991, when the Norwegian government introduced a CO_2-fee for emissions related to the petroleum industry. The goal was to encourage cost efficient methods to reduce emission of CO_2, and it was realized by improved energy efficiency [7]. Measures to reduce flaring, capture and storing of CO_2, as well as electrification of installations have all contributed to Norway's oil and gas production having only half of the average global CO_2-emission [6].

In 2005, Norway introduced an emission trading system, which in 2008 were merged with EU's emission trading system. This is a "cap-and-trade system", with an upper, fixed limit of emission, which is sold to industries as emission allowances. With time, the upper limit will reduce, and the price for allowances will increase. In this manner, industries will be encouraged to reduce their emissions instead of buying emission allowances [8].

For the Norwegian Oil and Gas Association to reach their goal for a zero-emission hydrocarbon production, further measures must be taken. The association believes that future technologies involving carbon capture and storage (CCS), hydrogen (H_2) and offshore wind, among others, will be the main contributors [6].

1.2 CO_2-Emissions Related to Oil and Gas Production

The oil and gas industry is the second largest source of GHG emission in Norway. In 2018 the industry was accountable for 27% of all Norwegian GHG emissions, where 66.7% of these came from gas turbines on offshore installations [9]. Gas turbines are used for power production, either for electricity generation or mechanical work for injection and compression. The gas turbines on Norways offshore installations are mostly operating on a simple cycle, and have a nominal average efficiency of 34.7%, meaning ~65% of the energy consumed is wasted and released into the atmosphere as heat via flue gases [10].

The main contributor to GHG emissions from oil and gas production world-wide is flaring and venting of gas, as Norway already have taken measures to reduce this activity to the bare minimum, the next challenge is emissions related to gas turbines on offshore installations.

1.2.1 Alternatives for Power Production on Offshore Installations

As a gas turbines primary function is to produce power, a more efficient way to deal with their emission is to take a step back and look at the power requirements on offshore installation, and alternatives beyond simple gas cycles.

By viewing the platform as a black box in need of power, several steps have to be considered for the procurement of this power. Figure 1-1 shows the power production selection process for an offshore installation, with specific alternatives for each step. The colour of the background illustrates the associated CO_2-emission for each level. The green colour indicates zero CO_2-emission, the black colour shows the emissions gas turbines on Norwegian offshore installations are accountable for today, and grey corresponds to somewhere in between.

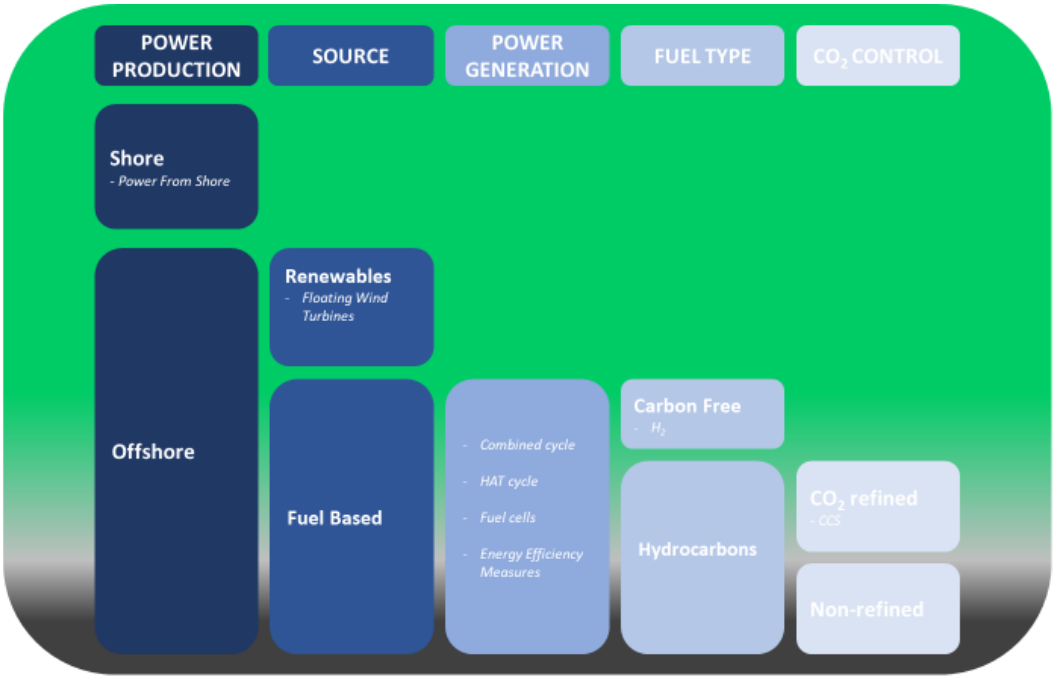

Figure 1-1: Power production selection model for offshore installations

Looking at Figure 1-1, energy can either be supplied as hydro power from shore without any CO_2-emission or produced offshore for direct use.

The offshore power production can be split into two sources, namely renewable energy from floating wind turbines or fuel-based energy.

Alternatives for fuel-based energy generation are many. This thesis will present energy production from combustion processes with combined cycle and Humid Air Turbine (HAT) cycle, and energy production from fuel cells, which do not directly involve any combustion. A small chapter on energy efficiency measures will also be provided, to demonstrate methods and results of emission reduction, with the original energy production by simple cycle gas turbines in place.

As CO_2 is a by-product of the combustion of the carbon fuel, emissions of CO_2 will not occur before hydrocarbons are present. The power generation column can therefore further be split into two, based on the fuel type. Hydrogen as an alternative to natural gas (NG) will be presented.

Lastly, measures to control the by-product of CO_2 can be implemented for complete removal of emissions from power production on offshore installations e.g. via CCS

1.3 Solutions for Reduced CO_2-Emission on Offshore Installations

This thesis aims to explore different options for CO_2-emission reduction related to power production on offshore installations, by looking at alternatives beyond simple cycle gas turbines. The base of the thesis will be the Greater Ekofisk Area (GEA), located in the southern part of the North Sea, which includes the fields Ekofisk, Eldfisk and Embla.

The thesis will present both alternatives available today, and new ideas that are still in a developing phase to ensure the most optimum solution for a high emission reduction to an affordable cost. The different options will be rated according to Technology Readiness Level (TRL), CO_2-emission reduction, efficiency improvement, and cost. Weight and size of equipment will also be an important factor, given these elements are limited on offshore installations. Some alternatives will be mentioned and explained briefly, and others will be investigated more thoroughly, depending on availability of data and information as well as the time frame for this thesis work. The goal of this thesis is to find the best solution for emission reduction on offshore installation, by comparing different alternatives based on abatement cost of reduced tons of CO_2.

2 Background

Searching for other alternatives for power production on offshore installations, a base area to hypothetically place the different solutions are chosen to be the Greater Ekofisk Area, which includes the fields Ekofisk, Eldfisk and Embla. A structured method for rating the different alternatives relative to each other is also essential to lay a good foundation for further comparison. The options will be rated by Technology Readiness Level, CO_2-emission reduction potential, efficiency, and cost. Lastly, a description of the conventional, simple gas turbine cycle is necessary, as most of the alternatives presented in this thesis originates from this technology. Chapter 2 will cover all three topics, providing the reader with the necessary background information for this thesis.

2.1 Greater Ekofisk Area

Greater Ekofisk Area lies in the southern part of the North Sea, about 300 km from shore and are made up by the fields Ekofisk, Eldfisk and Embla.

The Ekofisk field consists of 9 platforms plus 3 subsea templates. The oil and gas are produced with water injection from the three subsea templates and the injection platform Ekofisk K. The platform has 2 gas turbines of 22 MW each, running pumps for injection, and 3 turbines of 4.7 MW each for power generation. Ekofisk J is a process and transportation platform, serving as a hub for all three fields in the area. Oil and Natural Gas Liquids from Valhall and Hod, plus oil from Ula are also transferred here through pipelines before final transportation to UK and Germany. Ekofisk J is the largest energy producer in the GEA with 4 compressor turbines and 2 gas turbine generators, all of 22 MW each. The platform has a process capacity of 21.2 million Sm^3 of gas and 350 000 barrels of oil per day [10, 11]. In 2018 the process platform handled 67.9 million barrels of oil and 1.25 billion standard cubic meters of gas, consuming 593 891 MWh, or 7.84 kWh/bbl of oil equivalents from the compressors [12].

Eldfisk has 5 platforms whereas one of them controls the unmanned wellhead facility of Embla. Eldfisk E is an injection facility, providing water injection for the Eldfisk field as well as water support for the Ekofisk field [13, 14]. In total 4 gas turbines of 13.8 MW each are

operating pumps for this injection, along with a compressor of 22.7 MW used for gas lift and gas injection. The platform also provides the whole Eldfisk field with power, by operating 1 gas turbine generator of 5 MW and a steam generator of 10.3 MW running on waste heat from the compressor and four of the turbines dedicated for injection [10].

As a part of the development of Ekofisk South, with the installation of Ekofisk Z in 2013, the platform was designed to have space and weight capacity for a possible converter station of 120 MW [15]. An electrical cable between Eldfisk and Ekofisk is also present, installed in 2014, allowing the two fields to transfer and share power internally [16]. Table 2-1 gives an overview of the turbines located in GEA, their purpose and total power capacity.

Table 2-1: Gas Turbines at GEA [10]

	Electricity	Compression	Injection	Total Power Capacity
Ekofisk	2 x 22 MW 3 x 4.7 MW	4 x 22 MW	2 x 22 MW	190.1 MW
Eldfisk	1 x 5 MW 1 x 10.3 MW	1 x 22.7 MW	4 x 13.8 MW	93.2 MW

2.1.1 CO_2-Emissions and Power Requirements

Previous studies done in 2012 by ConocoPhillips, concerning Ekofisk gas concluded a burn value of 10.689 MWh/1000Sm^3 fuel. Burning 1000Sm^3 of the gas in a gas turbine with 35% efficiency returns 3.74 MWh fuel and 2.21ton CO_2 [15]. Based on these numbers, the CO_2-emission profile for GEA was created, from year 2000 to 2019. Figure 2-2 shows the emission profile for this period.

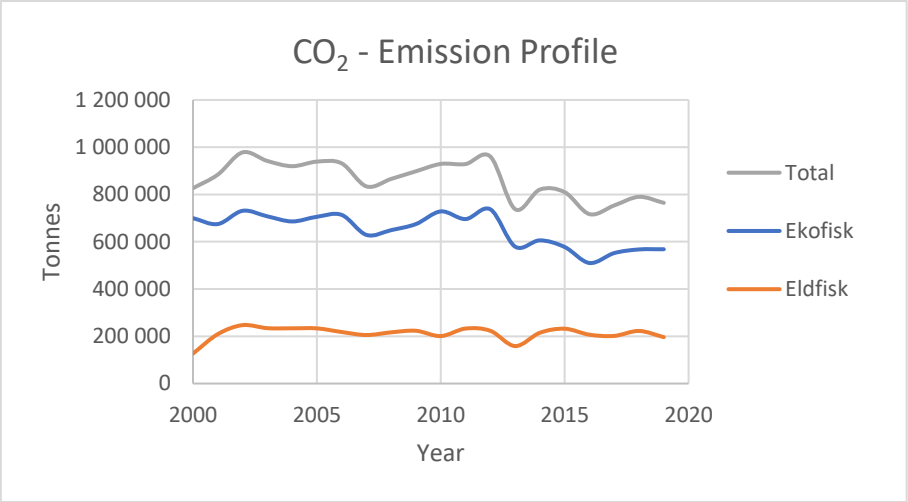

Figure 2-1: CO_2-emission profile for GEA [12]

In 2013 and 2016, the fields went under a shutdown, which explains the cut in CO_2-emissions at that time. In 2015, ConocoPhillips participated in a common industry project by The Norwegian Oil and Gas Association concerning energy management and efficiency. As a part of this project the Waste Heat Recovery Unit (WHRU) on Ekofisk K was optimized, reducing the use of a gas turbine for heat purposes. They have strived to use only one out of two pipeline compressors for gas export when possible, likewise for the two oil export booster pumps. The water injection headers have also been modified to optimize the distribution of injected water for the Ekofisk field. These energy efficiency measures explain the further reduction of CO_2-emissions from 2016 onwards [17]. Gas consumption from Ekofisk and Eldfisk were found in Diskos Reports under Field fuel, flare and cold vent report [12].

With the same procedure as for Figure 2-1, Table 2-2 was created, giving an overview of gas consumption, power generation and CO_2-emissions from gas turbines on GEA in 2018.

Table 2-2: Gas consumption, Energy Production and CO_2-emissions from GEA in 2018 [10]

	Gas Consumption [Sm^3]	Energy Production [MWh]	CO_2-emission [ton]
Ekofisk	256 741 941	960 215	567 400
Eldfisk	100 711 406	376 661	222 572
Total	**357 453 347**	**1 336 876**	**789 972**

The total CO_2-emission from GEA in 2018 (789 972 tons), are the number that this thesis has considered as a baseline for investigation of other power production alternatives to reduce CO_2-emissions. Energy requirements are assumed to be the same as the total Megawatt hours for 2018; namely 1 336 876 MWh.

2.2 Rating system

This thesis will use the TRL system for assessing the maturity of different technologies for power production on offshore installations. The alternatives will also be rated according to CO_2-emission reduction, efficiency improvement and cost. As size and weight are limited on offshore installations, compact and light equipment/systems are advantageable. It is not a part of the official rating system, but the dimensions will be remarked in this report.

As insecurities around cost and a low TRL level often are connected, cost can be left out of the rating system for some new technology options discussed in the thesis, due to high uncertainties. With too high inaccuracies, all cost estimates would be purely speculative, and is therefore better left unreviewed.

2.2.1 TRL

All new technologies go through a research and development phase before being deployed for commercial use. TRL are used to assess the maturity of a particular technology and determine the progress with nine different rating levels. TRL 1 being the lowest and TRL 9 the highest [18]. Table 2-3 gives a detailed description of each level.

Table 2-3: TRL Level Description [18]

Phase	TRL	Level Description
Research	1	Basic principles observed and reported.
	2	Technology concept and/or application formulated.
	3	Analytical and experimental critical function and/or characteristic proof-of-concept.
Development	4	Technology basic validation in a laboratory environment.
	5	Technology basic validation in a relevant environment.
	6	Technology model or prototype demonstration in a relevant environment.
Deployment	7	Technology prototype demonstration in an operational environment.
	8	Actual technology completed and qualified through test and demonstration.
	9	Actual technology qualified through successful mission operations.

2.2.2 CO_2-Emission Reduction

CO_2-Emission reduction will be measured as percentage of the emission from gas turbines on GEA. From ConocoPhillips' report, burning 1000Sm^3 of natural gas in the turbines generates 3.74 MWh of energy and produces 2.21 tons of CO_2. The amount of CO_2 produced per MWh generated is then:

$$CO_{2_{GT}} = \frac{2.21\ ton}{3.74\ MWh} = 0.59\ ^{ton}/_{MWh} \tag{2.1}$$

Where $CO_{2_{GT}}$, is the amount of CO_2 produced per MWh generated in a gas turbine.

The CO_2 emission reduction for alternative power production would then be calculated as:

$$\%\ CO_2\ emission\ reduction = -\frac{CO_{2_x}}{CO_{2_{GT}}} \cdot 100\% + 100\% \quad (2.2)$$

Where CO_{2_x}, is the CO_2-emission factor per generated MWh for option x.

For instance, reviewing an option with the same amount of CO_2-emission per MWh generated will equal 0% emission reduction, 0.295 tons of CO_2 per MWh equals 50% emission reduction and 0 ton/MWh equals 100% emission reduction.

2.2.3 Efficiency

Efficiency of power generation can be split into electrical efficiency and total efficiency and is denoted by η. The electrical efficiency is the power output divided by the energy input via fuel flow:

$$\eta_{el} = \frac{Power\ output}{Energy\ input} = \frac{W_{out}}{Q_{in}} \quad (2.3)$$

The total efficiency, also known as the fuel utilization factor, is the sum of power output and the utilized heat in the exhaust gas (e.g. in Combined Heat and Power plants) to the energy input via fuel flow:

$$\eta_{tot} = \frac{Power\ output + Utilized\ Heat}{Energy\ input} = \frac{W_{out} + Q_{out}}{Q_{in}} \quad (2.4)$$

A higher efficiency cycle will influence both the power output and the required energy input of fuel amount. Less specific CO_2 (i.e. CO_2-emission per unit of power output) will be produced as more of the fuel will transform into power or other energy products such as heat through innovative or combined cycles and cogenerations, and thus less fuel will be needed for the same amount of power output. Burning less fuel will further reduce the CO_2 output.

As some of the alternatives presented in this thesis is based on a cogeneration cycle, the efficiency rating will be based on the total efficiency. From this point, efficiency refers to total efficiency unless stated otherwise.

The efficiency improvement compared to the base case is calculated as:

$$Efficiency\ improvement = \frac{\eta_x - \eta_{GT}}{\eta_{GT}} \cdot 100\% \quad (2.5)$$

2.2.4 Cost

The cost of the emission reduction technology is an important factor when comparing and choosing between the available options. However, the main focus of this thesis is to study the effect of CO_2-emission reduction technology. Cost estimations will therefore be simplified and done without regards to discount rates and inflation. Although these factors play an important role in future investment decisions, the technical background of the author and time restrictions limits the capacity of investigating this further.

As the different alternatives have different emission reduction potential, looking at the total investment cost would be insufficient. The rating system will therefore be based on the abatement cost of reduced tons of CO_2. For an option to be profitable purely from an economical point of view, the abatement cost would have to be lower than the emission cost of CO_2, meaning the total cost of one emission allowance from EUs emission trading system and Norway's CO_2-fee for the petroleum industry.

In February 2020, the price for one emission allowance was 274 NOK/ton CO_2 [19], adding in the Norwegian CO_2-fee for 2020, which is 1.15 NOK/Sm^3 gas burned, or 491 NOK/ton CO_2 emitted [20], the price of releasing one ton of CO_2 into the atmosphere is 765 NOK.

An abatement cost equal to or lower than 765 NOK would therefore make the investment beneficial from both an economical and environmental point of view.

2.2.5 Rating System Table

Every option covered in this thesis will be rated according to the factors introduced in this subchapter and are to be inserted into Table 2-4.

Table 2-4: Rating table

Alternative	TRL	% CO_2-Emission Reduction	Efficiency	Abatement Cost	Comments

2.3 Gas Turbines

A gas turbine is a combustion engine designed to convert fuels such as natural gas to mechanical energy, either for direct use or as an intermediate for electricity. With their low weight and volume, their multi-fuel capability and rapid start-up and load changes, they are extremely versatile and can be applied in everything from a single unit in a domestic household to multiple machineries in a big gas power plant, in aviation, marine vessels and automotive applications. Gas turbines for power generation on offshore installations is a natural choice, as the need for both mechanical work and electricity is present, and the fuel is easily available [21].

2.3.1 The Gas Cycle

A simple gas turbine cycle consists of a compressor, a combustion chamber, and an expander. Atmospheric air is compressed to a high pressure in the compressor and diverted to the combustion chamber. Here it mixes with the fuel and combusts, generating a hot, high pressure exhaust gas. This gas expands in the turbine and generates mechanical work by rotating a shaft which is further used to drive the compressor, thereby finishing the cycle.

The surplus of the mechanical work is further converted to electricity through a generator [22]. See Figure 2-2 below for schematics of a simple gas cycle.

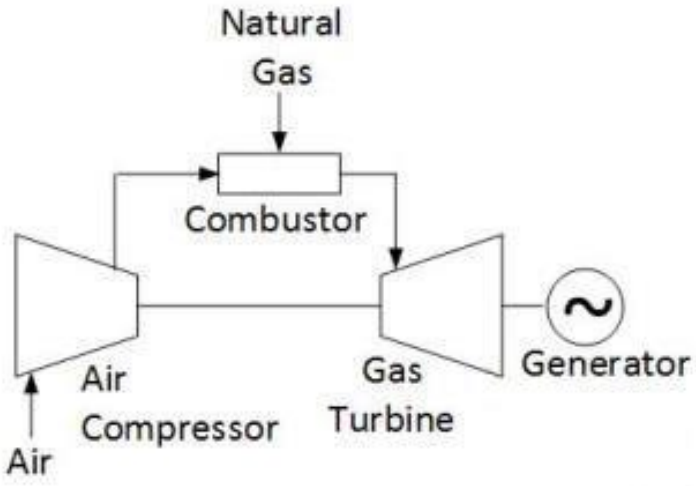

Figure 2-2: Schematics of a simple gas cycle [23]

The efficiency of a simple gas turbine cycle is not very high. Typical values are between 30-40%, depending on the fuel, engine, workload and operating temperatures [24]. The remaining energy from the fuel (~60%) is thermal energy released into the atmosphere unless recovered.

Typical gas turbine outlet temperature is somewhere between 450-650°C [22]. By installing a regenerator, the heat from the exhaust gas is transmitted to the delivery air from the compressor before entering the combustion chamber. Less fuel is then required to reach the same turbine inlet temperature, and the efficiency will increase [21]. Another possibility is to exploit the waste heat beyond the gas turbine, by installing a WHRU. For a gas turbine on an offshore installation, the heat could be utilized to warm up living quarters or used in separation processes for oil and gas. This would have a positive impact on the efficiency as the waste heat will contribute to a higher utilization of the fuel, as shown in equation (2.4). As the efficiency increases, the emission level per unit of useful energy produced, decreases.

The efficiency of a gas turbine also depends on the load level. On offshore installations more than half of the gas turbines run at 50-60% load, and a few at 70-80%. This is practiced as an insurance in case one of the turbines malfunctions, then one could easily increase the load

on the remaining ones to generate the same power output as before. Figure 2-3 shows how the efficiency varies with different load levels for certain gas turbine models [25].

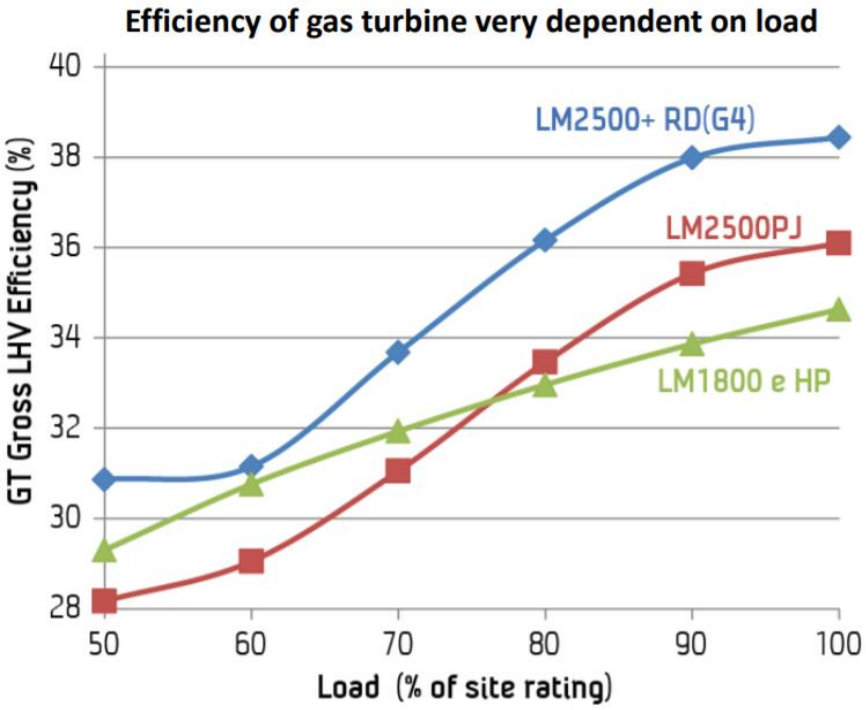

Figure 2-3: Load Level vs. Efficiency [25]

TRL

Gas turbines has been a well-known technology since the first unit was built in Paris in 1903 and is rated with TRL 9.

CO_2-Emission Reduction

As gas turbines serves as the basis for CO_2-emission reduction potential, CO_2-emission reduction is given as 0%.

Efficiency

Average nominal efficiency for the gas turbines on GEA is 34.7% [10].

Cost

As gas turbines are already installed on GEA, the investment cost is set to 0 NOK, and abatement cost is set to be equal to the CO_2-emission cost, namely 765 NOK/ton.

Summary Rating

Alternative	TRL	CO_2-Emission Reduction	Efficiency Improvement	Abatement Cost	Comments
Gas Turbines	9	0%	0%	765 NOK/ton	Base case

Power Production

Starting with the first column in the model of alternatives for power production presented in Chapter 1; offshore installations could either get power supplied from shore or it could be generated offshore for direct use. Chapter 3 is a detailed study of the first option, namely Power from Shore and a Partial Electrification of GEA with technological background, advantages/disadvantages and an economical evaluation of feasibility.

3 Power from Shore

Power from Shore (PFS) is a carbon-free energy alternative on offshore installations in Norway. Clean hydropower from shore is supplied to offshore installations in cables on the seabed, eliminating the need for electricity generating gas turbines. The first use of this technology on the Norwegian Continental Shelf (NCS) was on Troll A in 1996. A 69 km long 20 MW AC cable from shore to the platform provided the entire field with its energy demand [26]. The success of the operation led to a new obligation for all licensees operating on the NCS, to study the possibility for implementing PFS when presenting a Plan for Development and Operation (PDO). As of today, PFS have been installed on 7 different offshore fields on the NCS and 5 more installations are under development [27].

3.1 Technology

A PFS solution is a complex system, requiring submarine cables, transformers, and converter stations both offshore and onshore. This section aims to give a detailed description of the power transmission process, in addition to the components mentioned above.

3.1.1 Power Transmission

For a better understanding of power transmission in submarine cables, a brief introduction into electric power is necessary.

Power (P) is the product of voltage (V) and current (I).

$$P = V \cdot I \tag{3.1}$$

Voltage is defined as the difference in electric potential between two points. The current is the flow of electrons pushed or pulled in a conductor (wire) by voltage. The flow of electrons in a conductor produces heat due to friction, known as resistance (R). The resistance, along with the current is accountable for energy losses along the way when transporting electricity. The energy loss is related as:

$$Transport\ loss = R \cdot I^2 \tag{3.2}$$

When transmitting power, the usage of high voltage is advantageous [28]. It allows one to reduce the current for the same amount of power, as seen in equation (3.1), which leads to considerably reduced transport losses, shown by equation (3.2).

Power can be transmitted with two different currents, alternating current (AC) or direct current (DC). The AC transmission alters in strength and direction periodically, creating a sinewave. One wave equals one period, the number of periods per second is called the frequency and is measured in Hertz (Hz). 50 and 60 Hz are standardized frequencies used by consumers. The DC transmission is a steady flow of electrons in one direction, without any frequency [29].

For power transmission, AC has the advantage that it is much easier and less expensive to raise and lower voltages between generation, transport, and consumption. However, the transmission loss for AC is more complicated, as it not only depends on RI^2 (which is the case for DC) but also the relationship between voltage and current, known as the impedance. For a given current, the transmission loss for AC exceeds DC, so for larger distances with high power transmission, it is beneficial to choose a Direct Current, more specifically, a High Voltage Direct Current (HVDC) solution [29].

For power transmission to offshore installations, the distance is a key factor along with power requirements when choosing between AC or DC solution. When distance and power requirements call for a DC cable, converters both onshore and offshore will have to be installed, to transform the AC to DC for transporting, and back again for consumption. This increases the cost significantly.

Aker Kværner has developed a schematic (Figure 3-1) for the two different transmission technologies, and when it is most beneficial to choose one over the other. The chart is split into HVDC and AC power transfers, based on power requirements and distance to the installation. Examples of previously installed PFS solutions for some offshore installations on the NCS are also included in the figure [30].

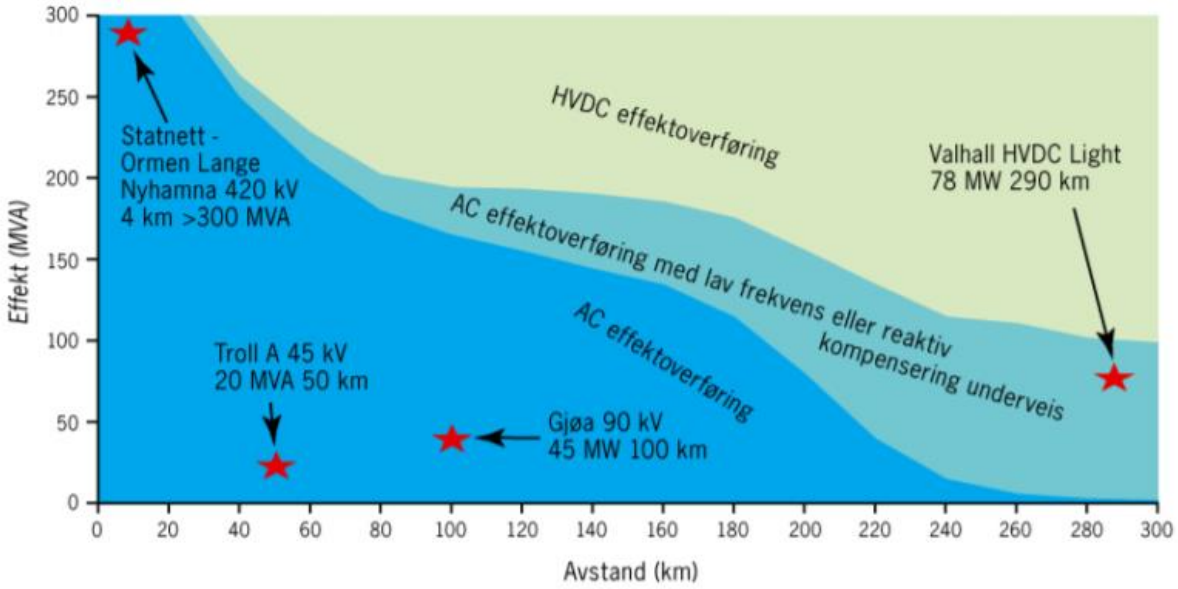

Figure 3-1: Schematic for AC/DC solution based on effect and distance [30]

3.1.2 Cables

The cables in a HVDC power transmission to offshore installations needs to be both resistant and durable. A cable breach on the seabed could take over a month to repair, resulting in full production stop for the same amount of time. The power amount and transmission distance also calls for the conductor material to be efficient, to limit the losses as much as possible. Copper and aluminium are both possible options. Aluminium has 2/3 of the electric conductive properties copper holds, but if weight is of importance, aluminium holds only 1/3 of coppers mass. For electrification on offshore installations, the cables would be placed on the seabed, and weight would not be a concern. Copper is therefore the best option for conductive material [31]. Insulation, reinforcement, armouring, and outer servings are also constituents in a HVDC cable but will not be discussed further here.

A power transmission will not take place unless a closed circuit is present. Installation of PFS to an offshore platform will therefore require two sets of cables in parallel, with a certain distance to each other to avoid electromagnetic disturbance. To protect the cables from taking potential damage on the seabed, they are buried in trenches or covered with rocks.

3.1.3 Transformers

Transformers are used to convert high-voltage power to low-voltage power and vice versa using electromagnetic induction. The basic principle involves two or more coils of insulated wire wound on a steel core. When voltage is introduced to the primary coil, an electromotive force induces the electrons in the secondary coil to move also, as they are connected through the steel core. The voltage ratio between the input and output coil depends on the number of windings around the steel core, for each coil. Figure 3-2 illustrates the principle of raising and lowering the voltage in transformers. When the primary winding is lesser than the secondary, the voltage increases as for the step-up transformer in the figure. To reduce the voltage the number of winding has to be higher for the primary coil than for the secondary, as for the step-down transformer [32].

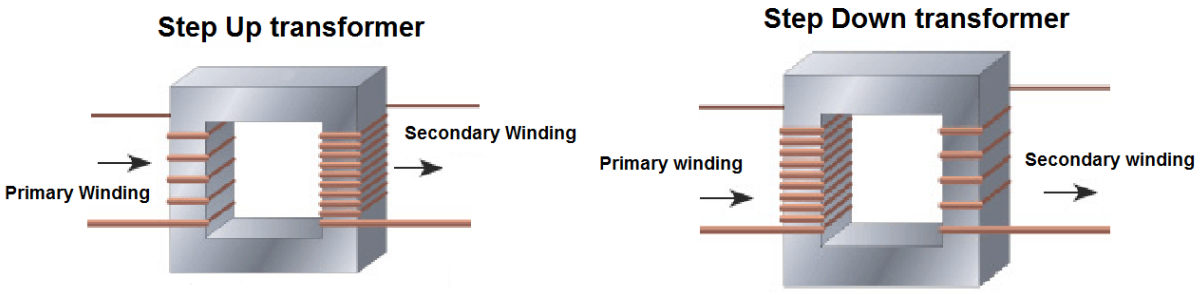

Figure 3-2: Illustration of Step-Up and Step-Down Transformers [33]

3.1.4 Converter Stations

Converters are necessary for transforming onshore AC power to DC for transportation and back to AC for consumption. For electrification of an offshore installations with HVDC technology, one converter will be installed onshore to ship off the power, and one offshore to receive it. This technology is often referred to as an AC-DC-AC converter [34].

HVDC LCC

HVDC classic, also known as HVDC Line Commutate Converter (LCC) works on a thyristor-based technology, meaning different phased Alternating Current is converted into one Direct Current by passing the AC power through a section of valves activated in a specific order for a Direct Current to be produced, as illustrated in Figure 3-3 [35].

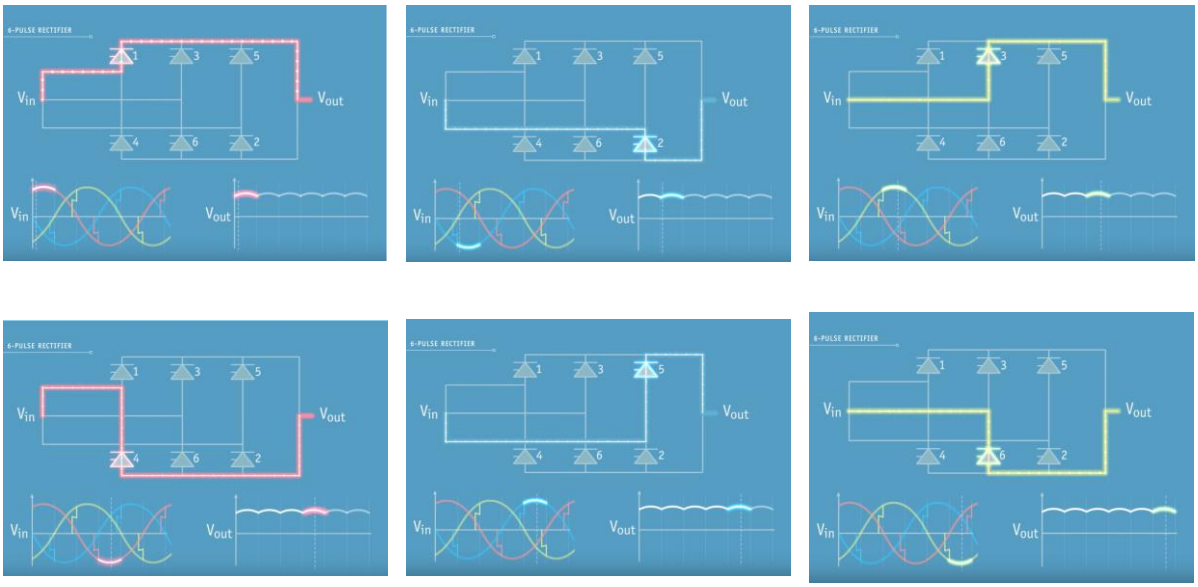

Figure 3-3: Illustration of a 6-phase rectifier (screenshot) [35]

To convert the DC back to AC, a 6-pulse inverter is used. Figure 3-4 illustrates the process step by step. 3 sets of full wave inverters are joined in parallel, and in 6 pulses the power is sent through different paths to create three phases of AC power: red, yellow and blue. With each pulse, one phase will receive the positive side of the DC power, one will receive the negative side and the last one will not be conducting [35].

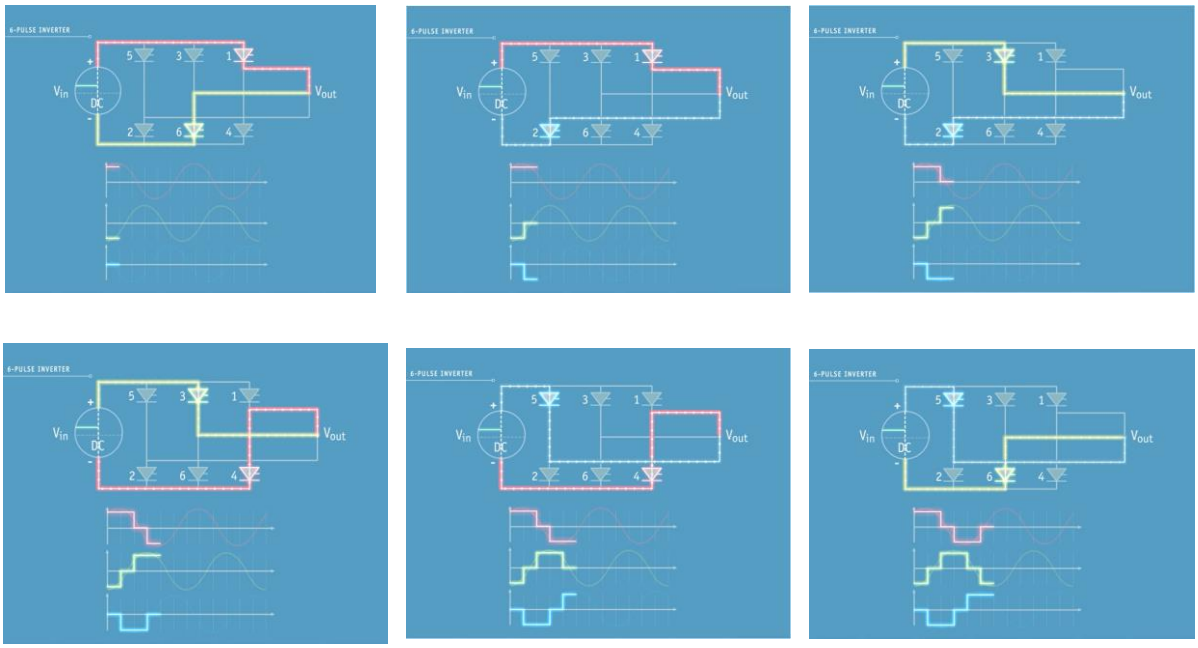

Figure 3-4: Illustration of a 6-pulse inverter (screenshot) [35]

For the input voltages and phases to be accurate, the HVDC LCC requires a strong and stable AC system. To strengthen the AC system, AC & DC harmonic filters are used to mitigate voltage distortions and interferences in the connected AC network. These filters are big and heavy and demands space that offshore installations do not have. The filters have been one of the limiting factors, along with the complexity of control (specifically during start-up), as to why HVDC technology has not been implemented by the oil and gas industry until the invention of Voltage Source Converters (VSC) by ABB in 1997 [36].

HVDC VSC

In 1997 ABB introduced the HVDC Light as an alternative to HVDC Classic. The phase commutate converter technology was replaced with a Voltage Source Converter, eliminating the need for filters, thereby reducing the size of the equipment on the offshore side with 50-60% [36].

The VSC operates with Pulse Width Modulation (PWM), a transistor-based technology using Insulated Gate Bipolar Transistor cells. By opening and closing the cells, one can control what path the power takes in the circuit, thereby manipulating the current into either AC or DC [37].

A demonstration of a PWM inverter is showed below, where the DC power is switched on and off repeatedly, creating the pattern of Figure 3-5. A cycle is the interval of one full repetition, illustrated by the yellow line. The duty cycle represents how much of the period the signal is high compared to low. Output voltage is then calculated by the max voltage times the duty cycle [38]:

$$V_{out} = 5V \cdot 0.50 = 2.5V$$

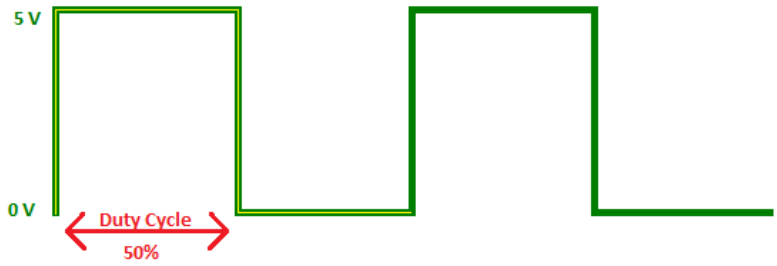

Figure 3-5: PWM pattern

By switching the power on and off rapidly, and varying the duty cycle, different voltages are produced, and the output voltage will appear as the blue AC sinewave in Figure 3-6 [36].

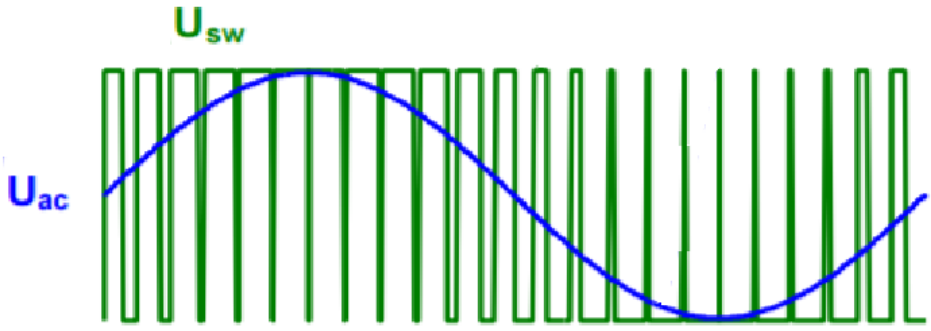

Figure 3-6: Principle of PWM [36]

The VSC has several advantages for offshore power supply compared to the HVDC LCC. The VSC has components that can interrupt the current by themselves, unlike the LCC requiring a current to commutate against. VSC can therefore feed power into a passive network, enabling a black start in case of a short circuit. PWM allows for the magnitude and phase of the voltage to be controlled freely and almost instantaneously, permitting full control of the power transmission. Lastly the essential filters needed for HVDC LCC is eliminated with the use of PWM, reducing the size of the module with 50-60% as mentioned earlier [36].

3.2 Advantages with PFS solutions

The advantages with replacing gas turbines with power from shore are many. The GHG emissions from burning the fossil fuel are avoided, which will eliminate the CO_2-emission cost. It will also free the previously consumed gas up for sale, generating an extra income. The total effect requirement will be less for an PFS solution compared to gas turbines, as the efficiency of the gas turbines generally lies between 30 and 40%, resulting in a waste of energy.

Gas turbines require a lot of maintenance, which always demands for maintenance personnel to be present. With a PFS solution, the need for offshore staff will be reduced as it requires less maintenance, which when needed, often is remotely controlled. The hazard of working near gas-fired rotating equipment is eliminated, along with the noise and vibration that gas turbines expel. Lastly a PFS solution would free up space and weight capacity on the offshore installations, as the module is lighter and more compact compared to gas turbines [39].

A downside to the PFS solution is the possibility of a power shortage/breach, or a cable breach. Given the cable is buried under the seabed, this would be unlikely, but must be accounted for. Repairing a cable at the seabed could take up to a month, resulting in a full production stop for the same amount of time [40].

3.3 Partial Electrification

As mentioned in Chapter 2.3, the mechanical work from gas turbines can either be used directly or converted to electricity via a generator. The mechanical work is used for driving pumps for injection and compression, whilst the electricity is used for heating, lights, and other power requirements. When electrifying an offshore installation, the term fully electrified speaks to replacing both the gas turbines generating electricity *and* the ones performing mechanical work. Partial electrification refers to replacing the turbines generating electricity only [30].

3.4 PFS on GEA

GEA has 17 gas turbines divided on three different platforms, 6 of these are for electricity generation whilst the remaining 11 are providing mechanical work [10]. For all power generation on the GEA to be replaced by PFS (i.e. a full electrification), the pumps and compressors would need to undergo extensive modifications as the system is set for mechanical drive. This would require a much more detailed study and lead to a considerably higher abatement cost. This study will therefore be limited to partial electrification as alternative power supply on GEA.

3.4.1 Energy Calculation

GEA's energy consumption from gas turbines for 2018 (Table 2-2) corresponded to 1 337GWh. The turbines generating electricity produced 20.88% of this (i.e. ~280 GWh). For the system to be able to handle peak consumptions, which can be up to 30% higher than normal usage, and to account for transmission losses, a PFS system with 50 MW capacity is studied as an alternative for GEA. Table 3-1 below shows the updated gas consumption, energy production and CO2-emission for GEA, if a PFS solution had been installed. The gas consumption has been reduced, but the total energy requirements (MWh) is assumed to be the same, as the gas turbines producing electricity have been replaced by hydro power.

Table 3-1: Gas Consumption, Energy Production and CO_2-emissions for GEA with PFS

	Gas Consumption [Sm^3]	Energy Prod. [MWh]	CO_2-Emission [ton]	[%]
Base Case	357 453 347	1 336 876	789 972	
PFS	282 816 114	1 336 876	625 024	
Reduction	**74 637 233**		**164 948**	**20.9%**

By installing a PFS system on GEA, close to 75 million Sm^3 of gas would have been freed up from the gas turbines and made available for sale. The CO_2-emission would have been reduced by nearly 165 000 tons per year.

3.4.2 TRL

Voltage Source Converters was introduced in 1997 by ABB. Today the functionality is still the same, but with a higher performance and reduced energy losses. The VSC is rated with TRL 9 from Table 2-3.

3.4.3 CO_2-Emission Reduction

The CO_2-Emission Reduction is calculated by Eq. (2.1) and (2.2) with the numbers from Table 3-1. PFS is assumed green, hydro power without any CO_2-emission, however, as the reduction potential only stands for ~21% of the CO_2-emission generated from gas turbines, the remaining CO_2-emission must be included in the equation.

$$CO_{2_{PFS}} = \frac{625\,024\ ton}{1\,336\,876\ MWh} = 0.4675\ {}^{ton}/_{MWh}$$

$$\%\ CO_2\ emission\ reduction = -\frac{0.4675}{0.59} \cdot 100\% + 100\% = 20.8\%$$

3.4.4 Efficiency

The efficiency of a PFS system is calculated with respect to energy losses in the converters and cables under transmission. The power transmission losses are assumed to be the same in this thesis as for ConocoPhillips' evaluation of PFS on GEA, namely 8%, i.e. 3% for the converter stations and 5% for the cable system [15]. Total efficiency for the PFS solution amounts to 92%, but is only true for the electricity generation, which is ~21% of total power requirements. To calculate the efficiency for total power generation, the gas turbines driving the pumps and compressors needs to be included.

$$Efficiency = \ 0.2088 \cdot 92\% + 0.7912 \cdot 34.7\% = 46.66\%$$

Efficiency improvement is calculated with Eq. (2.5)

$$Efficiency\ improvement = \frac{46.66\% - 34.7\%}{34.7\%} \cdot 100\% = 34.5\%$$

3.4.5 Cost

Cost estimates for Electrification of GEA are based on 2 separate 300km 50 MW DC cables from Lista in Agder Kommune, Southern Norway, to the Ekofisk Z platform, and two HVDC converters connected to each end of the cable. Expected lifetime of the fields are set to current production licence which expires in 2049, production and power requirements are based on that of 2018 and assumed to be continuous.

Price of future gas and electricity are highly uncertain, due to time restrictions this will not be forecasted, but calculated with three different prices. The average price from 2018, the average price from 2019 and average price from February 2020. The CO_2-emission cost will be set constant at the 2020 level (765NOK/ton CO_2).

Previously studies have been made on PFS for GEA by both the Norwegian Petroleum Directorate (NPD) and ConocoPhillips. *Kraft fra Land* [30] was published by NPD in 2008, and *Power from shore to the Ekofisk Area [15]* was published by ConocoPhillips in 2012. The cost estimation presented in this thesis will be based on those two reports, in addition to the study of electrification of Johan Castberg from 2016 [41]. The cost estimation of the converter station is based upon the module provided for Johan Sverdrup by ABB [42].

Equipment and Installation

The power requirement of GEA in 2018 called for a 50 MW power supply to cover the electricity demand of the area. Cost estimates of the converter stations and associated construction are based on Johan Sverdrup's 100 MW HVDC system supplied by ABB. The contract was worth 1.1 billion NOK, and included design, engineering, procurement, installation and start-up of the two converter stations [42]. In *very* general terms, price of HVDC system and Power Rating are related with the formula [43]:

$$Price_2 = Price_1 \cdot \sqrt{\frac{Power\ Rating_2}{Power\ Rating_1}} \tag{3.3}$$

It is therefore, assumed the acquisition and EPC for a 50 MW converter, including full installation and start up both onshore and offshore to be:

$$NOK = 1.1 \cdot 10^9 NOK \cdot \sqrt{\frac{50MW}{100MW}} = 777\,817\,460\ NOK$$

Procurement and EPC of DC cables are based on the study of electrification of Johan Castberg in the Barents Sea [41]. In this study 80% of the sea cable were to be buried under the seabed, and the remaining 20% were to be covered with rocks, the same assumptions are made for this thesis. Time spent on the different activities related to installation of the cable are stipulated from the values provided by the study from Johan Castberg. Total cost of cable installation adds up to 1 614 400 000 NOK. Table 3-2 gives a more detailed description of cost estimates related to installation of cables.

In addition, an administrative post for project management is calculated from the total equipment and installation cost, it is assumed to be 10% and to cover the whole project from start to finish.

Table 3-2: Cost Estimate Converter Module & Sea Cables

Description	Norm	Quantity		Estimated Cost
	NOK/unit	km	days	NOK
HVDC Light Converter Module	777 817 460			777 817 460
Procurement Sea Cables	2 550 000	600		1 530 000 000
EPC	1 000 000	600	37	37 000 000
Trenching	600 000	480	54	32 400 000
Rock Dumping incl. supply boats	1 000 000	120	15	15 000 000
SUM				2 392 217 460
Project Management (10%)				239 221 746
Total				**2 631 439 206**

Modifications

As part of the Ekofisk South development in 2013, the new drilling platform Ekofisk Z was installed. Although PFS was not implemented during this construction, the platform is designed with space and weight capacity for a 120 MW converter station and J-tubes for pulling cables, in case a PFS solution were to be implemented at a later stage [15]. In 2014 an AC cable was installed between Eldfisk S and Ekofisk Z with a 20 MW capacity, for more efficient power generation and distribution. Embla is already getting their power from Eldfisk through a similar cable.

For a PFS solution to be implemented, modifications on Ekofisk Z are necessary, involving preparations for installation, hook-up and integration. Adjustments related to PFS implementation on the other platforms at GEA are also required, but not of the same extent [15].

A time estimate for these modifications are hard to provide, as very few fields has gone through this upgrade. Valhall was in 2011 fully electrified, as part of a major upgrade of the entire field. A new combined production and accommodation platform replaced two old installations and included a HVDC module with power reception for PFS. Production stop was estimated to be 3 months in the original PDO. However, 6 months passed from when the old production platform was shut down until the new platform started producing. Thus was the actual loss of income doubled [44].

In NPDs report *Kraft fra Land* from 2008, a time estimation for installation of the power reception module was set to 11 days for Ekofisk and 8 Days for Eldfisk. This was based on the HVDC module being installed on a new Power host platform with a bridge connected to Ekofisk, where further distribution to Ekofisk and other fields would take place [45].

ConocoPhillips' own report on Power from Shore has reserved a 6 months installation window for the new system to be integrated at Ekofisk Z [15]. As the reception module would be installed separately from the current power sources, namely the gas turbines, a lot of preparation could be done without shutting the power off and thereby avoiding a production stop for the same amount of time. The report has no statements or assumptions regarding production stop, so this thesis will calculate the effect of 11 days, 3 months and 6 months for the final abatement cost.

The average saleable oil and gas production per day from GEA in 2018 was 1 486 817 bbl and 334 844 028 Sm^3 [12], the average oil and gas price were 568NOK/bbl and 2.21NOK/Sm^3 [46, 47], respectively. The Norwegian tax for the petroleum industry amounts to 78% of the total company profit [48]. For simplicity, the income from saleable production is calculated as 22% of the average oil and gas price from 2018. Average total income per day amounts to NOK 348 510 407. Table 3-3 shows the loss of income related to production stop for 11, 90 and 180 days.

Table 3-3: Loss of income due to production stop

Production Stop [days]	Loss of income (incl. tax) [NOK]
11	3 833 614 472
90	31 365 936 586
180	62 731 873 172

Operating Costs

ConocoPhillips' study of implementing a PFS solution estimated the operating and maintenance cost of the facilities to be 7.8 million NOK per year, and for the first three years an additional cost of 2.2 million NOK to cover subsea inspection of the cable system. Expenses related to operation of gas turbines generating electricity amounts to 20.2 million NOK per year, which will be deducted from the total cost of implementing PFS. These numbers are assumed to be the same today and are included in this thesis estimates. Table 3-4 shows that savings by switching to a PFS solution accumulates to 353 million NOK.

Table 3-4: Operating Cost of PFS and Gas Turbines

	Operating Cost [kNOK/year]	Years	Total Cost [NOK]
PFS	7 800	29	226 200 000
PFS	2 200	3	6 600 000
Gas Turbines	20 200	29	- 585 800 000
Total			**- 353 000 000**

Energy Costs

From Chapter 2.2.4, the price of releasing one ton of CO_2 into the atmosphere in Norway is set to NOK 765. Implementing PFS would reduce CO_2-emissions with 164 948 tons and cut the emission cost by NOK 126 185 220 per year. For a life expectancy of GEA to 2049, the CO_2-emission reduction accumulates to 4 783 492 tons of CO_2, which would end up saving 3 659 371 380 NOK in emission costs, assuming that PFS had been implemented from the year 2020.

With a PFS solution, 280 750 MWh of power would be supplied to GEA every year through cables. The 300km transmission distance will however result in a transmission loss of 8%, so the purchased electricity would amount to ~109% of power requirement, which equals to 306 017 MWh. 75 million Sm^3 a year of gas, previously used in gas turbines would now be available for sale, this amount minus tax would be deducted from the final cost of the PFS system.

As the gas and electricity prices are fluctuating variables, 3 different calculations are done for the abatement cost, with the average price of gas and electricity for 2018, 2019 and February 2020. Numbers are shown in Table 3-5 below, where power is viewed as an expense, while cost of CO_2-emission and excess gas are counted as extra income. Electricity prices are taken from SSB [49], and gas prices from YCHARTS [47].

Table 3-5: Energy Costs by switching to a PFS solution

	Quantity	Unit	Price [NOK/unit]			Total Cost [kNOK/year]		
			2018	2019	2020	2018	2019	2020
Power	306 017 000	kWh	0.316	0.322	0.318	96 640	98 537	97 313
CO_2	164 984	ton	765	765	765	- 126 185	- 126 185	- 126 185
Gas	74 637 233	Sm^3	2.211	1.495	0.956	- 36 301	- 24 550	- 15 698
Profit						**65 846**	**52 198**	**44 570**

The difference in gas prices between 2018 and February 2020 underlines the uncertainty of cost estimates for future investments. The cold winter of 2018 resulted in EU overbuying gas for the winter of 2019. The winter of 2019 was however milder than anticipated, a lot of gas ended up in storage and the price took a heavy fall [50].

If we were to disregard the total investment cost and just look at the cost associated with power, gas and CO_2-emissions; a minimum of 44 million NOK would be saved each year, assuming a PFS solution had been installed.

Abatement Cost

The Abatement cost is calculated with the formula:

$$\frac{Total\ investment\ cost\ of\ PFS - Operating\ cost\ of\ gas\ turbines\ incl.\ CO_2\ cost}{CO_2 - emission\ reduction\ for\ expected\ lifetime}$$

Total estimated cost of implementing PFS on GEA, including the abatement cost is summarized in Table 3-6 below. Due to uncertainties in both energy prices and estimated production stop during installation, a total of 9 different abatement costs are calculated. Table 3-6 refers to 2018 energy prices, and gives the cost for 11, 90 and 180 days of production stop. Cost estimates with energy prices from 2019 and Feb. 2020 can be found in Table 0-1 and Table 0-2 in the Appendix.

Table 3-6: Cost Estimate of PFS solution ref. 2018

Description	Unit	Production Stop [days]		
		11	90	180
Equipment & Installation	NOK	2 392 217 460	2 392 217 460	2 392 217 460
+ Project Management	NOK	239 221 746	239 221 746	239 221 746
+ Operating Cost PFS	NOK	232 800 000	232 800 000	232 800 000
+ Production stop	NOK	3 833 614 472	31 365 936 586	62 731 873 172
+ Energy Cost PFS	NOK	2 802 564 889	2 802 564 889	2 802 564 889
Total Cost PFS	NOK	9 500 418 567	37 032 740 681	68 398 677 267
- Operating Cost GT	NOK	- 585 800 000	- 585 800 000	- 585 800 000
- Gas Surplus	NOK	- 1 052 725 792	- 1 052 725 792	- 1 052 725 792
- CO_2 emission cost	NOK	- 3 659 371 380	- 3 659 371 380	- 3 659 371 380
Total Investment Cost	NOK	4 202 521 395	31 734 843 509	63 100 780 095
CO_2-emission reduction	ton	4 783 492	4 783 492	4 783 492
Abatement cost		**879**	**6 634**	**13 191**

The estimation is based on the assumptions stated under each section above. Taxes are not included, apart from the 78% tax of income with regards to saleable oil and gas. In addition, this cost estimate only covers the procurement and installation of the PFS system. All preparatory work both on- and offshore are neglected due to time restrictions and limited data.

Onshore investments would include land acquisition, buildings, connection to power grid, water supply and sewage as well as control and telecommunication facilities. Offshore preparatory work is explained in more detail under Modifications above.

Table 3-7 shows the abatement costs calculated for the different scenarios, ranging from 879 to 13 412 NOK/ton CO_2. Considering the Cost of CO_2-emission today is 765 NOK/ton CO_2, none of these scenarios are profitable purely from an economical point of view, although with a short production stop during the installation, the numbers come close.

Table 3-7: Summary Abatement Cost

Energy Prices	Production Stop [days]		
	11	90	180
2018	879	6 634	13 191
2019	961	6 717	13 274
2020	1 099	6 855	13 412

The big span of the abatement cost is due to uncertainties in future energy prices and production stop during installation. Variation in future energy prices is difficult to forecast, which leads to uncertainties regarding future investments.

The uncertainties regarding production stop would probably be smaller from a company's point of view, as they have access to much more detailed information than this thesis is based on. However, unforeseen circumstances do happen, which can lead to a longer period of production stop than first anticipated, and thereby a larger cost. This needs to be accounted for when doing risk analysis of future investments.

Previous Studies

The previous studies made by NPD and ConocoPhillips concluded with the abatement costs of 1 878 NOK/ton and 2 995 NOK/ton CO_2 reduced, respectively. Although 4 years separates these two studies, a gap of 1 117 NOK per ton CO_2 reduced, shows the big uncertainties associated with the cost estimates for this technology.

As this thesis' cost estimate vary greatly in size and is missing important numbers concerning onshore and offshore investments, the abatement cost from ConocoPhillips' study in 2012 are chosen for further comparison of alternatives for emission reduction on offshore installations.

3.4.6 Rating Table

Alternative	TRL	% CO_2-Emission Reduction	Efficiency Improvement	Abatement Cost	Comments
Gas Turbines	9	0%	0%	765NOK/ton	Base case
PFS	9	20.8%	34.5%	2 995 NOK/ton	Abatement cost from ConocoPhillips

Source

Power production for offshore installations can either happen onshore and be transmitted to the platform, as for PFS, or it can be generated offshore for direct use. Offshore power generation can further be split into two groups based on their source, namely renewables or fuel based. This refers to the second column in the alternative power production selection model for offshore installations. Chapter 4 will look closer at the renewable alternative for offshore power production, namely Floating Wind Turbines (FWT). A brief description of the structure and technology will be provided, in addition to areas of application. Lastly a general cost estimation for a floating wind park will be presented.

4 Floating Wind Turbines

Wind turbines was accountable for 4% of Norway's total power production in 2019, with 5.5TWh. It is expected for 16 new wind parks to be installed during 2020, raising Norwegian wind power production up to 11TWh a year [51]. Norway has enormous potential for wind power, as seen from Figure 4-1, which illustrates the annual mean wind speed in Norway. The figure clearly states the biggest potential for wind turbines to be offshore, with an average wind speed of over 11 m/s and large, unused areas.

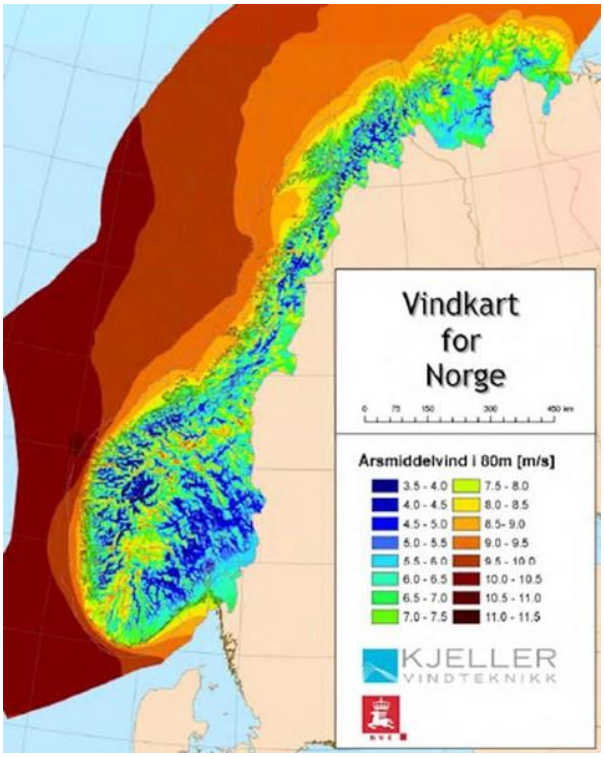

Figure 4-1: Average yearly wind speed in Norway [51]

A great number of offshore wind turbines has been installed along the costs of Europe in the last 20 years. In 2019 Europe had over 5000 offshore wind turbines with a total capacity of 22 072 MW, spread over 12 different countries [52]. The majority of these turbines are placed near the coastline in shallow water, with foundations that extend to the seabed. Even though the wind is much stronger further from the coast, the cost and technology were for a long time a limiting factor for harvesting wind power on deeper waters as it required usage of floating structures. Several pilot projects have been tested during the last 10 years, which are now being deployed throughout Europe.

6 floating wind farms, with a total capacity of 45 MW were installed as of 2019. Within the next 3 years this will expand to over 300 MW, with a series of new projects connecting to the grid, Norway's Hywind Tampen, among others [52].

The Hywind Tampen project consists of 11 floating wind turbines in the North Sea, located between Snorre and Gullfaks. Contrary to the other floating wind farms in Europe, who all delivers power to shore, Hywind Tampen will be the first wind farm in the world to provide electricity for offshore installations. With a capacity of 88 MW, it is assumed to cover at least 35% of the fields electricity demand per year, and cut CO_2 emission with 200 000 tons per year [53].

4.1 Technology

A wind turbine converts the kinetic energy from wind into electrical energy through a rotor and a generator. The wind turbines need to be placed up high both to reach the wind where it is strongest, and to be able to maximize the blade diameter. The size of the wind turbine and speed of the blades often increases when placed offshore compared to on land, as the restrictions for disturbance and geological footprint decreases considerably. Typical hight of offshore wind turbines is 180 meters, with a blade diameter of 160 meters [52].

4.1.1 Foundation

When moving the wind turbines from land to sea, the stability of the structure needs to be improved, to cope with both higher blade speed and to withstand high waves. In addition, the forward and backward rocking motion can ultimately cause a reduced power output, as it disrupts the path of the rotor blades, which also needs to be accounted for.

In shallow waters reaching up to 50 meters, the structure can be fixed into the seabed either as a monopile or a jacket/tripod. This would not be economical for waters deeper than 50 meters, so at this depth, the turbines are placed on floating structures moored to the seabed [54]. Figure 4-2 illustrates the four different foundations for floating wind turbines available today.

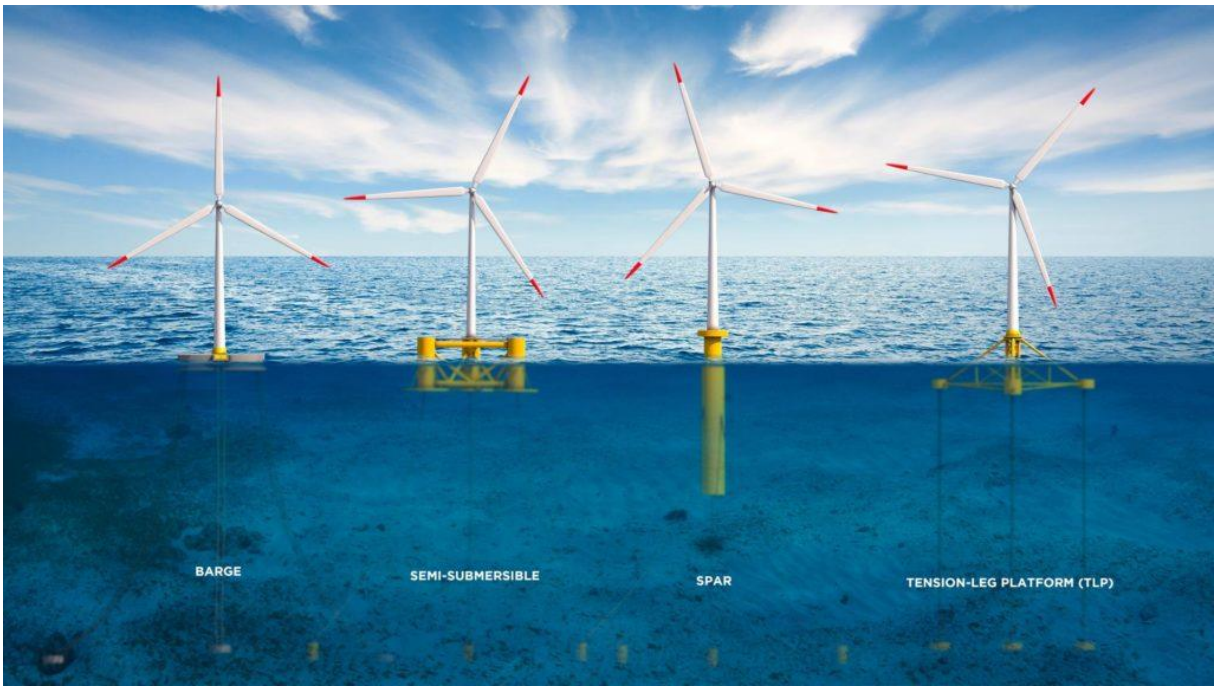

Figure 4-2: Foundations for Floating Wind Turbines [55]

The stability of floating wind turbines can be achieved in three different ways. The barge and semi-sub have a wide floater surface area and achieves stability through the equally distributed buoyancy force. A gravity-based stability is achieved when the center of gravity is as low as possible, and well under the center of buoyancy, as for the spar foundation. This technology requires waters deeper than 100 meters for the hull to be sufficiently submerged. Lastly the Tension Leg Platform (TLP) achieves stability through large external mooring forces, with stiff, vertical tethers [54].

4.1.2 Mechanical Components

Typical components in a wind turbine are illustrated in Figure 4-3. The blades, rotor and nacelle are located on top of the wind turbine tower. The nacelle contains the generator and all mechanical components required for power production. The blades are designed to catch the wind and turn the rotor. The rotor is further connected to a generator through a shaft, which in turns produces the electricity. For extreme conditions, with wind speed exceeding turbine design, a brake is activated for shutting the turbine down to avoid damage. The anemometer, controller, yaw -drive and -motor are components tasked with keeping the rotor perpendicular to the wind, for best possible utilization of the wind energy [56].

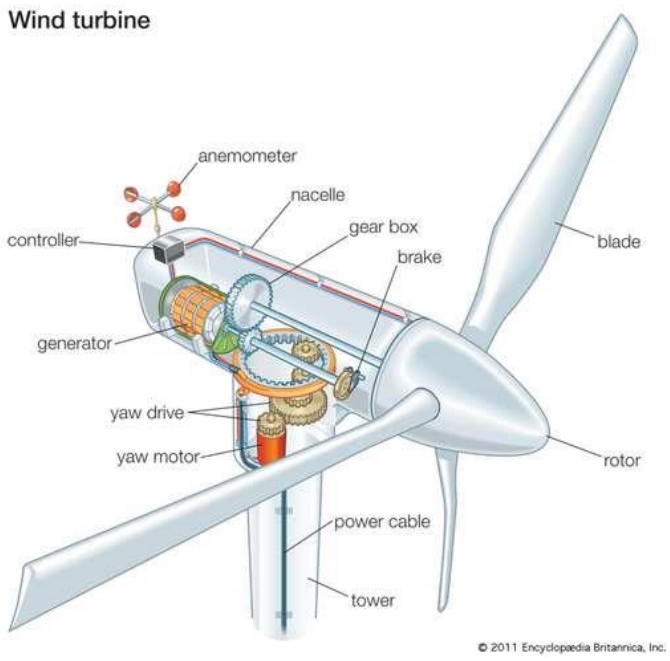

Figure 4-3: Typical Components of a Wind Turbine [57]

4.1.3 Wind Energy

The power of wind in a wind turbine can be broken down to the wind speed (U), the density of the air (ρ) and the area of blade disc (A), given by πr^2 where r is the length of a turbine blade, illustrated in Figure 4-4.

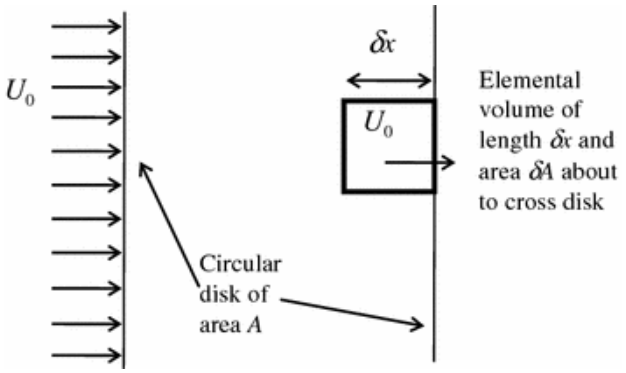

Figure 4-4: Wind flow past a circular disk representing the blades [56]

Given an elemental volume of air with length δx, area A and density ρ, its mass is given as $\rho A \delta x$ and its kinetic energy $KE = \frac{1}{2}\rho A \delta x U_0^2$. The time taken for the element to cross the blade disk δt, is given by $\delta x = U_0 \delta t$.

Total KE that passes the turbine blades represented by the disk in δt is symbolized as ΔKE and given by

$$\delta(\Delta KE) = \frac{1}{2}\rho A U_0 \delta t U_0^2$$

Summing over all elements and taking the limit as $\delta t \to 0$,returns

$$P = \frac{\delta(KE)}{\delta t} = \frac{1}{2}\rho A U_0^3 \quad (4.1)$$

P represents the total power of the wind energy and indicates that the power output depends on the cube of the wind speed. Output power of a wind turbine is in reality much lower, as capturing all of the wind energy hitting the blades would cause the wind to decelerate to rest, thereby stopping the turbine. A theoretical limit given by Betz' law, indicates the maximum power extracted from the wind to be 59% of the winds kinetic energy, this limit applies to all turbine designs. In *Introduction to Wind Turbine Technology* by David Wood, an assumption is made for 40% of the wind energy to be converted into electricity taking turbine performance, efficiency of drivetrain and generator and aerodynamic losses into account [56].

In addition to wind speed, wind resource surveys tend to specify the power density of the wind, meaning the flow of kinetic energy per swept area, denoted by Q with the unit W/m^2. The power density is expressed as

$$Q = \frac{P}{A} = \frac{1}{2}\rho U_0^3 \quad (4.2)$$

4.2 Application

The major downside to wind energy, as for most renewable energy, is the fact that the power production depends on the weather conditions. With no wind, the power production will stop until the conditions allow for it to start again. As of today, wind energy cannot be the only source of energy for an offshore installation. Instead it will work as an extra support when conditions allow for it.

A possibility for smoothening the energy profile from wind power, is battery storage. By charging up the batteries using the surplus of energy in windy periods, the batteries could deliver power in periods with no or little wind, instead of the back-up gas turbines, thereby preventing CO_2-emissions. Hydrogen production and storage through electrolysis is also an option, this will be described more thoroughly in Chapter 9.

A third possibility is to dedicate the power from the wind turbines to a consumer not in need for constant supply of energy, as for water injection pumps. With this application water will be injected only when the power supply from wind turbines is present, eliminating the need for gas turbines operating injection pumps. A short description of a wind powered water injection concept will be given in the subchapter 4.2.1 below.

4.2.1 WIN WIN

WIN WIN is a concept by DNV GL, which stands for WINd- powered Water INjection. The idea is a fully stand-alone system of a floating wind turbine which supplies power to a water injection process. In periods with low or no wind, a battery bank provides power for critical safety and communication functions. The concept will deal with all aspects of the water injection process, namely pumping the sea water to topside, filter the water down to specified qualities, treat the water with chemicals stored on board the fleet, and finally inject the water to the reservoir. The floating foundation of the wind turbine will be unmanned, and remotely controlled from the host platform of the field in question. The structure can also easily be moved from one location to another in case new injection wells are being drilled in order to replace former wells.

The WIN WIN concept is a good choice for fields and platforms with injection wells located far away from host platforms, or for fields with limited space and weight capacity on board their platforms.

System specification consists of a 6 MW wind turbine mounted on a spar foundation with 2 injection pumps of 2 MW each. Total injection capacity of the system is 80 000 bbl/day.

The case study was based on a reservoir with two injection wells, located 30 km from the production host at 200 meters water depth and a target injection rate of 44 000 bbl/day. The capital expenditure of the case study was estimated to be 697 million NOK and operating costs 44 million NOK/year [58].

WIN WIN is still in a developing phase. As of 2019 the concept had shown itself to be both cost efficient and technically feasible. As of today, the concept is ranked with TRL level 5 from Table 2-3, awaiting a prototype development [59].

The WIN WIN concept will not be studied as a possibility for GEA as their water injection volume amounts to over 500 000 barrels per day, requiring at least 7 floating wind turbines. Given the GEA's latest investment was made to a new subsea installation with 4 new injection wells in 2018, the sunk cost would be too high for the new concept to be profitable. Lastly, the relative shallow water depth of 70 meters would not be suitable for a spar foundation.

4.3 Floating Wind Turbines on GEA

As for the PFS system, replacing all power requirements on offshore installations with wind energy requires a lot of modification work, given the injection pumps and compressors operates on mechanical work. Wind power will therefore only be studied for the possibility of relieving the gas turbines generating electricity.

Previous studies by NVE in 2012 of wind strength and direction in the area indicates a mean wind speed of 10.5 m/s 100 meters above the surface, with a power density (Q) of 1 223 W/m^2 [60].

The water depth around GEA is similar to Scotland's Aberdeen Bay, where Kincardine Floating Offshore Windfarm are being developed with five 9.5 MW wind turbines installed on triangular-shaped semi-submergible foundations. The rotor blade diameter is 164 m, which gives a swept area of 21 124 m^2 per turbine. [61].

These foundations will be the basis for the estimations regarding offshore wind turbines at GEA. The turbines chosen is the upgraded version of Kincardine's turbines with capacity of 10 MW. The diameter and rotor swept area is the same [62]. 4 units with a total power capacity of 40 MW will be studied as an alternative to gas turbines producing electricity.

The turbine has a guaranteed lifetime of 25 years [62]. Platform, moorings and anchors are expected to last for 29, 26 and 31 years respectively [63]. Based on this data, the floating wind turbine system is expected to deliver power to GEA until 2045.

4.3.1 Energy Calculation

From Equation (4.1) and (4.2) the average power of wind hitting the turbines at GEA is

$$P = Q \cdot A = 1\,223\ {}^{W}/_{m^2} \cdot 21\,124\ m^2 = 25\,834\,652\ W = 25.83\ MW$$

With a turbine efficiency of 47.4%, theoretical power output from the turbine is

$$P_{Output} = 0.474 \cdot P = 0.474 \cdot 25.83MW = 12.24\ MW$$

The maximum capacity of the wind turbine is 10 MW, the power output cannot exceed this, but it proves the wind in the area to be strong enough to supply GEA with the necessary power on an average basis. The wind turbines would be considered to relieve the gas turbines producing electricity on the GEA. The power requirements would be the same as for PFS, namely 32 MW. Table 4-1 shows the gas consumption, energy production and CO_2-emission for the installation of 4 floating wind turbines. The gas consumption will however depend on the wind energy supplied and are expected to be greater in times with no wind, and lower in periods with higher wind speed. Either way, the numbers in Table 4-1 are assumed as average numbers, and will be the basis for further calculation of emission reduction and reduced gas consumption.

Table 4-1: Gas Consumption, Energy Production and CO_2-emissions for GEA with FWT

	Gas Consumption [Sm^3]	Energy Production [MWh]	CO_2-Emission [ton]	[%]
GEA Base	357 453 347	1 336 876	789 972	
GEA FWT	282 816 114	1 336 876	625 024	
Reduction	**74 637 233**		**164 948**	**20.88%**

4.3.2 TRL

Offshore wind turbine technology has been through extensive advancements for the past 10 years, with both higher power capacity and increased distance from shore. Wind power have never been supplied to offshore installations before, however the same technology is used for commercial offshore wind power, so the technology is rated with TRL 9 in Table 2-3.

4.3.3 CO_2-Emission Reduction

The CO_2-Emission Reduction for floating wind turbines would be the same as for PFS, as both options are without any CO_2-emissions and studied for replacement of the same amount of power generated by gas turbines.

The CO_2-emission reduction is calculated by Eq. (2.1) and (2.2), with the numbers from Table 4-1. Wind turbines produce power without any CO_2-emission, however, as the reduction potential only speaks to ~21% of the CO_2-emission generated from gas turbines, the remaining CO_2-emission must be included in the equation.

$$CO_{2_{PFS}} = \frac{625\,024\ ton}{1\,336\,876\ MWh} = 0.4675\ {}^{ton}/_{MWh}$$

$$\%\ CO_2\ emission\ reduction = -\frac{0.4675}{0.59} \cdot 100\% + 100\% = 20.8\%$$

4.3.4 Efficiency

Efficiency of a wind turbine is hard to determine, as it depends on the wind, and varies for different wind speed. Efficiency will in this context refer to the ratio between expected annual production from operator and annual production at full capacity, thus including capacity factor, losses, and turbine performance. To get a reasonable estimation of the efficiency, the expected production per year was compared to the maximum capacity for 5 different new offshore wind parks in Europe. The average number was taken to be the efficiency of wind turbines at GEA, namely 47.41%. Table 4-2 shows the selected offshore wind parks with their capacity and expected production.

Table 4-2: Average efficiency for floating wind parks

Floating Wind Farm	Year	Capacity [MW]	Ideal Production [GWh]	Expected Production [GWh]	Efficiency [%]
Hywind Tampen [64]	2022	88	770.88	384	49.81
Hywind Scotland [65]	2017	30	262.8	135	51.37
Kincardine [61]	2021	50	438	218	49.77
EolMed [66]	2022	24.8	217.25	100	46.03
Eoliennes Flottantes de Groix [67]	2022	28.5	249.66	100	40.05
Average					**47.41**

The efficiency of wind turbines is estimated to be 47.41% To calculate the total efficiency of power generation on GEA, the gas turbines driving the pumps and compressors would have to be included, as the electricity generation only represents ~21% of total power generated.

Total efficiency for power generation with wind turbines is then:

$$Efficiency = \ 0.2088 \cdot 47.41\ \% + 0.7912 \cdot 34.7\% = 37.35\%$$

Efficiency improvement compared to the simple cycle gas turbine is calculated from Eq. (2.5)

$$Efficiency\ improvement = \frac{37.35\% - 34.7\%}{34.7\%} \cdot 100\% = 7.6\%$$

4.3.5 Cost

Cost estimation for floating wind turbines on GEA is done with the basis in Carbon Trust' Report for the Scottish Government *Floating Offshore Wind: Market and Technology Review,* published in 2015 [63]. A detailed cost analysis was done for the prototype, pre-commercial, and commercial stage of the different floating turbine concepts, with a levelized cost of

energy (LCOE) approach, given in £/MWh. The cost was given in 2015 figures and will be converted to NOK with the average exchange rate of 2015. As the technology has matured since 2015, it is reasonable to assume cost will be lower for an installation done in 2020.

CAPEX

The analysis brakes down the capital expenditure (CAPEX) into 7 parts, where the turbine has the greatest share of 41%, followed by the platform with 22% of total expenditure. Balance of system includes the cost of electrical infrastructure (i.e. connection to grid, substations, cables) in addition to project development and managing

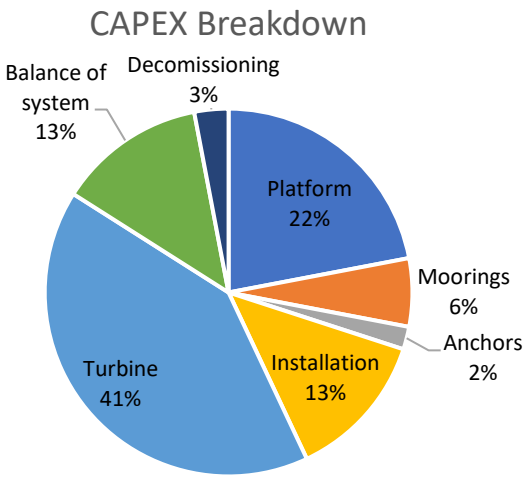

Figure 4-5: CAPEX breakdown for a floating wind farm

OPEX

Operational Expenditure (OPEX) for the different concepts was kept constant in Carbon Trust' report. Even though OPEX for semi-subs was assumed lower than for spar and TLP foundations, as the major repairs could be done more easily when the possibility of towing the full structure back to port is present. The annual operational expenditure for commercial floating wind turbines was given as 90 000 £/MW, or 1 110 735 NOK/MW.

LCOE

The levelized cost of energy combines the capital and operational expenditure, as well as yield, wind speed and power output, and returns the cost in £/MWh. With greater wind speed, the LCOE is reduced, as more power is generated.

The expected lifetime of the system is 25 years, meaning the total energy generated by the turbines would amount to 8 760 GWh assuming they operate at full capacity.

For a commercial, floating wind turbine with semi-sub foundation and an average wind speed of 10.5 m/s, the LCOE is estimated to be 84 £/MWh or 1 037 NOK/MWh. Total cost for floating wind system with capacity of 40 MW for 25 years amounts to 9 081 MNOK, as illustrated in Table 4-3.

Table 4-3: Total Cost of Floating Wind Turbine System

Description	Quantity	Unit
LCOE	1 037	NOK/MWh
Total Production	8 760 000	MWh
Total Cost	9 081 369 360	NOK

Gas Turbines

From Table 4-1, the average reduction in gas consumption due to power supply from wind turbines is close to 75 million Sm^3 per year, which further reduces the CO_2-emissions with nearly 165 000 tons per year. With the average price of gas for 2018 and cost of CO_2, an extra income of 4 billion NOK is generated.

The annual operational cost for gas turbines of 20.2 million NOK per year [15] cannot be eliminated completely, as GEA cannot rely on wind power alone. But an assumption is made for this operational cost to be cut in half, as the use of gas turbines generating electricity will decrease considerably.

Expected savings and income related to reduced use of gas turbines are shown in Table 4-4 below.

Table 4-4: Expected savings and income related to gas turbines

Description	Quantity	Unit	Price [NOK/unit]	Operating years	Total income
Excess Gas	74 637 233	[Sm3]	2.21	25	907 215 567
CO_2	164 948	[t]	765	25	3 154 630 500
Operational cost	10 100	[kNOK/y]	10 100 000	25	252 500 000
Total					**4 314 346 067**

Abatement Cost

The abatement cost is calculated with the formula

$$\frac{Total\ investment\ cost\ of\ FWT - Operating\ cost\ of\ gas\ turbines\ incl.\ CO_2\ cost}{CO_2\ emission\ reduction\ for\ expected\ lifetime}$$

Total estimated cost of installing floating wind turbines on GEA, including the abatement cost is summarizes in Table 4-5 below.

Table 4-5: Cost estimate of floating wind turbines

Description	Unit	Cost
Total Cost FWT	NOK	9 081 369 360
Expected savings from GT	NOK	4 314 346 067
Total Investment Cost	NOK	4 767 023 293
CO_2 emission reduction	ton	4 123 700
Abatement cost	**NOK/ton**	**1 156**

The abatement cost amounts to 1 156 NOK/ton CO_2 reduced, for a floating wind park with a lifetime of 25 years. As the cost is higher than the cost of CO_2, the investment would not be profitable from an economical point of view alone. It will however reduce the CO_2-emission

from GEA with 4.1 million tons over 25 years with the additional cost of 391 NOK per ton CO_2 compared to the conventional gas turbines.

The capital and operational expenditure are given on a general basis and not specified for turbines connected to GEA. In addition, the cost is given in 2015 figures, and due to inflation, the numbers will be somewhat higher today. From a technological point of view, the floating wind turbine expertise has matured since 2015, which will have a positive effect on today's cost, making it lower than first estimated. Taxes are neglected in the calculation, except for the estimated 78% tax of income from saleable gas. Necessary modifications on the platforms for preparation of receiving power from wind turbines are also overlooked in the calculation, due to limited resources and time.

The abatement cost of 1 156 NOK/ton CO_2 is therefore given with a high level of uncertainty, and the possibility of it being higher or lower than calculated in this thesis is great. It will however serve as a sufficient comparison towards other options for reducing CO_2-emission on offshore installation, as the main focus is to look at the CO_2-emission reduction potential for different power alternatives.

4.3.6 Rating Table

Alternative	TRL	% CO_2-Emission Reduction	Efficiency Improvement	Abatement Cost	Comments
Gas Turbines	9	0%	34.7%	765 NOK/ton	Base case
FWT	9	20.8%	7.6%	1 156 NOK/ton	

Power Generation

By choosing a fuel-based source for power production, several different engines and process are available for power generation, the conventional simple cycle gas turbine being one of them. In the power production selection model, the column Power Generation will present two alternative combustion processes, the Combined Cycle in Chapter 5 and HAT cycle in Chapter 6. Chapter 7 will cover fuel cells, which produces power through electro-chemistry rather than combustion. Chapter 8 is a presentation of energy efficiency measures, which when implemented on the present simple cycle gas turbine, contribute to emission reduction without extensive new investments or machinery.

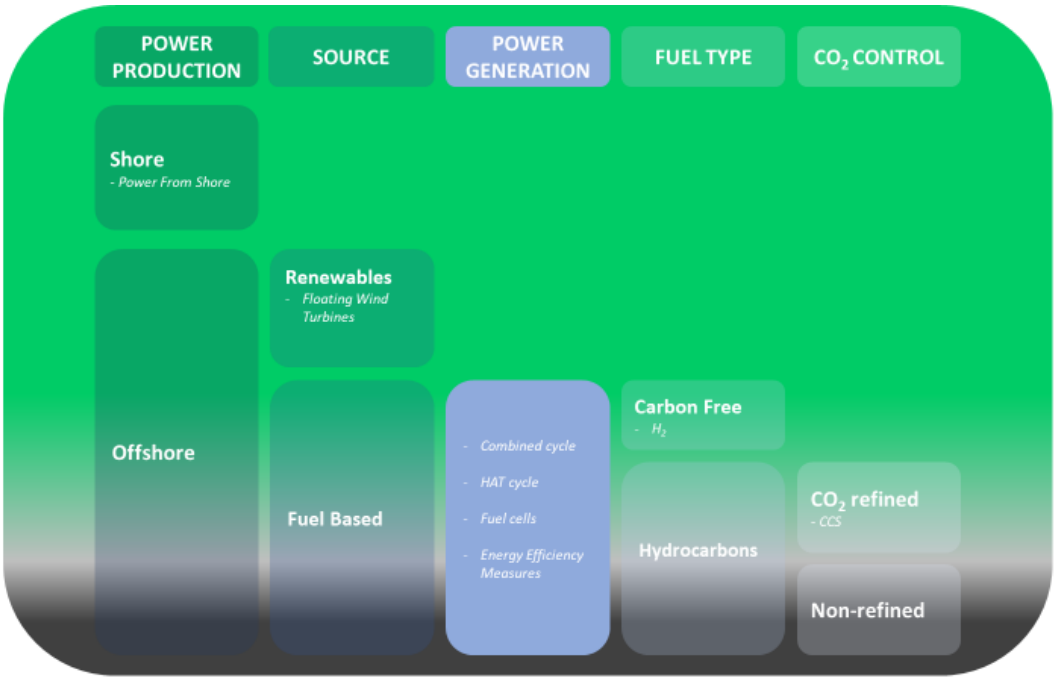

5 Combined Cycle

A combined cycle refers to two power cycles being connected in one plant. The most common combined cycle plant consists of a gas- and a steam cycle, connected through a Heat Recovery Steam Generator (HRSG). The gas turbine, referred to as the top cycle, burns fuel and generates exhaust gas of high temperature. This gas is expanded in a turbine to create mechanical work. The remaining thermal energy in the exhaust gas is recovered in a HRSG to generate steam, and further expanded in the steam turbine which makes up the bottoming cycle, to generate additional power [68]. See Figure 5-1 for illustration of a simple, combined cycle.

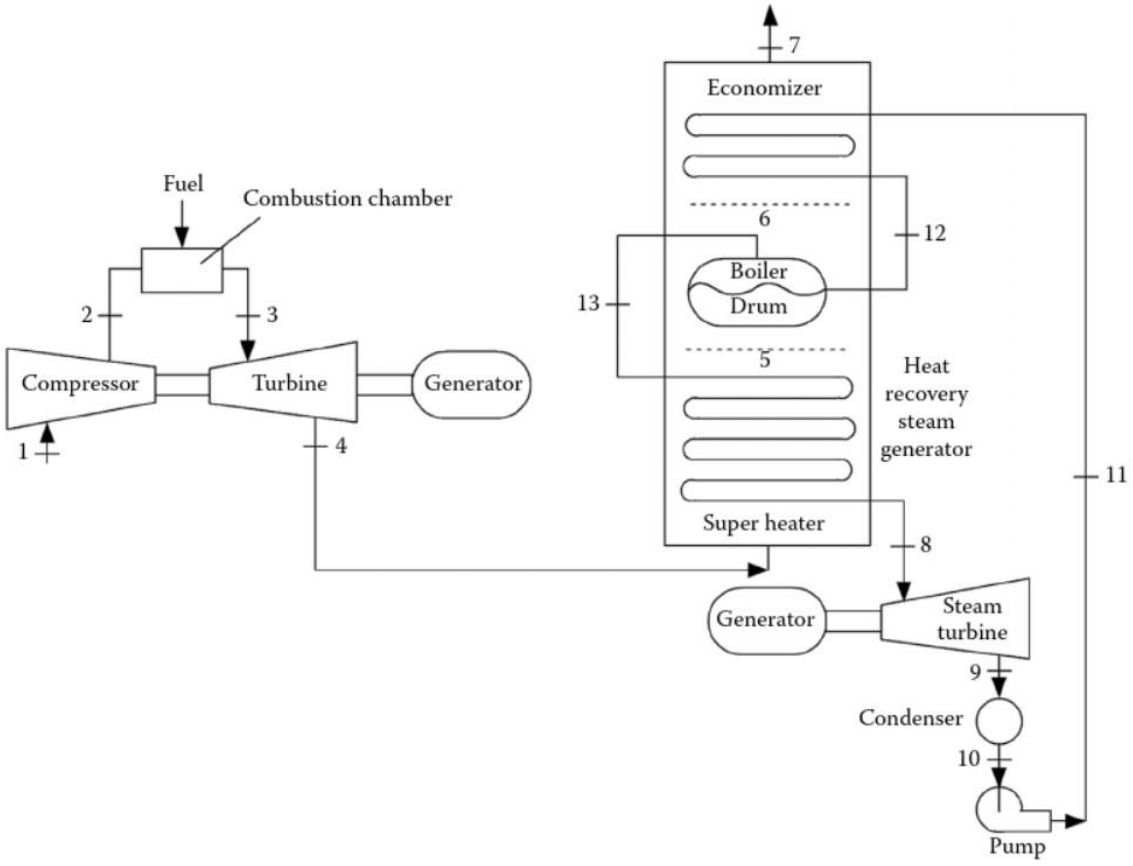

Figure 5-1: Combined cycle gas and steam turbines [69]

Due to weight limitations on offshore installations, combined cycles are scarcely implemented. The cycles are both bulky and heavy, the main contributor being the HRSG. For a combined cycle to be installed offshore, the HRSG needs to be both smaller and lighter, which reduces the efficiency to a maximum of 50%, compared to 64% on shore [70, 71]. Still

much more effective than a conventional, simple cycle gas turbine, the power demand, heat surplus and weight limitations on the offshore installation are the limiting factors deciding of whether or not to install it.

5.1 Technology

This subchapter will cover the three different systems in the combined cycle. As the gas turbine already have been introduced in Chapter 2.3, a brief summary will be provided in addition to a more detailed description of the components and the thermodynamic processes.

5.1.1 Gas Turbine

A simple gas cycle consists of a compressor, a combustion chamber, and a turbine/expander. Figure 5-2 illustrates the components of a simple ideal gas cycle, along with the TS- and PV-diagram for the thermodynamic processes.

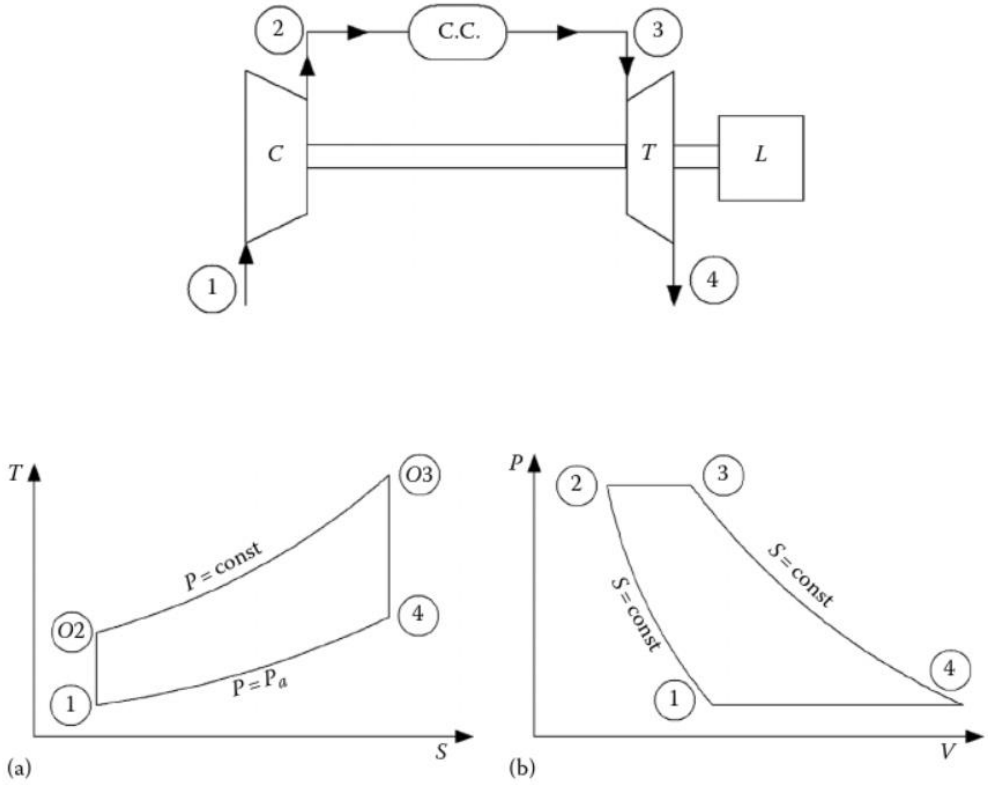

Figure 5-2: Simple cycle gas turbines, components, TS and PV diagram of cycle [69]

1: Air Inlet

The air inlet sucks air from nearby area and delivers it to the compressor at ambient values. $T_1 = T_a$, $P_1 = P_a$, $\phi_1 = \phi_a$. Where ϕ is the humidity.

2: Compressor

Fresh air is drawn into the compressor, where temperature and pressure increase in an isentropic compression process, giving:

$$\frac{T_2}{T_1} = \left(\frac{P_2}{P_1}\right)^{(\gamma-1)/\gamma} = \pi_c^{(\gamma-1)/\gamma} \tag{5.1}$$

Where $\gamma = {C_p}/{C_v}$ is the ratio of the specific heat values at constant pressure and volume of the ideal gas, and π_c is the pressure ratio $\frac{P_2}{P_1}$ [69].

The specific work for the compressor is:

$$W_c = C_p(T_2 - T_1) = C_p(T_2 - T_a) = C_p T_a \left(\pi_c^{(\gamma-1)/\gamma} - 1\right) \tag{5.2}$$

3: Combustion Chamber

High pressure air enters the combustion chamber where fuel is burned at constant pressure. The combustion process releases the chemical bound energy in the fuel, under formation of the emission gases CO_2, H_2O, Nitrogen Oxide (NO_x) and Carbon monoxide (CO). The combustion temperature influences the amount of NO_x and CO. High combustion temperatures generates NO_x, and low temperatures produces CO as a result of incomplete combustion. The combustion chamber must be compact and distribute the temperature evenly over the turbine inlet. The chamber must also allow for cooling, to protect the material from overheating [22, 69].

The heat added per unit mass flow in the combustion chamber is:

$$Q_{in} = h_3 - h_2 = C_p(T_3 - T_2) \tag{5.3}$$

4: Turbine

The high temperature gases generated in the combustion chamber enters the turbine, where they undergo an isentropic expansion process [69]. The temperature of the exhaust gases leaving the turbine range between 450-650°C [22]. For an ideal process, $P_2 = P_3$ and $P_4 = P_1$, giving:

$$\frac{T_3}{T_4} = \left(\frac{P_3}{P_4}\right)^{(\gamma-1)/\gamma} = \left(\frac{P_2}{P_1}\right)^{(\gamma-1)/\gamma} = \pi_c{}^{(\gamma-1)/\gamma} \tag{5.4}$$

The specific work generated from the turbine is:

$$W_T = C_p(T_3 - T_4) = C_p T_3 \left(1 - \frac{1}{\pi_c{}^{(\gamma-1)/\gamma}}\right) \tag{5.5}$$

5: Gas cycle

The net specific work of the cycle delivered to the load is then:

$$W_{net} = W_t - W_c = C_p(T_3 - T_4) - C_p(T_2 - T_1) \tag{5.6}$$

Finally, the thermal efficiency of an ideal, simple gas cycle can be expressed as:

$$\eta_{th} = \frac{W_t - W_c}{Q_{in}} = 1 - \frac{C_p(T_4 - T_1)}{C_p(T_3 - T_2)} = 1 - \frac{T_1\left(\frac{T_4}{T_1} - 1\right)}{T_2\left(\frac{T_3}{T_2} - 1\right)} \tag{5.7}$$

Given the processes 1-2 and 3-4 is isentropic, $P_2 = P_3$ and $P_4 = P_1$. Using Eq. (5.1) and (5.4), the equation above (5.7) can be simplified to:

$$\eta_{th} = 1 - \frac{1}{\pi_c{}^{(\gamma-1)/\gamma}} \tag{5.8}$$

Where $\pi_c = \frac{P_2}{P_1}$ [69].

5.1.2 HRSG

The exhaust gases from the turbine in the gas cycle is further directed to the HRSG for steam generation. In a combined cycle, the HRSG is the largest and heaviest constituent, as the steam production is directly linked to the heat transfer area within the generator. The HRSG typically consists of 3 sections: economizer, evaporator, and superheater. Figure 5-3 shows a single pressure HRSG and the T-Q diagram for the thermodynamic process.

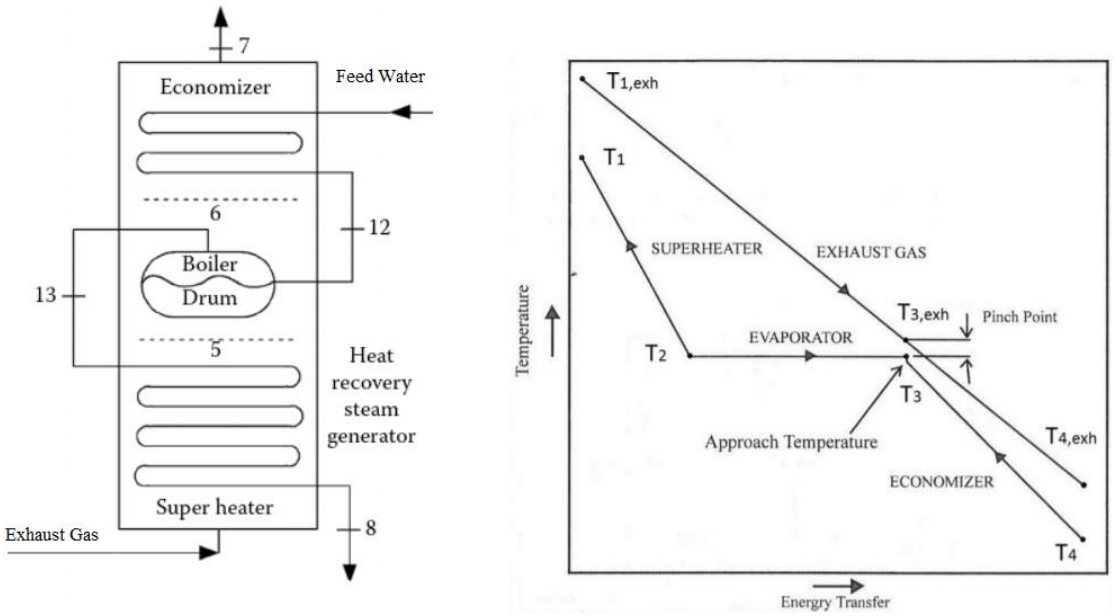

Figure 5-3: Components and T-Q diagram for a single pressure HRSG [68, 69]

The feed water is pumped into the economizer where it is heated to a temperature close to saturated condition. The liquid evaporates at constant pressure and temperature in the evaporator, before entering a drum where separation of the remaining water and steam takes place. The water is recirculated to the evaporator, and the dry steam is delivered to the superheater. The superheater heats the steam into required temperature for the steam turbine [22].

The temperature difference between water and exhaust gas should ideally be constant through the entire process to minimize the energy loss, but because the liquid evaporates at constant temperature, this is not the case. The pinch point temperature is the minimal temperature difference between the feed water and exhaust gas and occurs at the inlet of the evaporator. Typical values for onshore systems are 8-12 °C, and up to 35 °C for smaller scale where cost and weight limitations are important. The approach temperature is the

difference between economizer outlet and saturation temperature. If this was set to zero, steaming in the economizer could occur, leading to blockage of flow and saturation in the economizer [68].

The efficiency of a HRSG, η_{HRSG} can be expressed as the ratio of steam production to unused energy from the gas turbine [68]. The heat in the exhaust gas amounts to:

$$\dot{Q}_{exh} = \dot{m}_{fuel} \cdot LHV(1 - \eta_{GT}) \tag{5.9}$$

Where LHV is the lower heating value of the fuel. Steam production from HRSG is:

$$\dot{Q}_{HRSG} = \dot{m}_{exh} C_{p,exh} \left(T_{1,exh} - T_{3,exh}\right) \tag{5.10}$$

Finally, from Eq. (5.9) and (5.10), the efficiency of the HRSG is:

$$\eta_{HRSG} = \frac{\dot{Q}_{HRSG}}{\dot{Q}_{exh}} = \frac{\dot{m}_{exh} C_{p,exh} \left(T_{1,exh} - T_{3,exh}\right)}{\dot{m}_{fuel} \cdot LHV(1 - \eta_{GT})} \tag{5.11}$$

By implementing two or three pressure levels in the HRSG, more of the heat from the excess gases can be captured and the total efficiency of the combined cycle would increase. Adding pressure levels will however increase the size and weight of the HRSG [68].

5.1.3 Steam Turbine

In the steam turbine, superheated steam expands and drives a generator to produce electricity. The steam is further directed to a condenser, where it condenses back to water before being pressurized by a pump and finally delivered back to the HRSG [22]. Figure 5-4 shows the steam cycle and the TS-diagram for the process of the combined cycle pictured in Figure 5-1.

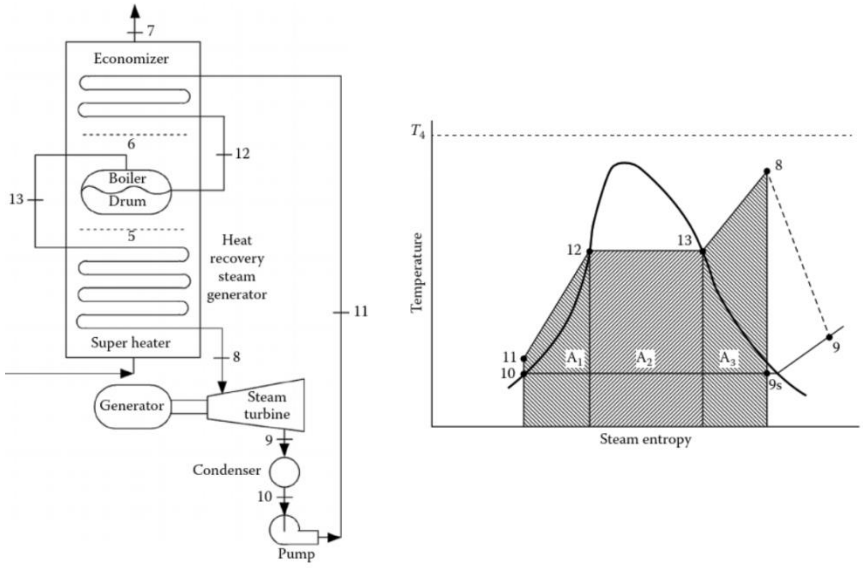

Figure 5-4: Components of the steam cycle with TS-diagram for the process [69]

The efficiency of the process depends on the HRSG, turbine and pump, and can be expressed as:

$$\eta_{ST} = \frac{\dot{W}_{out} - \dot{W}_{aux}}{\dot{Q}_{in}} \tag{5.12}$$

Where $\dot{W}_{aux}$ is the auxiliary power used for running the pumps, feed water etc [22].

5.1.4 Combined Cycle

The total power of the combined cycle is $W_{GT} + W_{ST}$, the gas turbine being the main contributor with about 60% of total power produced. The heat input is only from the gas turbine, and can be broken down to:

$$\dot{Q}_{in} = \dot{m}_{fuel} \cdot LHV$$

Where $\dot{m}_{fuel}$ is the fuel consumption and LHV the lower heating value of the fuel.

The electrical efficiency of the combined cycle can finally be express as:

$$\eta_{CC} = \frac{\dot{W}_{GT} + \dot{W}_{ST} - \dot{W}_{aux}}{\dot{m}_{fuel} \cdot LHV} \tag{5.13}$$

5.2 Combined Cycle Design on Offshore Installations

A study of optimization of combined cycles on offshore installations, with a special focus on the HRSG was done by Lars O. Nord and Olav Bolland at NTNU in 2012. The goal was to find the best design and performance of a combined cycle with limited space and weight capacity using process simulation. The study focused on a Once-Through heat recovery Steam Generator (OTSG) instead of a conventional HRSG, due to its compactness. The OTSG has no distinct sector for economizer, evaporator, and superheater. Instead, the OTSG uses a straight-through fluid path to produce wet steam, without the presence of a steam drum. With a once-through technology, water will only be circulated once and returned to the original environment. To avoid corrosion on the equipment, water needs to be free from salt and oxygen, among others. An offshore system would require a desalination plant for access to clean fresh water, in addition to a deaeration system to eliminate oxygen, carbon dioxide, argon and nitrogen from the water [70].

The study found that a once through technology with a single pressure level and a pinch point temperature of 25°C to be the best option for a combined cycle on offshore installations. The combined cycle net plant efficiency was found to be 51% with a power output of 42.9 MW. In comparison, the net plant efficiency of the onshore dual-pressure drum-type HRSG was estimated to be 53.8%. The weight of the HRSG was estimated to be 110kg, approximately 1/3 of the typical onshore HRSG [70].

5.3 Combined Cycle on GEA

The water injection platform, Eldfisk E has four 13.8 MW gas turbines dedicated for injection and one 22.7 MW for compression. The waste heat from three of these turbines (1x22.7 MW and 2x13.8 MW) is utilized by a bottom cycle steam turbine, with a maximum power output of 10.3 MW. The steam turbine is the main supplier of power for the entire field, in addition to the unmanned platform on Embla [72]. The steam turbine was installed in 1998 and upgraded in 2013 due to unstable operation and frequent use of the backup generator. The upgrade was done on the waste heat recovery system, to be able to cover exhaust heat from all four injection turbines (only two at a time) in addition to the compression turbine [73]. Figure 5-5 shows the flow diagram of Eldfisk steam power cycle.

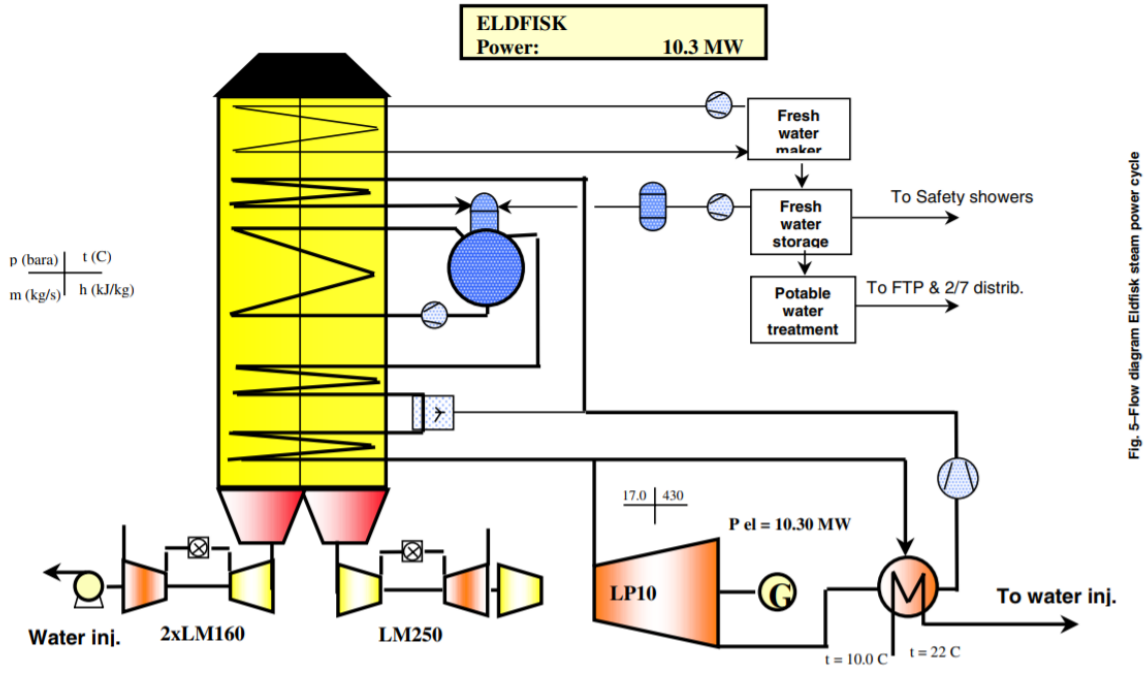

Figure 5-5: Eldfisk Steam Power Cycle [72]

The HRSG has three inlets for the three turbines and consists of four heat transfer zones. The economizer, evaporator and two superheating zones. Because of the varying power demand of the field, the HRSG produces 10% more steam than required from the steam turbine, to ensure control possibilities at load changes. The surplus steam is routed directly to the condenser via a bypass valve. To save energy, the condenser uses injection water instead of seawater as a cooling medium, eliminating the need for additional seawater lift [72].

5.3.1 Energy Calculation

Reduced fuel consumption due to steam bottoming cycle on Eldfisk E, compared to the simple cycle gas turbine solution, amounted to 23 million Sm^3 per year before upgrading the system [72], and 28.4 million Sm^3 per year after the upgrade [73].

To calculate the energy requirements of the combined cycle, the gas consumption, energy production and CO_2-emission table from 2018 is used. A scenario without the combined cycle in place is used for comparison, where 28.4 million Sm^3 is added to the total gas consumption, power generation stays constant. The results can be seen in Table 5-1 below.

Table 5-1: Gas Consumption, Energy Production and CO_2-emissions for GEA with and without combined cycle installed

	Gas Consumption [Sm^3]	Energy Production [MWh]	CO_2-emission [ton]	[%]
Gas Turbines	385 853 347	1 336 876	852 736	
Combined Cycle	357 453 347	1 336 876	789 972	
Reduction	**28 400 000**		**62 764**	**7 %**

With a CO_2-emission factor of 2.21, reduced CO_2-emission is 62 764 tons per year. The steam turbine began operation in the last quarter of 1999, since then the CO_2-emission reduction has accumulated to 1.1 million tons. With a life expectancy of the field to 2049, the steam turbine will contribute to a total of 2.9 million tons of CO_2 reduced

5.3.2 TRL

Combined cycle in commercial power plants is well known technology. It is not that common on offshore installations due to weight limitations. Studies for design optimization for combined cycles on offshore installations are being done, to make the alternative more attractive. As of today, combined cycles are installed on three different platforms on the NCS, proving the technology to be possible. Offshore combined cycles are therefore rated with TRL 9 from Table 2-3.

5.3.3 CO_2-Emission Reduction

The CO_2-emission factor for GEA with combined cycle installed is 0.59 ton/MWh. Had only simple cycled gas turbines been used on the fields, the CO_2-emission factor would have been:

$$CO_{2_{GT}} = \frac{852\,736\ ton}{1\,336\,876\ MWh} = 0.64\ {}^{ton}/_{MWh}$$

Calculated from Eq. (2.1) with numbers from Table 5-1.

The CO_2-emission reduction for the installed combined cycle can then be calculated from Eq. (2.2), and gives:

$$\%\ CO_2\ emission\ reduction = -\frac{0.59}{0.64} \cdot 100\% + 100\% = 7.81\%$$

5.3.4 Efficiency

The efficiency of the combined cycle on Eldfisk is taken as the average efficiency of the 5 gas turbines supplying the steam turbine with heat, listed in NPDs scheme of NO_x-taxable equipment [10]. The efficiencies for the turbines are given with the WHRU included, and net efficiency for combined cycle is calculated to be 40.53%. Table 5-2 gives the efficiencies and average of the five turbines.

Table 5-2: Efficiencies including WHRU for top cycle turbines on Eldfisk

Turbine	Operation	Efficiency [%]
LM – 1600	Injection	39.61
LM – 1600	Injection	39.61
LM – 1600	Injection	39.61
LM – 1600	Injection	39.61
LM – 2500 GJ	Compression	44.21
Average		**40.53 %**

Efficiency improvement is calculated from Eq. (2.5):

$$Efficiency\ improvement = \frac{40.53\% - 34.7\%}{34.7\%} \cdot 100\% = 16.8\%$$

5.3.5 Cost

No cost estimation for offshore combined cycles has been found online or in literatures. However, the average construction cost for combined cycle in US in 2017, was set to be 7 400 NOK/kW [74]. This cost is largely based on big industrial power plants, therefore the cost of a smaller offshore system, is assumed to be higher. With too high uncertainties and limited resources, cost estimations for offshore combined cycle would be purely speculative and are therefore chosen not to be studied any further.

5.3.6 Rating Table

Alternative	TRL	CO_2-Emission Reduction	Efficiency Improvement	Abatement Cost	Comments
Gas Turbines	9	0%	34.7%	765 NOK/ton	Base case
Combined Cycle	9	7.8%	16.8%	-	Cost estimate for offshore combined cycle has not been found

6 Evaporative Cycle

Evaporative cycles, or Humid Air Turbine (HAT) cycles, is an advanced gas turbine cycle with potential to reach similar efficiency figures as combined cycle plants. In the HAT cycle, water is evaporated into the compressed air before entering the combustion chamber, thereby reducing combustion temperature and the formation of NO_x. In addition, the increased mass flow expanded in the turbine has a positive effect on the thermal efficiency of the cycle [75].

Compared to the combined cycle, investment and operational costs is lower, due to the avoidance of the bottoming cycle. In addition, the fact that water is evaporated into the air stream (rather than boiling steam), lower water qualities can be used and the control of the process is much easier compared to combined cycle, since the humidification is self-controlled.

6.1 HAT cycle

Figure 6-1 shows a HAT cycle with two stages of compression and humid air as a working fluid.

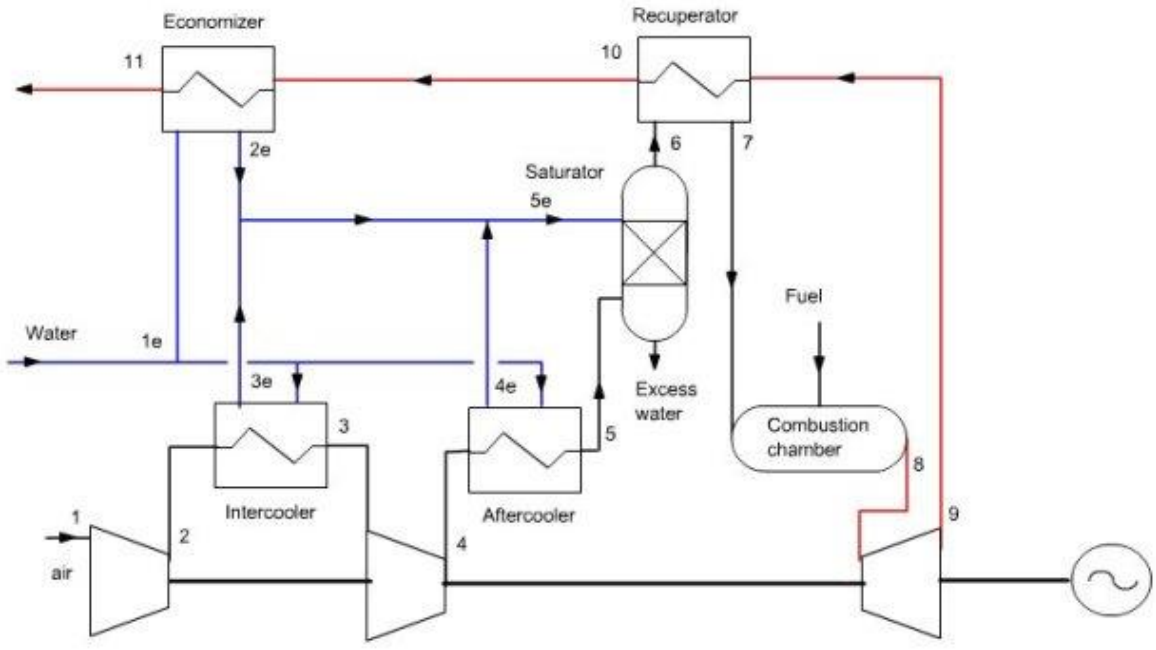

Figure 6-1: The Humid Air Gas Turbine Cycle [76]

In the cycle presented in Figure 6-1, the intake air is compressed in two stages in a low-pressure- and high-pressure compressor (1-4), before entering a saturator where water

evaporates and mixes with the air to create humidified air (5-6). The relatively cold, humidified air is preheated in a recuperator by the exhaust gases from the turbine (6-7), before entering the combustion chamber. In the combustion chamber, the hot, humidified air participates in combustion of natural gas (7-8) and the exhaust gas is expanded in the turbine (8-9) driving a generator to produce electricity. The exhaust gases heat up the humid air in the recuperator before it is directed towards the economizer for preheating of water entering the saturator (9-11). Water enters at 1e and is heated in either the economizer (2e), intercooler (3e) or aftercooler (4e) before being injected at the top of the humidification tower (5e). For a closed water loop, excess water not evaporated in the humidification tower is directed down to a mixing tank [76]. Due to evaporation of water in the cycle (which is leaving the power cycle via exhaust gas), new water must be added to the cycle to maintain the mass balance, this is known as makeup water.

Björn Nyberg and Marcus Thern at Lund University performed a thermodynamic simulation study on the HAT cycle and its components in 2011 [77]. They started off with simulations of a simple gas cycle, and step by step added components of the HAT cycle, to study the performance effect each part contributed with in the cycle. The efficiency increased from 36.5% in the simple cycle to 50% with all elements of the HAT cycle in place, and makeup water injected solely to the intercooler.

6.2 Key Components

This chapter is based on the thermodynamic study of the HAT cycle and its components by Nyberg and Thern and gives a description of each component in the HAT cycle.

6.2.1 Gas Turbine

The compressors, turbine and combustion chamber work by the same principle as for an ordinary gas turbine. However, modifications are required as standard GTs are designed for adjacent mass flow through compressor and expander, to balance the axial forces. Adding water after compression results in a larger mass flow rate through the expander, requiring a larger turbine than the standard one. Hence, the HAT cycle requires a more complex bearing setup to manage the mismatch of axial forces, which is yet to be developed in a commercial scale [78].

6.2.2 Intercooler

The intercooler is located between the two compressors. Discharge air from the low-pressure compressor enters the intercooler where cold water circulates to cool down the air in nearly isobaric conditions. When the temperature of the air decreases, the density increases. This lowers the compression work of the next compressor, and results in an increase of the total efficiency of the cycle. The energy absorbed by the water in the intercooler is brought back to the cycle via the humidification tower [77].

6.2.3 Aftercooler

The aftercooler is placed after the high-pressured compressor in the cycle and serves as a heat exchanger for water and dry air in preparation for the humidification tower. The specific work of the cycle is increased by the aftercooler, as the performance of the humidification tower increases, see Chapter 6.2.4, below. The efficiency of the cycle increases also, as the exiting temperature of the humidification tower decreases, enabling a higher heat exchange in the recuperator [77].

6.2.4 Humidification Tower

The humidification tower is the key component in the HAT cycle. The purpose of the tower is to increase the water content in the air passing through it, by use of simultaneous heat and mass transfer. Figure 6-2 shows the schematic of a humidification tower with its constituents.

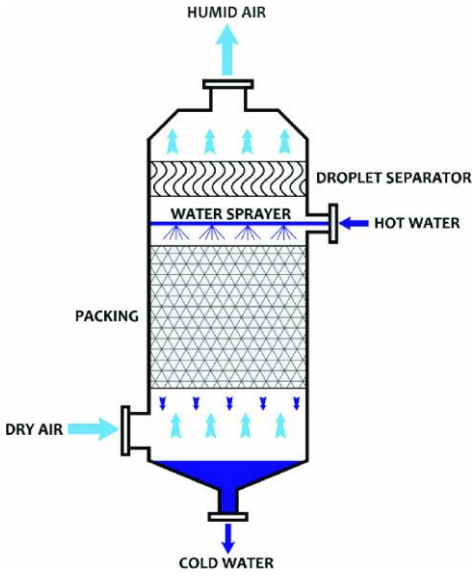

Figure 6-2: Schematic of a packed bed humidifier [79]

Dry, cooled air is injected at the bottom of the tower, and hot water is sprayed in through nozzles at the top. The packing ensures good contact between the air rising up and water running down, resulting in a large amount of the liquid evaporating into the gas stream. The evaporation in the tower is due to a natural driving force, being the temperature difference between the air and water. Here is where one can see the effect of the aftercooler. Without the prior heat exchange, the air would have been warmer than the water, resulting in condensing of air rather than evaporation of water, reversing the desired process [75].

The exiting humidified air will operate close to the saturation line, as the partial pressure of the vaporized liquid in the stream gets higher and higher, with the increased humidification of the air, resulting in an increased boiling point [75].

A droplet separator at the very top of the tower separates droplets from the exiting humidified gas stream, to avoid corrosion in the recuperator. The droplet separator works according to the density principle, i.e. the inertia difference between water and gas in the stream [80].

The humidification tower will also work as a distilling tower, as impurities in the water stream will be left in the ejected liquid flow exiting at the very bottom of the tank. Liquid soluble impurities will also be scrubbed out of the gas stream, resulting in the humid air exiting the tank being cleaner than both the air and water entering the humidification tank [75].

A pressure-drop of the water sprayed from the nozzles is expected and is compensated for by a water circulation pump. The pressure drop does not however, have a negative effect on the total efficiency of the HAT cycle, as the effect of lower compression work due to water circulation outweighs the work required by the pump [77].

The efficiency-increase of the cycle due to the humidification tower is explained by both the higher mass flow expanded over the turbine and a higher heat exchange in the recuperator. The humidification process lowers the temperature of the exiting fluid, thereby increases the heat exchange of the recuperator [77].

6.2.5 Recuperator

The recuperator is a gas-to-gas heat exchanger, where compressed, humidified air is heated by exhaust gases from the turbine. With a higher temperature of the humid air entering the combustion chamber, less fuel is needed to achieve the desired combustion temperature, which increases the efficiency of the cycle, while decreasing NO_x Emissions. Utilization of exhaust gases increases the efficiency further [77].

6.2.6 Economizer

The economizer is the final heat exchanger of the cycle. Remaining heat from the exhaust gases after the recuperator, is used to pre-heat water directed to the humidification tower. The temperature-increase of the water benefits the performance of the humidification tower, yielding a higher power output. The efficiency of the cycle increases too, due to a higher utilization of the exhaust gases [77].

6.2.7 Makeup Water

As water evaporates during the cycle, makeup water must be added to maintain the mass balance of the system. The makeup water can be injected in either of the three gas-to-water heat exchangers. Studies done at Lund University have found the temperature of the makeup water to be of importance for the total efficiency of the cycle, as well as the injection point. A lower temperature has a positive effect on the heat exchanged but decreases the mass flow of water into the humidification tower. The improved heat exchange has a positive effect on the total efficiency, and the decreased mass flow a negative effect. For two of the three heat exchangers, the latter dominates, resulting in a decreased total efficiency. For the intercooler however, the decreased compression work due to higher heat exchange, outweighs the negative effect of mass flow to the humidification tower, hence total efficiency of cycle is improved [77].

6.2.8 Flue Gas Condenser

A flue gas condenser installed after the economizer chills the gases in order to extract water and recover the remaining heat. The water can be reused as makeup water after being demineralized, and the heat can be utilized for district heating purposes, increasing the total efficiency of the cycle even further [80].

6.2.9 Carbon Capture

After the flue gas condenser, the CO_2-concentration in the remaining exhaust gases will be higher than in a GT of combined cycle, making the HAT cycle a suitable candidate for carbon capture. The concentration is higher due to part of the air being effectively replaced by steam within the cycle. Carbon capture will be studied further in Chapter 10.

6.3 Footprint

In Torbjörn Lindquist' doctorate, *Evaluation, Experience and Potential of Gas Turbine Based Cycles with Humidification,* a comparison of a mid-sized power plant of simple cycle, combined cycle and evaporative gas turbine (EvGT) cycle are presented. The electrical efficiency, footprint and power output can be found in Table 6-1. For an offshore installation where high-power to weight ratio dominates, the HAT cycle stands out as the best option for power generation with an electrical efficiency of 56% and a power output of 0.14 MW per square meter.

Table 6-1: Efficiency, Footprint and Power Output of Mid-Sized simple cycle, combined cycle and EvGT

Cycle	Electrical Efficiency [%]	Area [m^2]	Power Output [MW]	PO/Area [MW/m^2]
Simple Cycle	38.2	200	41	0.21
Combined cycle	55.6	800	60	0.075
EvGT	56.0	600	83	0.14

6.4 Advanced HAT cycle

In 2004 Hitachi began developing the Advanced HAT system (AHAT). The main difference in the advanced cycle is the use of Water Atomization Cooling, or an inlet air fogging, instead of an intercooler. Small droplets of water are sprayed into the inlet airflow to cool the air by evaporation. The cool air is denser, and increases the mass flow into the compressor,

thereby lowering the compression work. A Water Recovery System ensures for a near-zero make up water requirement. Figure 6-3 shows the schematics of the plant [81].

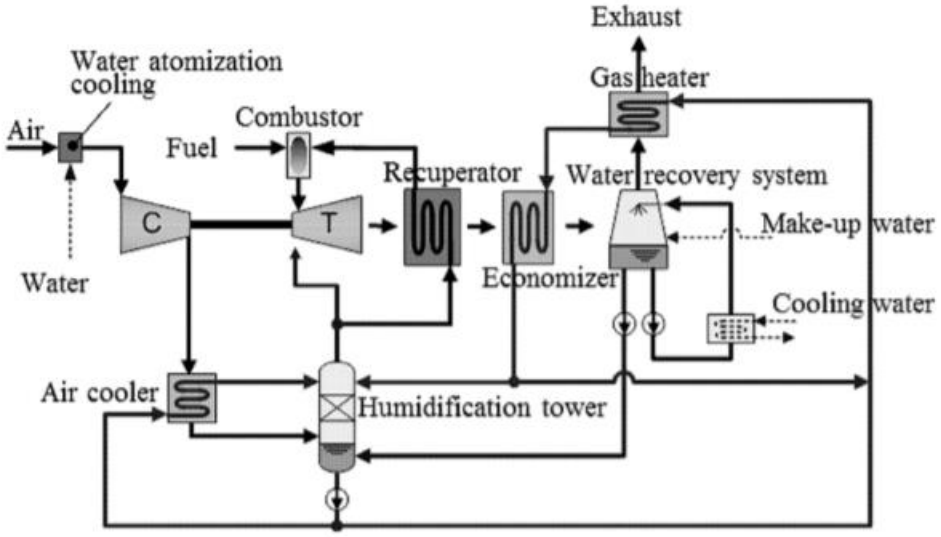

Figure 6-3: Schematic diagram of AHAT system [81]

In 2006 a 3 MW pilot plant proved the applicability of the system and flexibility with regards to load control. In 2008 phase II started, where the construction of a 40 MW full-scale power plant to investigate potential commercialization of such systems. The facility was completed in 2011, and tests started January 2012 to verify the practicability of the AHAT system further [81]. The tests verified that the key components of a medium class gas turbine can be applied to the AHAT system [82]. No update on the progress of development for commercialization has been found since 2014, however.

6.5 Humid Air Turbine on GEA

HAT cycles could be installed on GEA to increase the efficiency of the electricity generation. The plant is smaller and lighter compared to a combined cycle, and offers a higher total efficiency compared to the solutions for electricity generation on the GEA today, namely simple cycled gas turbines and a combined cycle.

The basis for calculations regarding HAT on GEA is taken from the simulation study *Techno-economic evaluation of the evaporative gas turbine cycle with different CO_2 capture options* by Yukun Hu et al. at the University of Stockholm [83]. The study takes basis in a LM1600PD

gas turbine with a capacity of 13.78 MW. The HAT-cycle performance was studied under the simulation tool Aspen Plus, where the calculated electrical efficiency was 52.1% and the CO_2-emission rate was 0.38 ton/MWh. Three different EvGT cycles are studied for their performance and cost, with two different CO_2-capture options, and one reference system without carbon capture. The reference study is what the calculations concerning HAT on GEA is based on.

6.5.1 Energy Calculation

The burn value of the fuel on GEA is 10.689 MWh/1000 Sm^3 fuel. With an efficiency of 52.1% and CO_2-emission factor of 0.38 ton/MWh, 1000Sm^3 of fuel would return 5.57 MWh and 2.12 tons of CO_2. The electricity demand on the field is still set to be ~21% of total energy demand, namely 280 GWh. Based on these numbers, a new gas consumption, energy production and CO_2-emission table were created for a scenario where the simple cycles and combined cycle generating electricity were exchanged for the HAT cycle.

Table 6-2: Gas Consumption, Energy Production and CO_2-emissions for GEA Humid Air Turbines

	Gas Consumption [Sm^3]	Energy Production [MWh]	CO_2-emission [ton]	[%]
Gas Turbines	357 453 347	1 336 876	789 972	
HAT cycle	332 931 599	1 336 876	729 486	
Reduction	**24 521 748**		**60 485**	**7.66%**

The CO_2-emission reduction of HAT cycle compared to simple cycle is 60 485 tons per year, representing a cost of 46.3 million NOK per year in terms of CO_2-fees and emission allowances. The excess gas would generate an extra income of close to 12 million NOK per year, calculated with the average gas price from 2018 of 2.211 NOK/Sm^3 and 78% tax.

As the HAT cycle make a good candidate for carbon capture, the emissions could be reduced even more. This will not be studied any further, however other options on carbon capture are reviewed in Chapter 10.

6.5.2 TRL

Proof of concept was demonstrated by Lindquist and Thern in 2002 with a non-intercooled HAT unit of 600 kW. A large-scale 40 MW AHAT system power plant was built in 2011 to verify the practicability of the system, however no news about progress on commercialization has been reported.

As of today, HAT power plants have not yet been commercialized. Two important points as to this is the water consumption in the cycle can be problematic and costly, depending on the availability of water at site. The recycled water needs to be condensed and cleaned for contaminants, increasing the complexity and cost. The HAT cycle also requires a suitable turbomachinery, to cope with the flow mismatch of the compressor and turbine due to the humified air, which is not developed yet [78].

With basis in Table 2-3, and Hitachi' 40 MW pilot unit, the technology is rated with TRL 5.

6.5.3 CO_2-Emission Reduction

The CO_2-emission factor for the HAT cycle is calculated from Eq. (2.1) with numbers from Table 6-2.

$$CO_{2_{HAT}} = \frac{729\,486 ton}{1\,336\,876\,MWh} = 0.55\,{}^{ton}/_{MWh}$$

With Eq. (2.2) the CO_2-emission reduction can be calculated:

$$\%\,CO_2\,emission\,reduction = -\frac{0.55}{0.59} \cdot 100\% + 100\% = 6.8\%$$

The total emission reduction of the field amount to 6.8% when the gas turbines producing electricity is replaced by humid air turbines.

6.5.4 Efficiency

The efficiency of the HAT cycle is set to be 52.1% from the base case. This is true for electricity generation only, which is ~21% of total power requirements. The gas turbines running compressors and pumps has an average efficiency of 34.7% and represents ~79% of the total energy production. Efficiency for total power generation is calculated to be:

$$Efficiency = 0.2088 \cdot 52.1\% + 0.7912 \cdot 34.7\% = 38.33\%$$

Efficiency improvement can be calculated from Eq. (2.5):

$$Efficiency\ improvement = \frac{38.33\% - 34.7\%}{34.7\%} \cdot 100\% = 10.5\%$$

6.5.5 Cost

Cost estimations will not be studied for the HAT cycle, as the low TRL offers too great uncertainties for final installation and operation cost estimations.

6.5.6 Rating Table

Alternative	TRL	% CO_2-Emission Reduction	Efficiency Improvement	Abatement Cost	Comments
Gas Turbines	9	0%	34.7%	765NOK/ton	Base Case
HAT	5	6.8%	10.5%	-	Too low TRL for cost estimations

7 Fuel Cells

Unlike the other alternatives for fuel-based power generation presented in this thesis, fuel cells produce electricity without direct combustion of the fuel. The power conversion is through electrochemical means, with an anode and cathode to provide positive and negative charge and an electrolyte layer to transport ions while blocking electrons, forcing them round in an external circuit, which produces electricity. Air and fuel such as natural gas or hydrogen is consumed to produce DC electricity in addition to by-products of heat, CO_2 and/or water. As each cell only produces a low voltage (~1V), the cells are placed in series linked together, forming a fuel cell stack. A fuel cell system is typically made up of the fuel cell stack, a DC-AC converter and a fuel reformer to produce hydrogen, if required [84].

Potential applications for fuel cells are broad, as the power range from µW in hearing aids to MW in grid-connected electricity production. Compared to gas turbines, fuel cells can deliver efficiencies of 60-80%, no noise pollution and reduced CO_2-emissions. The cells can even be designed to capture produced CO_2, thereby eliminating emissions completely [27]. Fuel cells on offshore installations have been evaluated for a long time but has not yet been implemented. This is because the fuel cells designed to operate on natural gas, which is the most convenient fuel offshore, operate on high temperatures. This further requires materials capable of withstanding excessive heat and the mechanical stresses linked to expansion with a rise in temperature. The increased cost and weight associated with these materials are problematic with respect to implementation on offshore installations.

7.1 Technology

Numerous different types of fuel cells are available on the market today, with different technologies for the components. Fuel cells are often divided into operation in low-, medium- and high- temperatures, in the range from 50°C to 1000°C. Low temperature operations often require clean hydrogen fuel, while higher temperatures allow for direct internal processing of more complex fuel such as natural gas. High temperature operations have the advantages of higher efficiency, less formation of CO and the opportunity to manage without the use of noble metals as catalysts, as the temperature alone provides a

sufficient reaction rate. The high temperature does however increase the size and weight of the system, as it requires heavy isolation.

Solid Oxide Fuel Cell (SOFCs) is an example of a high temperature operating fuel cell capable of operating on natural gas. On the low temperature end, the hydrogen operating Proton Exchange Membrane Fuel Cell (PEMFCs) is the most known and used fuel cell worldwide. The PEM cell is light and compact, as it was originally developed to be used in private cars. The size of a PEMFC compared to the SOFC is only 10% [85].

To be able to utilize fuel cells on offshore installations, a combination of the two fuel cells introduced above are being developed by Prototech AS. The new Clean Highly Efficient Offshore Power (CHEOP) system includes the two fuel cells, steam reformation, hydrogen membranes and heat transfer between the processes. The CHEOP-system, when commercialized, will be capable of delivering the same amount of power as a gas turbine, with higher efficiency and decreased CO_2-emissions, noise pollution and size [86].

The next subchapters will explain the technology behind SOFCs, PEMFCs and CHEOP more thoroughly.

7.1.1 SOFCs

Solid oxide fuel cells have a solid electrolyte as the name suggests. The ceramic electrolyte is conductive of the oxide anion O^{2-} at high temperatures. Air is supplied to the cathode where it is reduced to its ionic state and further conducted to the anode. At the anode oxygen ions react with the fuel (H_2 and CO) to produce water, carbon dioxide, heat and electrons. Lastly the electrons are pushed around the electrolyte in an external circuit to produce electricity [84]. Figure 7-1 shows the schematics of a solid oxide fuel cell.

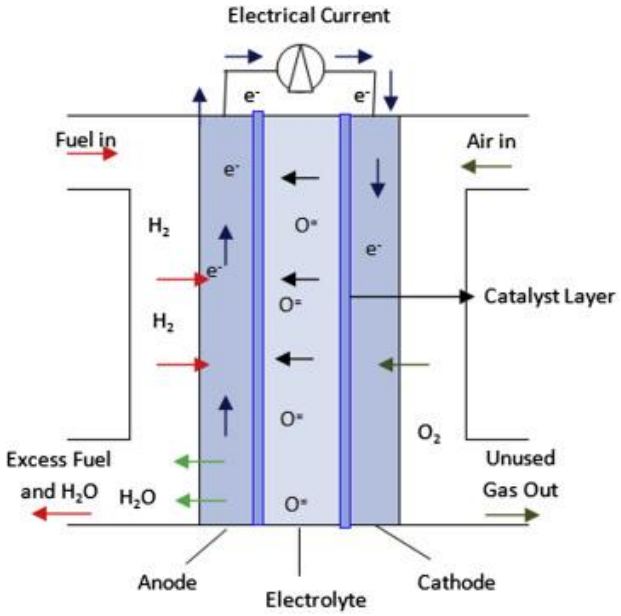

Figure 7-1: Schematics of a Solid Oxide Fuel Cell [87]

The reactions taking place in the cell are shown below [85].

Anode: $$H_2 + O^{2-} \rightarrow H_2O + 2e^- \quad (7.1)$$

Cathode: $$\frac{1}{2}O_2 + 2e^- \rightarrow O^{2-} \quad (7.2)$$

The high temperature in the cell allows for oxidation of carbon monoxide present in the gases from reforming of hydrocarbons. The oxidation contributes to even more electricity production from the cell, according to reactions below [85].

Anode: $$CO + O^{2-} \rightarrow CO_2 + 2e^- \quad (7.3)$$

Cathode: $$\frac{1}{2}O_2 + 2e^- \rightarrow O^{2-} \quad (7.4)$$

The cell can run on both natural gas and hydrogen fuel. Operating temperatures are typically between 800-1000°C, and efficiencies of over 60% are normal [84].

7.1.2 PEMFCs

The electrolyte in the PEM fuel cell is a thin permeable polymeric membrane. The cell operates on low temperatures of around 80°C and is therefore in need of catalysts to boost the reaction rate, placed on either side of the membrane. Within the cell, fuel is supplied to

the anode and split into H^+ ions and electrons. The protons pass through the membrane to the cathode, where they react with supplied oxygen to produce water. The electrons are diverted around the membrane in an external circuit to produce electricity [84].

The most effective operation of the PEMFC happens when the electrolyte is saturated with water, as the conductivity of the membrane depends on the degree of its hydration. If the temperature increases, the risk of dehydration occurs. Then the ionic resistance in the membrane will increase rapidly and the performance of the cell will suffer drastically. An excess of water will however cause flooding of the cell by blocking the pores and preventing gases from reaching the active layer between the electrolyte and electrodes. This too will result in a decreased performance of the fuel cell. Water management is therefore one of the greatest challenges associated with PEMFCs, and must be part of the design consideration, to ensure optimal efficiency and power output from the cell.

Figure 7-2 shows the schematics of a PEM fuel cell.

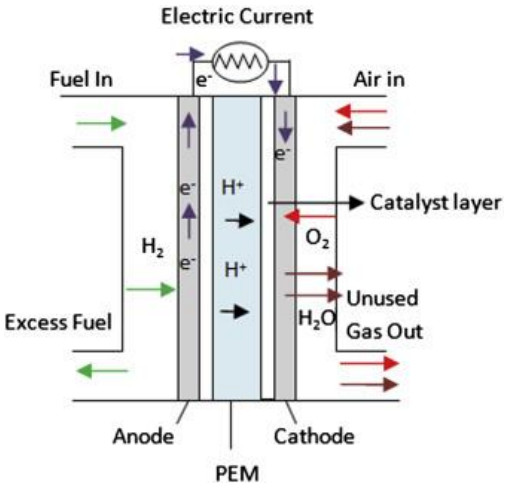

Figure 7-2: Schematics of a Proton Exchange Membrane Fuel Cell [87]

Reactions taking place at the anode and cathode are shown below [85].

Anode: $$H_2 \rightarrow 2H^+ + 2e^- \quad (7.5)$$

Cathode: $$\frac{1}{2}O_2 + 2e^- + 2H^+ \rightarrow H_2O \quad (7.6)$$

The PEMFC run on pure hydrogen, with efficiencies ranging between 40-60% [84].

7.1.3 CHEOP

The CHEOP system development started in 2015, with a goal to develop a compact 3 MW fuel cell stack with the size and weight equivalent of 1/10 of a 30 MW gas turbine, and further replace the gas turbine with the CHEOP-system containing 10 fuel cell stacks [27]. The system consists of the two fuel cells SOFC and PEMFC, a reformer with a hydrogen membrane and a heat recovery unit. Schematics of the system are shown below in Figure 7-3 [88].

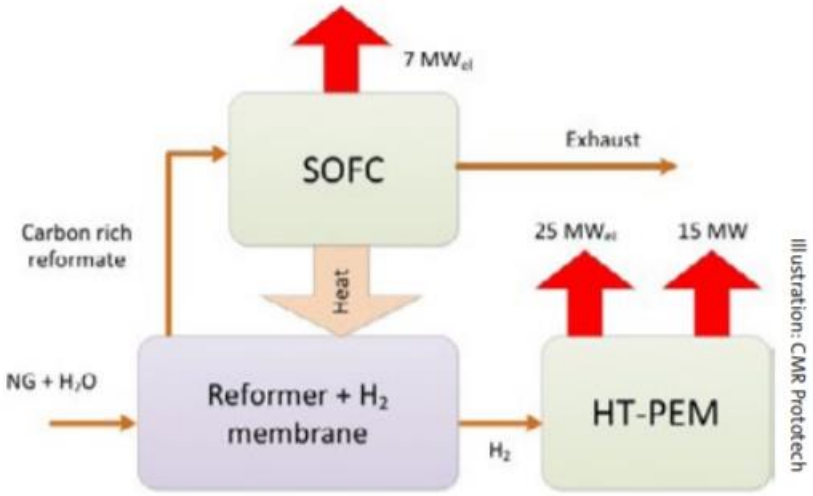

Figure 7-3: Schematics of a CHEOP system [88]

Natural gas and water enter the reformer and H_2 membrane, where CO and H_2 is produced and separated. The H_2 is further converted to electricity in the high temperature PEMFC of 180°C with total capacity of 25 MW. 15 MW of heat in the form of oil between 160-180°C are also produced from this cell. The CO from the reformer is directed towards the SOFC operating on 800°C. The high temperature allows for the carbon fuel to be oxidized as shown in Eq. (7.3) and (7.4), providing an additional power capacity of 7 MW. Lastly, the waste heat from the SOFC is recovered and utilized in the reformer. The remaining fuel from the SOFC is diverted out through an exhaust pipe and combusted [88].

An illustration of how the CHEOP module might look like is shown in Figure 7-4. A comparison of the CHEOP and a 32 MW gas turbine are shown in Table 7-1.

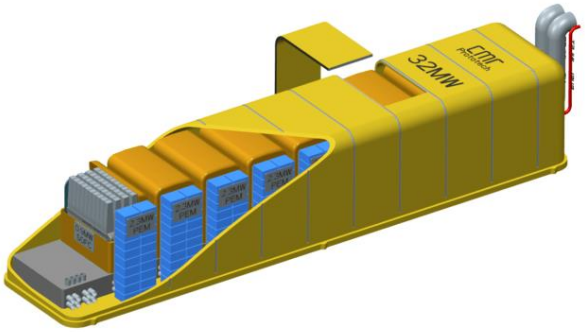

Figure 7-4: Illustration of the CHEOP module [86]

Table 7-1: Characteristics of a gas turbine and the CHEOP module [89]

Description	Gas Turbine	CHEOP Module	Unit
Power	32	32	MW
Weight	97	100	Ton
Volume	530	300	m^3
Efficiency	33	60	%
Noise	~87	Very low	DB

A simultaneous project is under development of a CHEOP Carbon Capture (CHEOP-CC) module, with an oxygen membrane at the cathode of the SOFC unit. This membrane will separate oxygen from the unused gas leaving the cathode, which will further be utilized in the final combustion of the unused fuel from the anode, i.e. an oxyfuel combustion. When the fuel is combusted with pure oxygen instead of air, the exhaust gases will only contain CO_2 and water, and the CO_2 can be separated by condensing and dehydration, further explained in Ch. 10.1.1 [90].

7.2 Fuel Cells on GEA

When commercialized, the CHEOP system would make a good alternative to the current gas turbines producing electricity at GEA. The CHEOP-modules will increase the efficiency of the power production, thereby reducing emissions, in addition to reducing the noise pollution. Combined with a carbon capture unit (CHEOP-CC), CO_2-emissions from power generation will be completely eliminated. CHEOP-CC will be studied further in Ch. 10.2.

7.2.1 Energy Calculation

The burn value of the fuel on GEA is 10.689 MWh/1000 Sm^3 fuel. With an efficiency of 60% and CO_2-emission factor of 2.21 kg/Sm^3, 1000Sm^3 of fuel would return 6.41 MWh and 2.21 tons of CO_2. Total energy requirement in 2018 was 1 337 GWh. The turbines producing electricity was accountable for roughly 21% of this (i.e. ~280 GWh). Based on these numbers, Table 7-2: Gas consumption, energy production and CO_2-emission for GEA with the CHEOP system installed was created. The case for CHEOP is split into two, as the fuel cell only covers the electricity production. The remaining energy required for mechanical work is still supplied by gas turbines.

Table 7-2: Gas Consumption, Energy production and CO_2-emissison for GEA with the CHEOP system

		Gas Consumption [Sm^3]	Energy Production [MWh]	CO_2-emission [ton]	[%]
Base Case		357 453 347	1 336 876	789 972	
CHEOP	*Electricity*	43 525 018	279 143	96 190	
	Mechanical	282 816 114	1 057 733	625 024	
Reduction		**31 112 215**		**68 758**	**8.7 %**

From Table 7-2, a reduction of 8.7% in total gas consumption and CO_2-emissions can be accomplished by implementing CHEOP. As the fuel cell system allows for integration of a

carbon capture unit (CHEOP-CC), the emissions could be even further reduced. The CHEOP-CC will be reviewed in Ch. 10.2.

7.2.2 TRL

Fuel cells in general are well known technology rated with TRL 9. The CHEOP technology, however, a combination of the SOFC and PEM technology, is still under development. The SOFCs has never been demonstrated in MW size before, and the process of enhancing power capacity while at the same time reducing its size is still undeveloped technology.

As of today, the project has reach phase 2 which will end with a 200kW fuel cell system for onshore testing. Phase 1 involved building and validating a SOFC stack of 10kW, in addition to designing the 32 MW system for future applications. The main focus of the current phase is to demonstrate the system in a sufficient size before scaling up even further in phase 3 [91]. As of today, the CHEOP technology is rated with TRL 3 from Table 2-3, while Prototech AS are currently working on reaching TRL 4 where the system will be validated in a laboratory environment.

7.2.3 CO_2-Emission Reduction

The CO_2-Emission Reduction is calculated by Eq. (2.1) and (2.2), with the numbers from Table 7-2. To get the emission reduction for all power generation on GEA, emissions from gas turbines producing mechanical work are also included.

$$CO_{2_{CHEOP}} = \frac{96\,190 + 625\,024\ ton}{1\,336\,876\ MWh} = 0.54\ ^{ton}/_{MWh}$$

$$\%\ CO_2\ emission\ reduction = -\frac{0.54}{0.59} \cdot 100\% + 100\% = 8.6\%$$

7.2.4 Efficiency

Electrical efficiency of the CHEOP-module is stated to be 60% and are accountable for ~21% of total energy production. The gas turbines producing mechanical work represents the remaining ~79% and have an average efficiency of 34.7%. Total efficiency for power generation becomes:

$$Efficiency = 0.2088 \cdot 60\% + 0.7912 \cdot 34.7\% = 40\%$$

Efficiency improvement compared to simple cycle gas turbines is then calculated from Eq. (2.5)

$$Efficiency\ improvement = \frac{40\% - 34.7\%}{34.7\%} \cdot 100\% = 15.2\%$$

7.2.5 Cost

As the CHEOP system is still in an early stage of development, with TRL 3, any cost estimation would include a lot of uncertainties as core components of the system has not yet been verified. Early estimations done by Prototech AS suggests the technology would be competitive to PFS financially, but this too is given with a high level of uncertainty [91].

7.2.6 Rating Table

Alternative	TRL	CO_2-Emission Reduction	Efficiency Improvement	Abatement Cost	Comments
Gas Turbines	9	0%	34.7%	765 NOK/ton	Base case
CHEOP	3	8.6%	15.2%	N/A	Too low TRL for cost estimations

8 Energy Efficiency Measures

This chapter will cover small energy measures already taken by ConocoPhillips on GEA to increase efficiency of power generation. The measures do not involve any new technology or expensive investments, but rather describes small actions taken with the existing power solution to save energy, and thereby reduce emissions.

Five different examples of energy efficiency measures are provided, with estimated annual and total CO_2-emission reduction, in addition to a simplified calculation of the abatement cost for 3 of the measures, given in NOK/ton CO_2 reduced.

The measures taken and the abatement costs presented aims at illuminating the positive impact of possible improvements to encourage further studies for identification of improvement potential at existing installations.

8.1 Modification of Oil Export Pump

One of the oil-export pumps on Ekofisk 2/7 J produced a greater pressure increase than required. By reducing the pressure drop from 50 to 25 bar over a valve, the power demand was reduced by 1 MW. This further reduced CO_2-emissions with 5 500 tons per year.

The measure was implemented in 2009, with the current production licence, which is valid until 2049, total CO_2-emission reduction amounts to 220 000 tons. The investment cost was estimated to be somewhere between 0.1 to 1 MNOK [92]. The range given is wide, however to underline the positive effect these efficiency measures provide, the abatement cost is further calculated with the highest given cost of 1 million NOK to prove the investment cost is still insignificant compared to amount of CO_2 reduced.

$$\frac{Total\ investment\ cost}{CO_2\ emission\ reduction\ for\ expected\ lifetime} = \frac{1\ 000\ 000}{220\ 000} = 4.55\ NOK/ton\ CO_2\ reduced$$

8.2 Upgrade of Combined Cycle System

The original WHRU for the combined cycle on Eldfisk 2/7 E, recovered heat from two water injection turbines and one gas compression turbine. Unstable operation led to an upgrade of the system in 2013, for the WHRU to cover all four injection turbines (only two at a time) in addition to the compression turbine. With a higher flexibility regarding waste heat recovery, the power output increased by 27%, from 7.5 MW to 9.5 MW. Reduced CO_2-emissions were estimated to be 12 000 tons per year [73]. Accumulated to the end of current production licence, total CO_2-emission reduction amounts to 420 000 tons. Investment cost for the upgrade has not been found.

8.3 Operations Optimization of Gas Compressor to Pipeline

The operation philosophy regarding pipeline gas compressors was optimized in 2014. Previously, two compressors were running simultaneously to ensure high regularity. As of 2014, only one compressor is operating whenever the pressure in the pipeline operated by Gassco is below 117 bars. The annual emission reduction due to reduced use of compressor is estimated to be 32 000 ton CO_2. Investment cost is given as <100 000 NOK [93].

A simplified abatement cost with the highest possible investment cost of 100 000 NOK and total CO_2 reduction over 34 years of 1 088 000 ton are given as:

$$\frac{Total\ investment\ cost}{CO_2\ emission\ reduction\ for\ expected\ lifetime} = \frac{100\ 000}{1\ 088\ 000} = 0.09\ NOK/ton\ CO_2\ reduced$$

8.4 AC Cable Between Installations

In 2014 an AC cable with 10 MW capacity was installed between Ekofisk 2/4 Z and Eldfisk 2/7 S. The cable provides the two fields a higher flexibility concerning power generation, as specific gas turbines can operate on higher load, i.e. reach a higher efficiency. The net result is a more optimal utilization of energy between the two fields, hence a reduced CO_2-emission [94]. Investment cost and estimated CO_2-emission reduction from the power cable has not been found.

8.5 Operations Optimization of WHRU

The WRHU on Ekofisk 2/4 K were originally connected to three of the power turbines and one of the gas injection turbines on the platform. The WHRU is mainly used for production of fresh-water and heating of living quarters, requiring operation of only one power turbine and one injection turbine to supply sufficient heat. An optimization of the WHRU were done in 2015 by blinding parts of the WHRU connected to turbines not normally in operation, to eliminate the heating medium from being cooled down by cold exhaust pipes. The flow rate of the heating medium through the WHRU was also reduced, to increase the temperature of the working medium.

The measures taken increased the heating medium temperature by 7 degrees, eliminating the need to operate the power turbine for 9 out of 12 months, as the installation is normally powered through a cable from the Ekofisk Complex.

CO_2-emission reduction due to reduced use of the gas turbine is approximately 6 300 tons per year. Accumulated to end of current production license makes a total of 207 900 tons CO_2 reduced. Investment cost is given as <100 000 NOK [95].

A simplified abatement cost with the highest possible investment cost of 100 000 NOK and total CO_2 reduction over 33 years is given as:

$$\frac{Total\ investment\ cost}{CO_2\ emission\ reduction\ for\ expected\ lifetime} = \frac{100\ 000}{207\ 900} = 0.48\ NOK/ton\ CO_2\ reduced$$

8.6 Total CO_2-Emission Reduction

Below in Table 8-1, is a summary of the energy efficiency measures with associated abatement cost and CO_2-emission reduction with the current production licence to 2049. The combined annual CO_2-emission reduction from the three measures given with investment cost, make up 5.5% of the CO_2-emissions related to gas turbines on GEA in 2018. The abatement cost calculated for these measures is insignificant and well below the break-even abatement cost of 754 NOK/ton CO_2 reduced, proving these small measures to be both economically and environmentally beneficial. Total abatement cost for the measures given with investment values are calculated as:

$$\frac{Total\ investment\ cost}{CO_2\ emission\ reduction\ for\ expected\ lifetime} = \frac{1\,000\,000 + 100\,000 + 100\,000}{220\,000 + 1\,088\,000 + 207\,900} = 0.73 NOK/ton$$

Table 8-1: Summary of CO_2-emission reduction due to energy efficiency measures and associated abatement cost

Description	Abatement Cost [NOK/ton CO_2 reduced]	Annual CO_2-emission reduction [tons]	Total CO_2-emission reduction [tons]
Modification of oil export pump	4.55	5 500	220 000
Upgrade of combined cycle system	-	12 000	420 000
Gas compressor to pipeline	0.09	32 000	1 088 000
AC cable between installations	-		-
Upgrade of WHRU	0.48	6 300	207 900
Total CO_2-Emission Reduction		**55 800**	**1 935 900**

Fuel Type

Fuel based power generation include not only different options for cycles and processes, but type of fuel too. The column for power generation can therefore further be split into two, namely carbon free fuel, or hydrocarbon fuel. CO_2 is not generated as a by-product before the hydrocarbons are present, meaning CO_2-emissions could still be avoided by choosing a carbon free fuel type. Chapter 9 is therefore a presentation of hydrogen as an alternative fuel to natural gas. The chapter will go into detail about characteristics of the fuel, production methods and utilization. Finally, a study of the possibility of implementing hydrogen production and combustion on GEA is presented.

9 Hydrogen

Being an energy carrier capable of delivering and storing tremendous amounts of energy, hydrogen is often referred to as the future of energy. Hydrogen is the most abundant and simplest element on the Earth's surface and has the highest energy content of any common fuel by weight. When combusted with oxygen, only water is produced, making the element environmentally attractive as a fuel. However, the compound seldom exists by itself in nature. Typically, it is bound to other chemicals such as oxygen in water or carbon in hydrocarbons. To utilize the hydrogen for energy purposes, it will first need to be separated from other elements, a process referred to as *hydrogen production*.

9.1 Production

To produce hydrogen, three necessities are required. A hydrogen source, a separation method, and a primary energy source to perform the separation. By combining these three factors in different ways, hydrogen production methods are numerous. From steam methane reforming, hydrogen can be separated from natural gas by heat. In electrolysis, hydrogen is produced by separating water molecules into hydrogen and oxygen with electricity. Biological processes produce hydrogen gas by letting bacteria and microalgae consume plant material. Hydrogen can also be produced in several ways using sunlight [96]. This chapter will focus on hydrogen production from steam methane reforming, partial oxidation, and electrolysis, as these methods are most relevant for offshore installations.

9.1.1 Production from Hydrocarbons

Steam Methane Reforming

In the Steam Methane Reforming (SMR) process, natural gas (CH_4) reacts with steam at high temperature to produce CO and H_2 in the following reaction.

$$CH_4 + H_2O \leftrightarrow CO + 3H_2 \qquad (\Delta H = +206 kJ/mol) \qquad (9.1)$$

The reaction is endothermic, meaning heat input is required for hydrogen to be produced. This heat is usually generated by burning a fraction of the natural gas, or by utilization of waste heat. To enhance the hydrogen production and eliminate CO, the SMR is followed by a Water-Gas Shift (WGS) reaction, illustrated by the chemical reaction below.

$$CO + H_2O \leftrightarrow CO_2 + H_2 \qquad (\Delta H = -42kJ/mol) \qquad (9.2)$$

This reaction is mildly exothermic, meaning heat is produced. The water to gas shift reaction is usually conducted in two stages with different temperatures. The high temperature shift reactor operates in the range of 350-475°C and is accountable for most of the hydrogen production. The second stage requires more active catalysts since the temperature is lower (in the range of 200-250°C) and contributes to bringing down the CO concentration to only a few mole% [97]. The final step is the hydrogen purification process, most often done by Pressure Swing Adsorption (PSA). PSA technology relies on differences in the adsorption properties of gases, by flowing feed gas upwards through an adsorber vessel. Hydrogen being a highly volatile component with low polarity, are practically non-adsorbable opposed to other gases such as N_2, CO, CO_2, H_2O and hydrocarbons. In this way, clean hydrogen (99.99%) exits at the top of the vessel. Desorbed impurities cling on to the surface of the adsorber material until the vessel is depressurized and the substances can leave from the bottom [98].

Partial Oxidation

Hydrogen can also be produced from hydrocarbons using partial oxidation. In this process, hydrocarbons react with oxygen to form hydrogen and carbon monoxide, as for the chemical reaction below.

$$CH_4 + \frac{1}{2}O_2 \leftrightarrow CO + 2H_2 + Heat \qquad (\Delta H = -35.7kJ/mol) \qquad (9.3)$$

The chemical reaction is exothermic, meaning heat is produced. The hydrogen to carbon ratio is however lower than for the SMR reaction, with the ratio 2:1 for partial oxidation and 3:1 for SMR. As for the SMR process, the hydrogen production by partial oxidation can be maximized when followed by a WGS reaction and cleansed for impurities by PSA [97].

9.1.2 Electrolysis

Hydrogen can also be produced from water by splitting up the molecule using electricity in an electrolyser. An electrolyser typically consists of an anode and a cathode separated by an electrolyte, in addition to a power supply. The electrolyte can either be an aqueous solution (acidic or alkaline) or a membrane. This subchapter will first give a background into the thermodynamics of water electrolysis, and further introduce two methods for water splitting, namely alkaline water electrolysis and Proton Exchange Membrane (PEM) water electrolysis.

Fundaments of Water Electrolysis

The basic water electrolysis reaction is:

$$H_2O(l) + Electricity \rightarrow H_2(g) + \frac{1}{2}O_2(g) \tag{9.4}$$

The reaction is endothermic and the required energy for splitting the water molecule is given by:

$$\Delta H = \Delta G + T\Delta S \tag{9.5}$$

Where ΔH is the enthalpy change associated with the reaction and represents the total amount of energy required to decompose water into oxygen and hydrogen. ΔH is the sum of the electrical energy and thermal energy, represented by ΔG and TΔS respectively. ΔG is the Gibbs free energy change and is positive (non-spontaneous) up to 2250°C. T is the absolute temperature of the process, and ΔS is the entropy change, which is positive for this reaction [99].

Water electrolysis technologies are classified into low temperature processes (T<150°C), medium temperature processes (150°C<T<600°C) and high temperature processes (T>600°C) From Eq. (9.5), the required electrical energy (ΔG) decreases with increasing temperature of the process. A high operating temperature is therefore beneficial for the process, as less electricity is needed, which is more costly than heat. Figure 9-1 shows the electricity input requirements for different temperatures in a water electrolysis process [99].

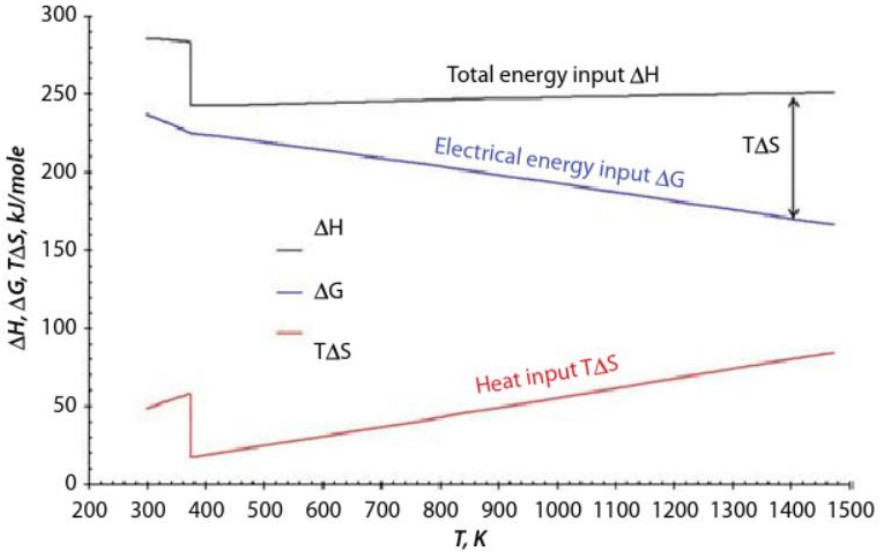

Figure 9-1: Temperature dependence of main thermodynamic parameters for water electrolysis [99]

There are two different thermodynamic voltages used for characterization of water electrolysis. The free electrolysis voltage E and the thermo-neutral voltage V defined below.

$$E = \frac{\Delta G}{n \cdot F} = 1.229\ V \tag{9.6}$$

$$V = \frac{\Delta H}{n \cdot F} = 1.48\ V \tag{9.7}$$

Where n is the numbers of electrons in the reaction, which is 2, and F is the Faraday Constant = 96 485.3365 C/mole.

E is the standard thermodynamic voltage. At standard conditions, electrolysis will start for voltages above E, but the cell will consume heat from the surroundings as the voltage is too low to maintain isothermality. For an efficient electrolysis, the voltage needs to be higher than the thermoneutral voltage V. With a voltage above 1.48, current density increases, and the electrolysis can be carried out at high speed. This process however, requires cooling as the reaction will be exothermic [99, 100].

The cell efficiency of an electrolyser measures the ratio of theoretical amount of energy to the real amount of energy required to split one mole of water and can be expressed as the thermo-neutral voltage divided by the cell voltage, U [100].

$$\eta_{el} = \frac{V}{U} \cdot 100\% \tag{9.8}$$

An efficiency of 100% can easily be obtained by running the cell on the thermo-neutral voltage. However, operation at this voltage yields a low current density and therefore also a low specific hydrogen production. To increase the productivity, thereby decreasing capital expenditure, a higher voltage is advantageable. Too high voltage will lead to an increasing share of the electricity being degraded into heat in the cell, meaning an increase in operational expenditure. A balance between CAPEX and OPEX must therefore be found in the right cell voltage. Typical electrical efficiencies for electrolysers are 60-80% for alkaline and 80% for PEM, with a production rate of 1-500 and 1-230 Nm^3/h respectively. [99, 100].

Alkaline Water Electrolysis

The alkaline water electrolysis is a low-temperature electrolysis, with typical operating temperature between 60-80°C. The electrolysis is performed with two electrodes immersed in an alkaline aqueous solution of typically NaOH or KOH. When connected to a power supply, water is reduced at the cathode to produce hydrogen gas and hydroxyl ions, according to Eq. (9.9). At the anode, hydroxyl ions are oxidized to water and oxygen, as for Eq. (9.10).

Cathode: $$2H_2O + 2e^- \rightarrow H_2 + 2OH^- \tag{9.9}$$

Anode: $$2OH^- \rightarrow \frac{1}{2}O_2 + H_2O + 2e^- \tag{9.10}$$

As water is consumed during the process, a constant water supply is necessary to keep the concentration of the aqueous solution at an optimum level. Water vapour and traces of electrolyte can be carried away by the gas products, a purification process of the hydrogen gas is therefore necessary before utilization. A porous separator is placed between the two electrodes, to avoid the two product gases to react with each other. The schematics of alkaline water electrolysis are shown in Figure 9-2.

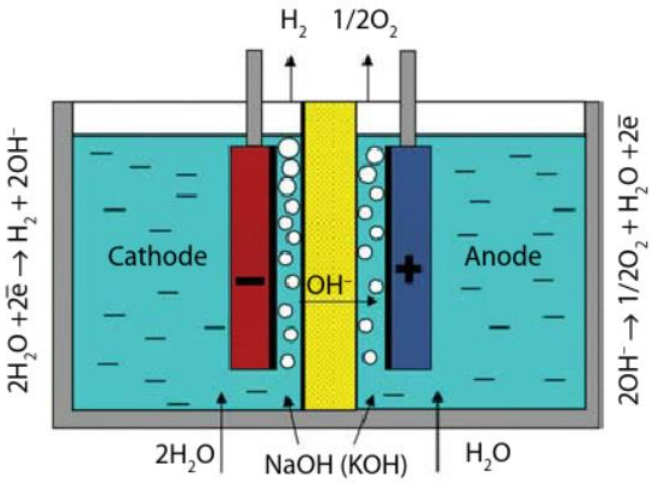

Figure 9-2: Schematic diagram of the alkaline water electrolysis cell [99]

PEM Water Electrolysis

The PEM cell, illustrated in Figure 9-3, consists of a thin (~0.2mm) membrane of a proton-conductive polymer electrolyte, serving the purpose of both carrying ionic charges and separating the two product gases to avoid reformation of water. Catalytic layers are placed on either side of the membrane, which is further connected to electrodes supplying DC charge. Together the five constituents make up the Membrane-Electrolyte Assembly. The assembly is further placed between bipolar plates with channels for water and gas transportation, and lastly immersed in water for electrolysis to start [99, 100].

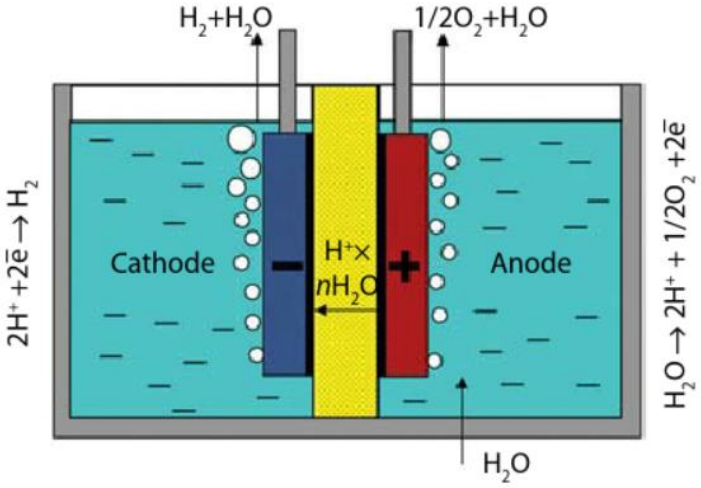

Figure 9-3: Schematics of a PEM electrolysis cell [99]

When connected to a power supply, the water will oxidize at the anode, producing O_2 according to the half reaction in Eq. (9.11) below. The hydrated hydrogen ions are further transported across the PEM, and reduced at the cathode to form hydrogen according to Eq. (9.12).

Anode: $$H_2O \rightarrow \frac{1}{2}O_2 + 2e^- + 2H^+ \quad (9.11)$$

Cathode: $$2H^+ + 2e^- \rightarrow H_2 \quad (9.12)$$

The acidic hydrogen ions transported by the membrane can lead to corrosion of the electrodes connected to the membrane. To avoid corrosion, precious metals have to be used, making the PEM electrolysis cell rather expensive [99].

9.2 Utilization

Today, hydrogen is mainly used for fertilizers and petroleum refining. However, hydrogen as fuel for transportation purposes is a growing market. The largest potential for hydrogen is for fuel cells and renewable energy storage, whereas numerous studies are being performed today. Hydrogen can also be combusted directly in a combustion engine, thereby replacing natural gas, and avoiding CO_2-emissions as only water is produced as a by-product. This however, requires modifications to the original machinery to cope for the differences in combustion characteristics between the two gases.

This thesis will cover hydrogen utilization in combustion engines, fuel cells and for storage purposes, as these options are most relevant for energy production on offshore installations.

9.2.1 Combustion engines

Gas turbines are versatile, fuel-flexible combustion engines and can easily be modified to operate with different fuels, including hydrogen. However, differences in combustion characteristics for hydrogen and natural gas must be considered before switching the fuel. Table 9-1 shows the different characteristics for methane and hydrogen.

Table 9-1: Comparison of fuel properties [101]

Property	Units	Methane	Hydrogen
Formula		CH_4	H_2
Molecular Weight	[gram/mol]	16	2
LHV (per volume)	[MJ/Nm^3]	35.8	10.8
LHV (per mass)	[MJ/kg]	50	120
Flame Speed	[cm/s]	38.3	170

Hydrogens volumetric-energy density is ~1/3 that of natural gas, meaning the gas turbine requires 3 times as much gas for same power output with hydrogen as fuel compared to natural gas. The fuel system of the turbine must therefore be adjusted to accommodate the increased fuel flow [102]. As the flame speed of hydrogen is higher than of natural gas, the fuel speed must also be increased, to balance the flame on the burner rim to prevent flash back. Flash back happens when the flame speed is higher than fuel speed, resulting in the flame propagating into the burner tube. Even though no CO_2 is formed when combusting H_2, formation of NO_x is present at the high temperatures when combusting with air. To reduce NO_x emissions, water is injected into the fuel before combustion, known as Wet Low Emission (WLE). This water needs to be treated for impurities, demanding extra space and resources [103].

As of today, there are few commercialized gas turbines operating on 100% hydrogen, but most gas turbines can operate with varieties of fuel containing substantial hydrogen volumes. GE Power has achieved hydrogen volumes of 95% in their aeroderivative gas turbines, configurated with a single annular combustor (SAC) [102]. The SAC is a diffusion burner, meaning only fuel is supplied to the burner, therefore the mixing of oxidizer (air) and combustion happen simultaneously. Opposed to the pre-mixed combustion process where fuel and air are mixed before entering the burner for combustion [104].

Siemens has pledged to reach 100% H_2 combustion in gas turbines by the year 2030. As of 2019, three of their aeroderivative WLE gas turbines has burned on 100% H_2 [103].

Fuel Blends

Fuel blends of hydrogen and natural gas is a near-term alternative to 100% hydrogen combustion. As hydrogen and natural gas has different heating values, the reduction in CO_2 emissions would have to be calculated from the heat input ratio opposed to volume or mass percentage. Figure 9-4 shows the relationship between heat input and volume flow for a methane/hydrogen fuel mix. To reduce CO_2 emissions by 50% in a combustion process by using a methane/hydrogen blend, 77 vol% of the fuel needs to be hydrogen [101].

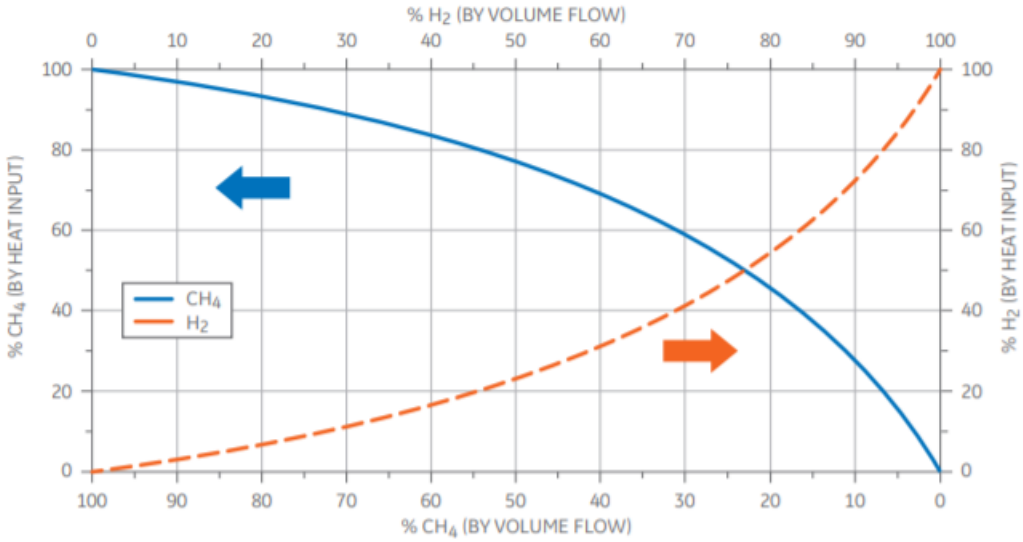

Figure 9-4: Relationship between mass flow (heat input) and volumetric flow for a methane/hydrogen fuel mix [101]

9.2.2 Fuel cells

A fuel cell converts fuel to electricity through chemical reactions without any combustion and operate best on pure hydrogen where the by-products are only heat and water. For a more thoroughly description of fuel cells, see Ch. 7.

9.2.3 Storage

Hydrogen storage is often linked with renewable energy production, such as wind or solar energy, as a solution to the disadvantage of energy only being available when weather conditions allow for it. Hydrogen production and -storage from renewable energy sources would allow us to save the energy and use it when needed. There are several different technologies for storing hydrogen today, including pressurized and cryogenic storage, chemical storage and hydride storage. This subchapter will briefly discuss pressurized storage in compression tanks, cryogenic vessels and underground reservoirs. A common factor for all alternatives is the necessity to first increase the volumetric energy density of hydrogen, for the most efficient utilization of the storage capacity [97].

Compression and Liquification

Compression of hydrogen is usually done in two or three stages, as it requires less energy than for one-stage compression. Storage tanks for the high-density gas needs to be made of high strength materials to ensure durability and safety. Standard compression tanks today use a pressure of about 10-20 MPa [97].

Liquified hydrogen has a volumetric energy density 860 times higher than of hydrogen gas at ambient conditions. The liquification involves cooling the gas to below -252.87°C in several compression stages and by use of liquid nitrogen or helium cooling. Specific containers known as cryogenic vessels is required for storing liquid hydrogen safely. Although liquid hydrogen has a much higher volumetric energy density than compressed hydrogen, a compressed gas is simpler and less expensive to both manufacture and handle [97].

Underground Storage

For large scale hydrogen storage, underground reservoirs and caverns are advantageous. Several academic studies have been performed on the possibility of storing hydrogen underground, either in depleted reservoirs, aquifers or salt caverns. The criteria for underground storage are strict, as hydrogen has a high penetrability and high reactivity on rock matrix. The storage facility needs to be tight, and the effect of hydrogen reactions with the surrounding rock and fluid needs to be examined thoroughly [105].

Around 30% of gas injected into a storage facility cannot be recovered. This is known as the cushion gas, and its role is to exercise the minimum pressure needed to prevent water inflow into pore spaces and to provide optimum conditions for the recoverable gas. The remaining ~70% is known as the working gas and can be recovered at any time [105].

Large-scale practical experiments have been done in salt caverns with volumes of over 500 000m^3 and working gas capacity of 3.72 million kg H_2 with good results. No experiments have been done on depleted oil fields or aquifer reservoirs however, even though these reservoirs tend to be bigger than salt caverns. The main reason for this is the high cost of hydrogen production today. Lowering the cost will result in an increased amount of hydrogen and thereby an increased amount of storage requirements [105]. On the NCS, a huge potential lies in offshore wind turbines combined with hydrogen production and -storage, when technology allows for it to be done in an efficient and economic manner.

9.3 Hydrogen on GEA

This chapter will investigate the possibility of hydrogen production from natural gas by steam methane reforming. The hydrogen will be burned as fuel in the gas turbines, and the CO_2 produced from the SMR process will be captured and stored, furthered studied in Chapter 10.

The basis for calculation of natural gas consumption, hydrogen production and CO_2-emissions with respect to SMR is taken from Spallina et al. *Techno-economic assessment of membrane assisted fluidized bed reactors for pure H_2 production with CO_2 capture* (2016) [106]. The simulation study compares two membrane-based technologies for hydrogen production to a reference technology for hydrogen production based on SMR with and without CO_2 capture.

In this plant, natural gas is first preheated to convert sulphur compounds to H_2S which is absorbed over a bed of ZnO. NG is further mixed with H_2O to achieve a steam to carbon (S/C) ratio of 3.4 in the reformer. An adiabatic pre-reforming is carried out to remove higher hydrocarbons in the gas, and finally the SMR process is introduced to create syngas (H_2/CO). The syngas is further cooled before entering a WGS reactor where more than 70% of the CO

in the syngas reacts with H_2O to produce CO_2 and H_2. The gas is cooled to ambient temperature before entering the PSA unit, where H_2 is produced with a purity higher than 99.999%. The PSA off-gas, rich in CO, is directed towards the furnace, where it is combusted to provide heat for the SMR process.

9.3.1 Energy Calculation

The SMR is a small-scale plant with a production capacity of ~30 000 Nm^3/h, a H_2-yield of 2.49 mol per mol CH_4, and hydrogen production efficiency of 74%. Required heat input and H_2/CO_2 output for the SMR plant are shown in Table 9-2.

Table 9-2: Gas Consumption, Hydrogen Production and CO_2 Production from SMR [106]

	Gas Consumption		Hydrogen Production		CO_2 Production
	[Nm^3]	[kg]	[Nm^3]	[kg]	[ton]
Per hour	9 432	11 731	2 700	30 033	25
Per year	82 624 320	102 766 567	23 652 000	263 092 325	215 736

From Table 9-1 the heating value of hydrogen is 10.8 MJ/Nm^3, compared to 40MJ/Nm^3 of NG [107]. The annual hydrogen produced in the SMR process has a total heating value of 2 841 TJ, which corresponds to ~71 million Sm^3 of natural gas. The new and old gas composition (vol%) are shown in Table 9-3, where the volume and heat input represent required amount to cover GEA's annual energy need, namely 1 336 876 MWh.

Table 9-3: Composition, volume and heating value of NG and NG/H_2 mix

Fuel	Component	Content	Volume [m^3]	Heating Value [MJ]
Original	NG	100 %	357 453 347	14 298 133 880
	H_2	-	-	-
Fuel Blend	NG	52 %	286 418 419	11 456 736 772
	H_2	48 %	263 092 325	2 841 397 108

With the new gas composition, an updated gas consumption, energy production and CO_2-emission table can be made shown in Table 9-4.

Table 9-4: Gas consumption, energy production and CO_2-emission table for GEA with SMR and a fuel mix of NG/H_2

Activity	NG Consumption [Sm^3]	Energy Production [MWh]	CO_2-emission [ton]
Base Case	357 453 347	1 336 876	789 972
SMR	102 766 567		215 736
Combustion	286 418 419	1 336 876	632 985
Reduction	**- 31 731 639 (-8.88%)**		**- 58 748 (-7.44%)**

From Table 9-4, one can clearly see an increase in total gas consumption and CO_2-emission by producing hydrogen through SMR for further combustion in gas turbines along with natural gas. A more efficient SMR process would yield a higher hydrogen flow rate, thereby decreasing the emission of CO_2. However, a net decrease in CO_2-emission could also be accomplished by implementing CCS. CCS would eliminate most of the CO_2-emissions related to the SMR process (up to ~216 000 tons per year). This will be further studied in Ch. 10.3.

9.3.2 TRL

SMR has not yet been applied to offshore installations, the main cause being the size and weight of the process equipment's. The process is however a well-known, commercially available technique for hydrogen production and is rated with TRL 9 from Table 2-3.

Gas turbines are versatile combustion engines, and experiments done by GE Power finds their aeroderivative turbines capable of operating with hydrogen concentrations up to 95 vol%, when configurated with a SAC. Burning a ~50/50 NG-H_2 fuel blend on GEA's gas turbines are therefore also rated with TRL 9.

9.3.3 CO_2-Emission Reduction

The CO_2-Emission Reduction is calculated by Eq. (2.1) and (2.2), with the numbers from Table 9-4.

$$CO_{2_{H_2}} = \frac{215\,736 + 632\,985\ ton}{1\,336\,876\ MWh} = 0.64\ ^{ton}/_{MWh}$$

$$\%\ CO_2\ emission\ reduction = -\frac{0.64}{0.59} \cdot 100\% + 100\% = -7.6\%$$

9.3.4 Efficiency

The H_2-production efficiency is given as 74%. The gas turbine cycle efficiency for combusting a fuel blend of hydrogen and natural gas on GEA's gas turbines are assumed to be the same as with combustion of 100% natural gas, namely 34.7%. This assumption is based on the fact that heat input and energy output from the turbines are the same.

From these two efficiencies, a *chain conversion efficiency* can be calculated to demonstrate the overall efficiency of fuel utilization. When neither of these are 1, energy loss is expected in both processes which when combined will increase the efficiency loss even further.

The chain conversion efficiency from H_2 production and combustion is:

$$\eta_{ch.con} = \eta_{H_2} \cdot \eta_{GT} = 0.74 \cdot 0.347 \cdot 100\% = 26\%$$

Efficiency improvement can further be calculated from Eq. (2.5)

$$Efficiency\ improvement = \frac{26\% - 34.7\%}{34.7\%} \cdot 100\% = -25\%$$

9.3.5 Cost

Cost estimations are based on the study of Spallina et al. [106]. The SMR process plant is assumed to have a lifetime of 30 years. Costs were given in Euro in 2016 figures and converted to NOK with the average exchange rate for 2016. The investment is calculated to last for current production licence which expires in 2049. Cost associated with the upgrade on GEA's gas turbines for SAC configuration will not be reviewed.

Bare Erected Cost (BEC)

The Bare Erected Cost (BEC) comprises the cost of all process equipment related to the SMR process facility and is given as ~360 million NOK. The largest cost is associated to the reactor and the heat exchanger used for cooling down the exhaust gas from the furnace. A detailed cost description of BEC is provided in Table 9-5 below.

Table 9-5: Bare Erected Costs for SMR Process plant [106]

Description	Cost [NOK]	% of BEC
Reactors	98 101 344	27.3 %
Convective cooling HEX	99 123 233	27.5 %
Turbomachines	31 771 458	8.8 %
H_2 compressors	13 563 254	3.8 %
Syngas coolers & heat rejection	38 738 883	10.8 %
PSA unit	78 499 655	21.8 %
Bare Erected Cost	**359 797 827**	**100 %**

Total Overnight Cost (TOC)

Total Overnight Cost (TOC) includes all "overnight" capital expenses incurred during the capital expenditure period. TOC is calculated from BEC with the methodology from Table 9-6 below.

Table 9-6: Methodology for calculation of the TOC [106]

Description	Abbreviation	Cost
Bare Erected Cost	BEC	[NOK]
Total Installation Cost	TIC	80%BEC
Total Direct Plant Cost	TDPC	BEC + TIC
Indirect Cost	IC	14%TDPC
Engineering, Procurement and Construction	EPC	TDPC + IC
Contingencies & Owners Cost	C&OC	15%EPC
Total Overnight Cost	TOC	EPC + C&OC

Calculation of the TOC of the SMR plant can further be seen in Table 9-7.

Table 9-7: Total Overnight Cost [106]

Description	[NOK]
BEC	359 797 827
+ TIC	287 838 262
= TDPC	647 636 089
+ IC	90 669 052
= EPC	738 305 141
+ C&OC	110 745 771
= TOC	**849 050 912**

Operating Cost

Operating and maintenance cost are divided into fixed and variable cost. Fixed costs include operating labour, maintenance, insurance cost, chemicals, and membrane replacement. Variable costs cover consumables such as cooling water and process water. Fixed and variable operating costs are given in Table 9-8.

Table 9-8: Operating and maintenance costs of SMR processing plant [106]

Description	Lifetime [years]	Cost [NOK/year]	Total [NOK]
O&M Fixed	29	61 313 340	1 778 086 860
O&M Variable	29	5 852 637	169 726 473
Total			**1 947 813 333**

Energy Cost

From Table 9-4, the increase in gas consumption due to SMR and fuel blend in gas turbines amounts to ~31.7 million Sm^3 per year. This further increases the CO_2-emissions with 58 748 tons per year. With the average price of gas for 2018 (minus 78% tax) and cost of CO_2, an extra loss of income of 3.34 billion NOK is expected.

The costs related to increased gas consumption and CO_2-emissions are shown in Table 9-9 below.

Table 9-9: Additional energy costs related to SMR and NG/H_2 fuel blend

Description	Quantity	Unit	Price [NOK/unit]	Operating years	Energy Costs
NG	31 731 639	[Sm3]	2.21	29	447 409 770
CO_2	58 748	[t]	765	29	1 303 333 542
Total					**1 750 743 313**

Abatement Cost

The abatement cost is calculated with the formula:

$$\frac{Total\ investment\ cost\ of\ SMR + Additional\ energy\ costs\ incl.\ CO_2\ cost}{CO_2\ emission\ reduction\ for\ expected\ lifetime}$$

Total estimated cost of an SMR process plant, including the abatement cost is summarizes in Table 9-10 below.

Table 9-10: Cost estimate of SMR and NG/H_2 fuel blend

Description	Unit	Cost
TOC	NOK	849 050 912
+ O&M	NOK	1 947 813 333
+ Additional Energy and CO_2 Costs	NOK	1 750 743 313
Total Investment Cost	NOK	4 547 607 558
CO_2-Emission Reduction	ton	-1 703 704
Abatement cost	**NOK/ton**	**-2 669**

The increase in CO_2-emissions (shown by the negative sign in Table 9-10) is due to increased total gas consumption for production of hydrogen. The abatement cost comes out with a negative sign as well, meaning cost of the hydrogen production plant is 2 669 NOK per ton CO_2 increased.

Based on the abatement cost calculated here, investing in a SMR process plant alone for GEA is neither economically nor environmentally beneficial. However, SMR allows for easily pre-combustion capture of CO_2, which if implemented and combined with storage of CO_2, can lower the net emissions with up to 216 000 tons per year, if 100% of the CO_2 from the SMR process is captured. This will be further studied in Ch. 10.3.

9.3.6 Rating Table

Alternative	TRL	CO_2-Emission Reduction	Efficiency Improvement	Abatement Cost	Comments
Gas Turbines	9	0%	34.7%	765 NOK/ton	Base case
H_2	9	-7.6%	-25%	-2 669 NOK/ton	H_2 production from SMR, and NG/H_2 fuel blend for combustion

CO_2-Control

The last column in the Power Production Selection Model presented in the Introduction, is CO_2-Control. Even though power generation is conducted with hydrocarbons and the by-product of CO_2 is formed, CO_2-emissions could still be limited/avoided by implementing Carbon Capture and Storage. Chapter 10 will go into detail about the technology of CCS and further study the possibilities of implementing carbon capture (CC) from fuel cells and from hydrogen production through SMR.

10 Carbon Capture and Storage

In 1996, Norway was the first country in the world to implement CCS, at the gas-field Sleipner. The gas from Sleipner has a 9% CO_2-content, which is much higher than the market specifications of maximum 2.5%. To be able to sell the gas, CO_2 is removed from the natural gas by absorption at a processing platform before being delivered to pipelines and exported. The extracted CO_2 is further injected to a saline formation 1 km below the seabed. At the course of 24 years, more than 20 million ton CO_2 from the Sleipner gas has been stored in this formation [108].

10.1 Technology

CCS technology can be split into three sections, namely capture, transportation and storage. Capturing the CO_2 can be done either pre-combustion or post-combustion, with different technologies, including oxy-fuel combustion. Transportation of CO_2 from capture site to storage site can either be conducted through pipelines or by marine vessels. The storage facility needs to be both porous and permeable to allow large volumes of CO_2 to be injected, and the reservoir must be overlain by an impermeable cap rock to avoid CO_2 leakage [109].

10.1.1 Capture

Capturing the CO_2 involves separating the gas from other substances, either from fuel or flue gases, and accumulate it for further handling. Carbon capturing in electricity generation can be done in at least three different ways: Pre-combustion capture, Post-combustion capture and oxy-fuel combustion [110].

Pre-Combustion Capture

Pre-combustion capture technology involves converting the original fuel to a mixture of H_2 and CO_2 by gasification, involving partial combustion, reforming and WGS. The reactions in the process are shown in Table 10-1, and the schematics of the pre-combustion capturing are shown in Figure 10-1 [111].

Table 10-1: Gasification Process [111]

Process	Reaction
Partial Oxidation	$CH_4 + \frac{1}{2}O_2 \rightarrow CO + 2H_2$
Reforming	$CH_4 + H_2O \rightarrow CO + 3H_2$
WGS	$CO + H_2O \leftrightarrow CO_2 + H_2$

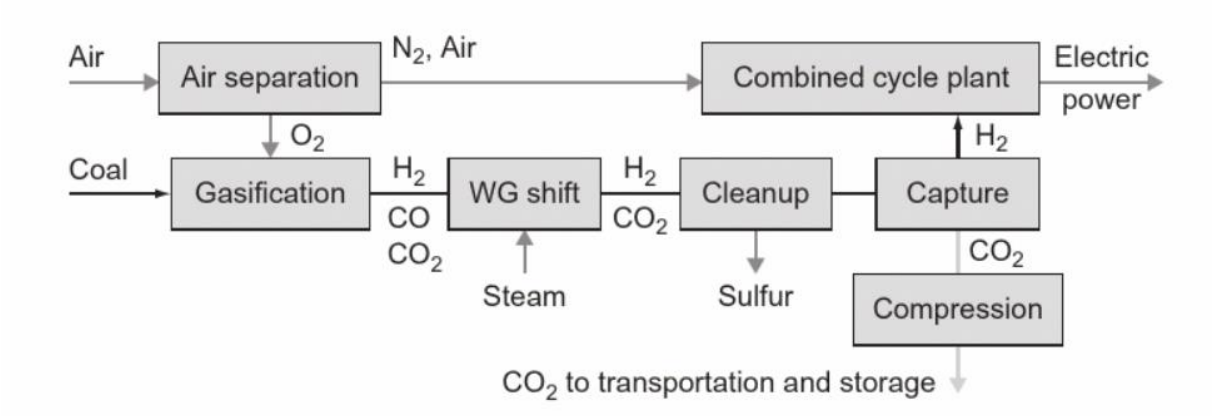

Figure 10-1: Schematics of pre-combustion capturing [111]

The CO_2 concentration in the gas stream after the gasification process is typically >20% and can be separated from the gas in different ways, of which the use of physical solvents (usually by Selecsol or Rectiso) is currently the most commercially developed. CO_2 absorption by a physical solvent is proportional to the partial pressure of the CO_2, meaning the absorption rate is highest for CO_2 at elevated pressures.

For gasification processes at atmospheric pressure, the most common and mature technology is chemical absorption. Cooled gas stream enters the bottom of an absorption tower, and a liquid solvent (typically amine-based) is injected at the top. The solvent reacts with the CO_2, forming a heavy solution which will sink to the bottom of the tower where it will be extracted and transferred to a stripper tower. Here, the solution is heated up to around 120°C to separate the CO_2 and the liquid solvent. The solvent exits from the bottom of the tank to be reused. CO_2 and steam are directed towards a condenser, where steam is

condensed and separated from the CO_2 stream. Finally, the clean CO_2 stream is compressed and transported towards final storage destination [111]. Figure 10-2 shows the schematics of an absorption process.

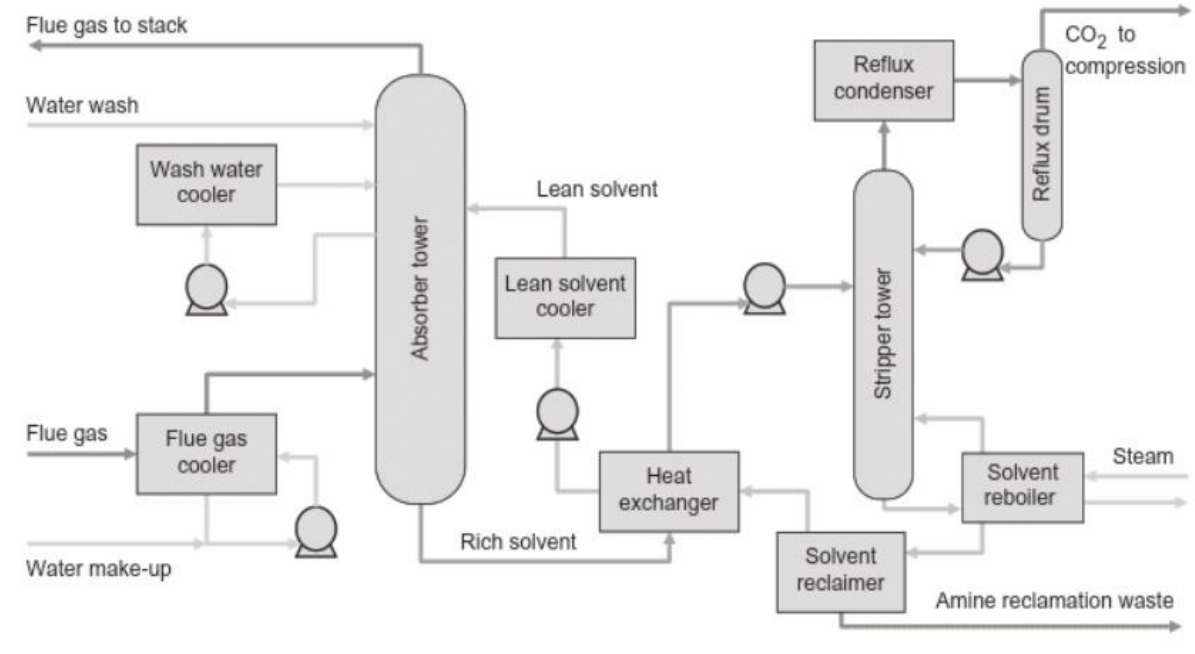

Figure 10-2: Schematics of chemical absorption [111]

Post-Combustion Capture

In a Post-combustion capture process, the CO_2 is removed from the flue gases after combustion of the fuel. The separation of CO_2 from the remaining constituents (mainly N_2) of the gas is the same as for atmospheric pre-combustion capturing, namely chemical absorption, explained above [111]. The main advantage of post-combustion capture is its ability to be applied to existing plants as an "end-of-pipe" technology.

Oxy-fuel Combustion

By combusting the fuel with pure oxygen instead of air, the flue gases will mainly consist of CO_2 and H_2O, as the nitrogen in the air is eliminated. The final separation before compression and storage of the CO_2 requires only dehydration. The combustion temperature with pure oxygen is a lot higher than of air, as the nitrogen acts as a cooling substance in the process. A portion of the flue gases are therefore recirculated back to the combustion chamber to control the temperature [110].

As for the dehydration process, most of the water will be removed by a condenser. However, separation of the last H_2O molecules can be very complicated and costly, depending on the required quality specification for CO_2 with respect to transport and storage (Table 10-2 in Pipeline Transportation). Final purification can further be done by absorption [112].

The main disadvantage of oxy-fuel combustion is the high energy requirement for producing oxygen of high purity, making the plant retrofit unattractive.

10.1.2 Transport

When transporting CO_2, pressure and temperature are important factors, as they determine the fluids properties. Figure 10-3 shows the phase diagram for CO_2, where the critical point can be found at P_C=7.39MPa and T_C=31.04°C. For most efficient transportation, a dense fluid is advantageable as it requires less energy to move [111].

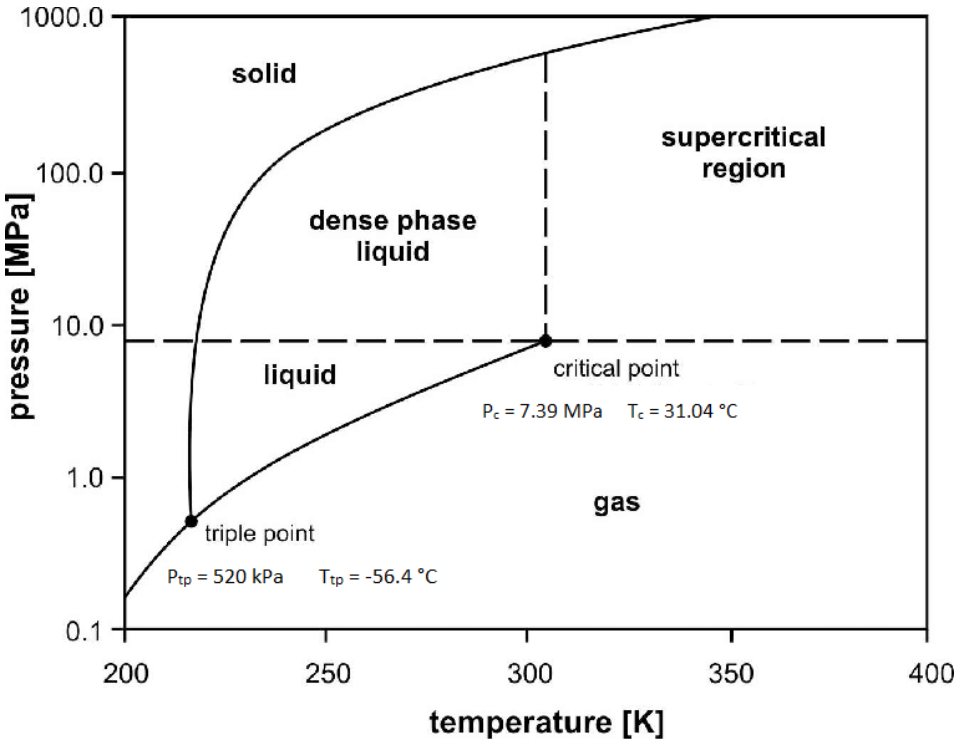

Figure 10-3: Phase Diagram for CO_2 [113]

Transporting CO_2 from capture site to storage site can happen either by pipelines or marine vessels. For large quantities and shorter distances, pipelines are best suited. Marine vessels are most often used for smaller quantities and larger distances [111]. Figure 10-4 shows the

optimal CO_2 transport solution, developed by Geske et.al. in a study, revealing cost savings can reach up to 40% by choosing the right transportation method with respect to quantity and distance [114].

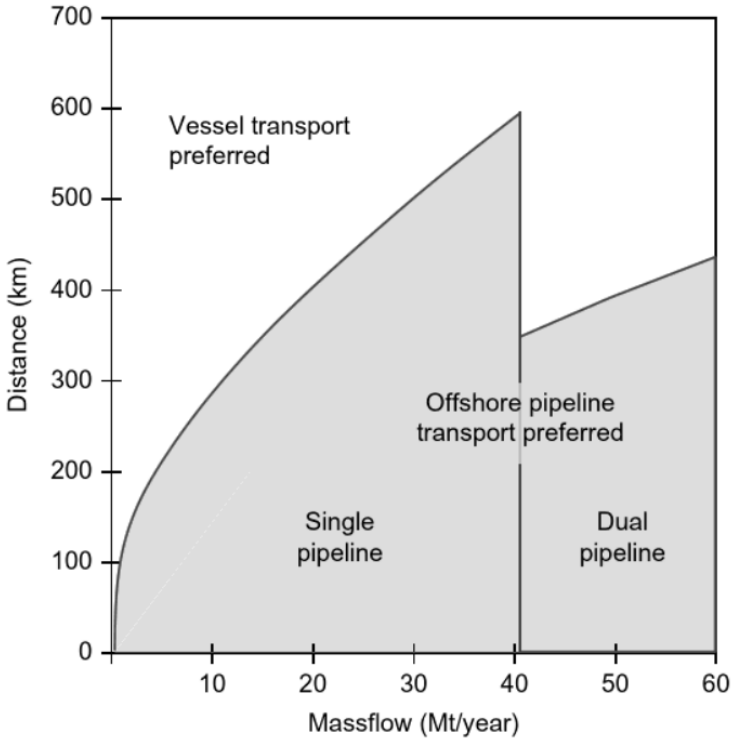

Figure 10-4: Optimal CO_2 transport solution [111]

Pipeline Transportation

CO_2 transportation in pipelines are most beneficial in a subcooled liquid phase. This phase is present when $P>P_C$ and $T<T_C$. The high density and low compressibility associated with this phase allows for a smaller pipeline diameter, lower pressure drops and further lower energy requirements for transportation. To ensure the temperature stays below the critical point along the full length of the pipeline, thereby avoiding the gas phase, the CO_2 is typically cooled to below 15°C before transport [111].

Impurities in the fluid can have a negative effect on both the flow-determining properties and the pipelines itself. Increase in compression requirements occur with only a few mol% of H_2 in the gas. Presence of water and hydrogen sulfide will lead to corrosion on the pipeline walls [111]. A recommended quality specification for pipeline transportation of CO_2 has been published by EU Dynamis project, and are shown in Table 10-2. The specifications have however been criticized, as later experiments have found pipeline corrosion occurring at

concentration of 50 ppm in the CO_2 gas. For pipeline corrosion to be completely avoided, the water content should be below this limit [111].

Table 10-2: EU Dynamis recommended CO_2 specification for transportation and storage [111]

Component	Concentration Limit	Limitation
H_2O	500 ppm	Prevention of free water
H_2S	200 ppm	Health and Safety
CO	2000 ppm	Health and Safety
SO_x	100 ppm	Health and Safety
NO_x	100 ppm	Health and Safety
O_2	< 4 vol% < 1000 ppm	For aquifer storage Technical limit, for EOR
CH_4	< 4 vol% < 2 vol%	For aquifer storage For EOR
N_2 + Ar + H_2	< 4 vol% total	Lower for H_2 in view of economic value of its energy content
CO_2	**> 95.5%**	**Balanced with other compounds in CO_2**

Marine Vessels

Transport of CO_2 by ships have the same efficiency principle as for pipelines, namely transport efficiency is maximized when the density of the liquid is as high as possible. CO_2 is either a gas or a solid in atmospheric pressure, meaning liquifying the fluid requires compression above atmospheric pressure. At the triple point (520 kPa and -56.4°C), the density of CO_2 is at its highest, namely 1200 kg/m^3. Optimal vessel transport condition is therefore set to pressure and temperature slightly above the triple point. To avoid formation

of dry ice during loading, which occur when $T<T_{TP}$, operating conditions are usually set in the range of 0.6 to 1.5MPa and -30°C to -50°C [111].

10.1.3 Storage

The final step of the CCS process is storage. The CO_2 will be pumped into the storage facility in a supercritical phase, where the CO_2 inherits a liquid density and a reduced mobility. The liquid density maximizes the storage capacity and the reduced mobility minimizes the possibility of leakage. For the fluid to remain in supercritical phase, the hydrostatic pressure and temperature has to be larger than the critical pressure and temperature of CO_2, which is the case 800 meters below the surface. Suitable CO_2 storage sites are saline formations or former/depleting oil and gas fields. Saline formations are porous rocks containing salty water and are found in the subsurface all over the world. Former oil and gas fields are also a possible storage site, but the risk of leakages is larger in these reservoirs cap rocks, as they have been penetrated by numerous production-, injection- and exploration wells. CO_2 injection as an alternative to natural gas injection in operative oil and gas fields are also a possibility, for Enhanced Oil Recovery (EOR). In that way, energy rich natural gas can be utilized, and a storage site is made available for the damaging CO_2 [111].

Trapping

After injection, CO_2 is trapped underground with one or more of five different trapping mechanisms. The most common trap mechanisms are *stratigraphic* and *structural trapping*, which is the same mechanism oil and gas are trapped by. When injected, the liquid naturally floats upwards, until stopped by an impermeable layer of rock known as a cap rock. Naturally occurring structures in the subsurface, as anticlines or fault seals, and stratigraphic traps such as pinchouts or unconformities, surrounded by caprocks makes it possible for the CO_2 to accumulate in such places, forming CO_2 reservoirs [109]. Figure 10-5 illustrates these trapping mechanisms.

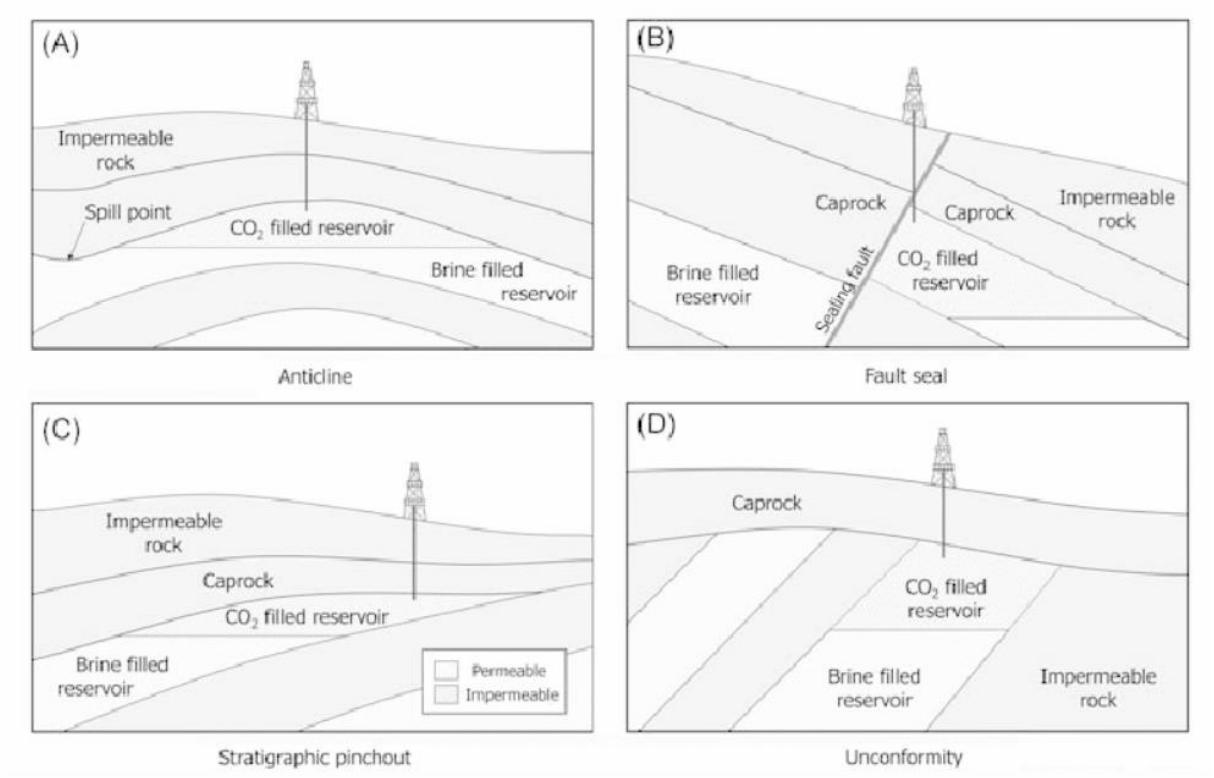

Figure 10-5: Structural and Stratigraphic Trapping of CO_2 [111]

In saline aquifers, the pore spaces of the rock contain water. When CO_2 is injected and starts rising up towards a cap rock, the water will be expelled from the pore spaces and replaced by CO_2. When injection of CO_2 stops, water will return from the surrounding rocks and begin to move back to the pores. The CO_2 will be immobilized by the added pressure of the water, and become trapped by the mechanism known as *residual trapping* [109].

With time, the injected CO_2 will dissolve into the fluid surrounding it, be water or oil. This is known as *solubility trapping*. The dense fluid will further sink into the bottom of the reservoir where it may react chemically with the surrounding rocks to form stable minerals. The product of this reaction is the most secure form of storage, known as *mineral trapping*. It is a slow process however, and can take thousands of years [109]. Table 10-3 summarizes the trapping mechanisms, the indicative specific capacity and effective timescale for trapping of CO_2.

Table 10-3: Indicative Specific Capacities of Trapping Mechanisms [111]

Trapping Mechanism	Indicative specific capacity [$kgCO_2/m^3$]	Effective timescale [years]
Structural Trapping	50 – 200	10 to 1 000
Stratigraphic Trapping	50 – 200	10 to 1 000
Residual Trapping	10 – 50	10 to 1 000
Solubility Trapping	1 – 20	100 to >1 000
Mineral Trapping	1 – 100	1 000 to >10 000

Storage Capacity

The storage capacity of a reservoir depends on several factors, the pore volume being the most important one. Pressure communication between other reservoirs, the compressibility of the rock and fluids and the solubility of the CO_2 are other elements that play a part in the total storage capacity. If the reservoir is not pressure communicating with other reservoirs, the capacity primarily depends on how high pressure it can withstand without fracturing. If the rock and fluid have a high compressibility, the reservoir can withstand higher pressure [109].

The amount of CO_2 to be stored in a saline aquifer is given by the formula:

$$M_{CO_2} = Vb \cdot \varphi \cdot \frac{n}{g} \cdot \rho_{CO_2} \cdot S_{eff} \tag{10.1}$$

Where M_{CO_2} is the amount of CO_2 in tonnes, Vb is the bulk volume, φ is the porosity of the rock, $\frac{n}{g}$ the net to gross ratio, ρ_{CO_2} the density of CO_2 and S_{eff} the fraction of stored CO_2 relative to the pore volume [109].

An evaluation of theoretical storage capacity in the North Sea was done by NPD in 2011, with a step-wise-approximation by the maturation pyramid shown in Figure 10-6. The

technical maturity of the storage volume increases with higher levels of the pyramid, as well as the suitability for storage.

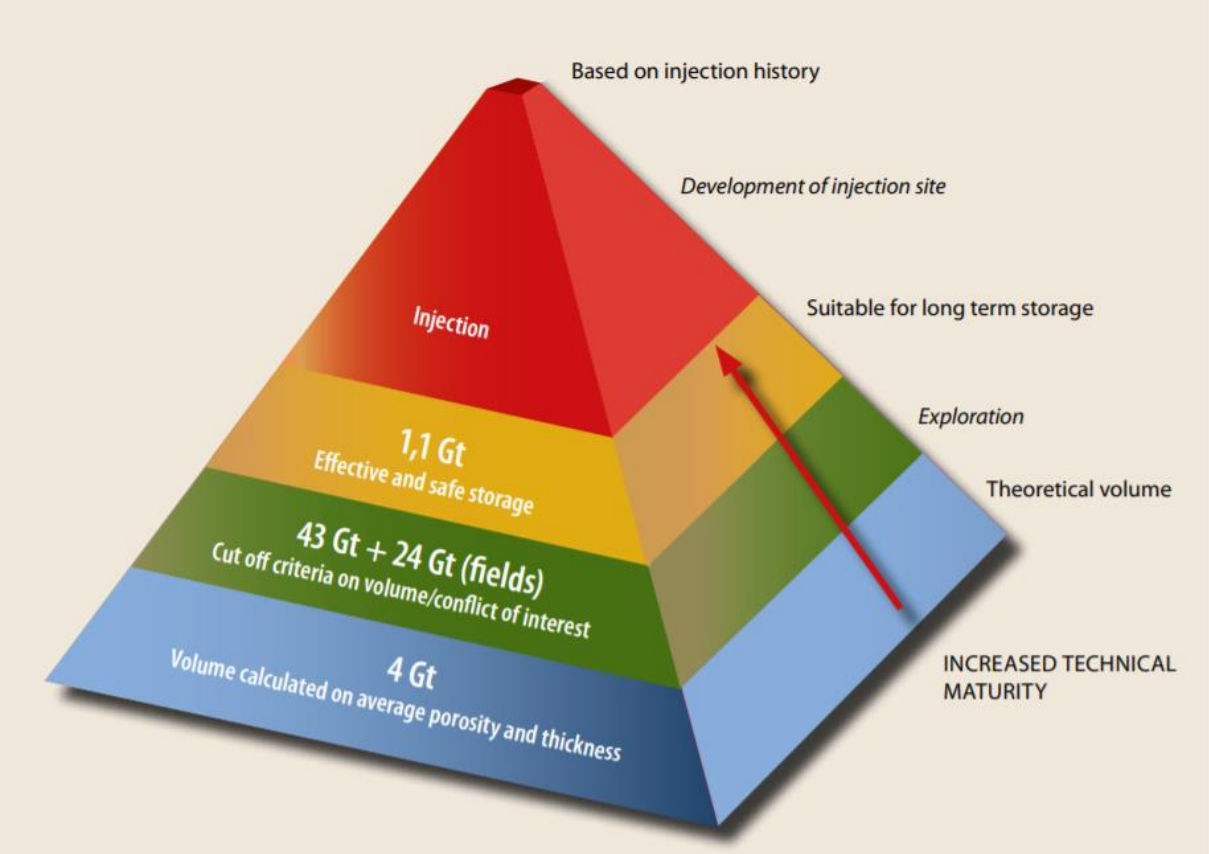

Figure 10-6: Methodology of evaluation of geological volumes suitable for injection and storage of CO_2 [109]

Areas with capacity for 1.1 Giga ton (Gt) of CO_2 have already been demonstrated to be effective and safe storage for CO_2 through injection projects (Sleipner Area) or detailed evaluation. The estimated storage capacity in aquifers and future abandoned hydrocarbon fields amounted to 43Gt and 24Gt, respectively, with a storage efficiency ranging between 0.8% and 5.5% for the different areas. Further evaluation and data are however required to define whether these areas are suitable, secure storage sites, thereby increasing the level of technical maturity with respect to the pyramid [109].

10.2 CHEOP-CC at GEA

This chapter will study the possibility of a carbon capture unit integrated in the CHEOP fuel cell system presented in Ch. 7.2. The unused fuel from the SOFC in the initial CHEOP-system contains a lot of carbon in the form of CH_4, CO and CO_2. This is originally combusted with air to prevent CH_4 and CO from entering the atmosphere. In the CHEOP-CC system, this final combustion is replaced with an oxyfuel combustion process, thereby eliminating nitrogen from the end products, meaning only CO_2 and water is present in the exhaust gas. Carbon separation can further be done by dehydration. The oxyfuel combustion is made possible by an oxygen membrane designed by fuel cell technology to separate out oxygen from the unused gas in the cathode [90]. The additional oxygen membrane will consume around 5% of total electricity generated by the system, this will however be compensated for by adding extra fuel cells to each stack. Capacity of the CHEOP-CC will still be 32 MW [91]. The energy penalty does not include final compression of the CO_2 before transportation, due to lack of information and immature TRL, this will not be studied any further.

10.2.1 Energy Calculation

As the oxygen membrane demands 5% of the electricity generated in the fuel cell, the efficiency will drop by 3%, and an increased gas consumption to reach the desired power output is expected. The burn value and CO_2-emission factor of the fuel is still 10.698 MWh and 2.21 ton per 1000Sm^3, respectively. With an efficiency of 57% in the fuel cell system, 1000Sm^3 fuel would return 6.09 MWh and 2.21 tons CO_2. Electricity demand on GEA for 2018 was ~21% of total energy requirement, namely ~280GWh. Based on these numbers a new gas consumption, energy production and CO_2-emission table were created. Table 7-2 can be seen below.

Table 10-4: Gas Consumption, Energy production and CO_2-emissison for GEA with the CHEOP-CC system

		Gas Consumption [Sm^3]	Power [MWh]	CO_2-emission [ton]	[%]
Base Case		357 453 347	1 336 876	789 972	
CHEOP-CC	*Electricity*	45 815 809	280 744	(101 253)	
	Mechanical	282 816 114	1 056 132	625 024	
Reduction		**28 821 424**		**164 948**	**20.9 %**

CO_2-emissions from electricity production are placed in brackets, as this will be captured and stored and is therefore not considered as emissions. From Table 7-2, a total reduction in CO_2-emissions with the CHEOP-CC system installed amounts to 164 948 tons per year, a reduction of 20.9% compared to the base case of simple cycle gas turbines. The emission reduction is however expected to be less than calculated above, as the captured CO_2 must be compressed before transportation for final storage, which will require additional energy hence additional CO_2 emission not included here.

10.2.2 TRL

The CHEOP-CC system is developed alongside the original CHEOP, and is currently rated with the same TRL, namely TRL 3, from Table 2-3. More information about the technology level is available in Ch. 7.2.2.

10.2.3 CO_2-Emission Reduction

The CO_2-Emission Reduction is calculated by Eq. (2.1) and (2.2), with the numbers from Table 7-2. Only the CO_2 produced by the gas turbines are included, as the CHEOP-CC will capture any CO_2 produced while generating electricity.

$$CO_{2_{CHEOP-CC}} = \frac{625\ 024\ \ ton}{1\ 336\ 876\ MWh} = 0.47\ ^{ton}/_{MWh}$$

$$\%\ CO_2\ emission\ reduction = -\frac{0.47}{0.59} \cdot 100\% + 100\% = 20.8\%$$

10.2.4 Efficiency

Electrical efficiency of the CHEOP-module is stated to be 57% and are accountable for ~21% of total power production. The gas turbines producing mechanical work represents the remaining ~79% and have an average efficiency of 34.7%. Total efficiency for power generation becomes:

$$Efficiency = \ 0.2088 \cdot 57\% + 0.7912 \cdot 34.7\% = 39.4\%$$

Efficiency improvement compared to simple cycle gas turbines is then calculated from Eq. (2.5)

$$Efficiency\ improvement = \frac{39.4\% - 34.7\%}{34.7\%} \cdot 100\% = 13.4\%$$

10.2.5 Cost

As for the CHEOP system in Ch.7.2, cost estimations will not be studied any further due to the low TRL rating of the technology.

10.2.6 Rating Table

Alternative	TRL	CO_2-Emission Reduction	Efficiency Improvement	Abatement Cost	Comments
Gas Turbines	9	0%	34.7%	765 NOK/ton	Base case
CHEOP	3	8.6%	15.2%	N/A	Too low TRL for cost estimation
CHEOP-CC	3	20.8%	13.4%	N/A	Too low TRL for cost estimation

10.3 H_2 w/CC at GEA

This subchapter is a continuation of Ch. 9.3. The same hydrogen production plant is studied for pre-combustion capture of the CO_2 produced in the SMR process. The basis for calculation of gas consumption, CO_2-production and economics are based on the same paper as for Ch. 9.3, namely Spanilla et al. *Techno-economic assessment of membrane assisted fluidized bed reactors for pure H_2 production with CO_2 capture* (2016) [106].

The reforming process with carbon capture is similar to the process described in Ch. 9.3 (except for a S/C ratio of 4) up to the WGS reactors. For carbon capture to be most efficient, the syngas is shifted in a two stage WGS to enhance both hydrogen and CO_2 production. After the LT-WGS reactor, the H_2-CO_2 rich mixture is cooled down to ambient temperature and condensed for H_2O. The CO_2 is further separated from the hydrogen by means of methyl-de-ethanol amine (MDEA) absorption. The pure CO_2 stream exiting from the chemical absorption process is further compressed to be ready for transport and final storage.

The hydrogen flow rate is the same as for the plant without CC. However, the H_2 yield is lower, with 2.48 mol per mol CH_4, and hydrogen production efficiency is reduced to 69% compared to 74% without CC. The decrease in H_2 yield and efficiency is due to a higher heat input in the reformer because of higher S/C ratio, and a higher electricity requirement due to CO_2 compression.

Required heat input and H_2/CO_2 output for the SMR plant are shown in Table 10-5.

Table 10-5: Gas Consumption, Hydrogen Production and CO_2 Production from SMR [106]

	Gas Consumption		Hydrogen Production		CO_2 Production
	[Nm^3]	[kg]	[Nm^3]	[kg]	[ton]
Per hour	10 116	12 582	2 700	30 033	4
Per year	88 616 160	110 219 104	23 652 000	263 092 325	36 833

Hydrogen production volume is the same as for the option without CC. Gas composition to be used in the gas turbines and required amount of NG is summarized in Table 10-6 below.

Table 10-6: Composition, volume and heating value of NG and NG/H2 mix

Fuel	Component	Content	Volume [m^3]	Heating Value [MJ]
Original	NG	100 %	357 453 347	14 298 133 880
	H_2	-	-	-
Fuel Blend	NG	52 %	286 418 419	11 456 736 772
	H_2	48 %	263 092 325	2 841 397 108

10.3.1 Energy Calculation

From the new gas composition in Table 10-6, a new gas consumption, energy production and CO_2-emission table can be made, with reduced CO_2 emission from the SMR process due to carbon capture, shown in Table 10-7.

Table 10-7: Gas consumption, energy production and CO_2-emission table for GEA with SMR w/CC and a fuel mix of NG/H_2

Activity	NG Consumption [Sm^3]	Power [MWh]	CO_2-emission [ton]
Base Case	357 453 347	1 336 876	789 972
SMR	110 219 104		36 833
Combustion	286 418 419	1 336 876	632 985
Reduction	- 39 184 177 (-11%)		120 154 (15.21%)

From Ch. 9.3, hydrogen production through SMR caused gas consumptions to increase by 8.8% compared to the base case of simple cycle gas turbines. Implementing CC to the SMR process increases gas consumption even further, to an 11% increase compared to the base case. The increase is due to additional heat and electricity requirements from the capture

unit, as mentioned above. However, the CO_2-emissions decrease with 15% compared to the base case, which when accumulated to end of production license in 2049 amounts to a total reduction of ~3.5 million ton.

10.3.2 TRL

Carbon capture through chemical absorption is a commercialized technology, however not yet implemented on offshore installations due to size and weight of equipment. The technology is still rated with TRL 9 from Table 2-3.

10.3.3 CO_2-Emission reduction

The CO_2-Emission Reduction is calculated by Eq. (2.1) and (2.2), with the numbers from Table 10-7.

$$CO_{2_{H_2w/CC}} = \frac{36\,833 + 632\,985\ ton}{1\,336\,876\ MWh} = 0.50\ ^{ton}/_{MWh}$$

$$\%\ CO_2\ emission\ reduction = -\frac{0.50}{0.59} \cdot 100\% + 100\% = 15.1\%$$

10.3.4 Efficiency

The H_2-production efficiency is given as 69%. The efficiency for combusting a fuel blend of hydrogen and natural gas on GEA's gas turbines are assumed to be the same as with combustion of 100% natural gas, namely 34.7%. This assumption is based on the fact that heat input and energy output from the turbines are the same.

The chain conversion efficiency for H_2 production and combustion is:

$$\eta_{ch.con} = \eta_{H_2} \cdot \eta_{GT} = 0.69 \cdot 0.347 \cdot 100\% = 24\%$$

Efficiency improvement can further be calculated from Eq. (2.5)

$$Efficiency\ improvement = \frac{24\% - 34.7\%}{34.7\%} \cdot 100\% = -30.8\%$$

10.3.5 Cost

The cost estimate for H_2 w/CC will be a so-called gate-to-gate study, where only the separation and compression of the CO_2 will be included. The cost for transportation and storage will be neglected, due to lack of evaluation data regarding safe storage facilities in the North Sea.

Cost estimations are based on the study of Spallina et al. [106]. The SMR process plant is assumed to have a lifetime of 30 years. Costs were given in Euro in 2016 figures and converted to NOK with the average exchange rate for 2016. The investment is calculated to last for current production licence which expires in 2049.

Bare Erected Cost (BEC)

The Bare Erected Cost (BEC) comprises the cost of all process equipment related to the SMR process facility and is given as ~551 million NOK. The largest cost is associated to the CO_2-absorption unit. Cost description of BEC is provided in Table 9-5 below.

Table 10-8: Bare Erected Costs for SMR Process plant w/CC [106]

Description	Cost [NOK]	% of BEC
Reactors	103 210 789	19 %
Convective cooling HEX	123 276 973	22 %
Turbomachines	34 372 630	6 %
H_2 compressors	12 820 062	2 %
Syngas coolers & heat rejection	61 127 542	11 %
PSA unit	54 810 410	10 %
MDEA unit	132 752 671	24 %
CO_2 compressors	28 984 488	5 %
Bare Erected Cost	**551 355 565**	**100 %**

Total Overnight Cost (TOC)

TOC includes all "overnight" capital expenses incurred during the capital expenditure period. TOC is calculated from BEC with the methodology from Table 9-6. Figures can be seen in Table 9-7.

Table 10-9: Total Overnight Cost

Description	[NOK]
BEC	551 355 565
+ TIC	441 084 452
= TDPC	992 440 017
+ IC	138 941 602
= EPC	1 131 381 619
+ C&OC	169 707 243
= TOC	1 301 088 862

Operating Cost

Operating and maintenance cost are divided into fixed and variable cost. Fixed costs include operating labour, maintenance, insurance cost, chemicals, and membrane replacement. Variable costs cover consumables such as cooling water and process water. Fixed and variable operating costs are given in Table 9-8.

Table 10-10: Operating and maintenance costs of SMR processing plant [106]

Description	Lifetime [years]	Cost [NOK/year]	Total [NOK]
O&M Fixed	29	90 576 525	2 626 719 225
O&M Variable	29	7 617 718	220 913 822
Total			2 847 633 047

Energy & Emission Cost

From Table 10-7, an increase in gas consumption will be ~39.2 million Sm^3 per year compared to the base case of simple cycle gas turbines. Due to carbon capture, a decrease in CO_2-emissions amounts to 120 154 tons per year. With the average price of gas for 2018 (minus 78% tax) and the cost of CO_2, total savings related to energy and emission costs are expected to be ~2.1 billion NOK for the current licence period until 2049.

Expected savings and income related to reduced gas consumption are shown in Table 9-9 below. The volume and cost of NG are shown with a negative sign to indicate an increase in consumption and therefore an expenditure, opposed to the reduced CO_2-emissions representing an extra income.

Table 10-11: Expected savings and income related to SMR w/CC and NG/H_2 fuel blend

Description	Quantity	Unit	Price [NOK/unit]	Operating years	Total income
NG	-39 184 177	[Sm3]	2.21	29	- 552 489 056
CO_2	120 154	[ton]	765	29	2 665 624 651
Total					**2 113 135 595**

Abatement Cost

The abatement cost is calculated with the formula:

$$\frac{Total\ investment\ cost\ of\ SMR\ w/CC - Expected\ savings\ from\ energy\ \&\ emission\ costs}{CO_2\ emission\ reduction\ for\ expected\ lifetime}$$

Total estimated cost of an SMR process plant with CC, including the abatement cost is summarized in Table 9-10 below.

Table 10-12: Cost estimate of SMR w/CC and NG/H_2 fuel blend

Description	Unit	Cost
TOC	NOK	1 301 088 862
+ O&M	NOK	2 847 633 047
- Expected savings from energy & emission costs	NOK	2 113 135 595
Total Investment Cost	NOK	2 035 586 314
CO_2-Emission Reduction	ton	3 484 477
Abatement Cost	**NOK/ton**	**584**

The final estimated abatement cost for hydrogen production with pre-combustion capture through SMR and chemical adsorption amounts to 584 NOK/ton CO_2 reduced. As this is below the cost of CO_2-emission of 765 NOK/ton, the investment would have been economically profitable. However, the estimated abatement cost only includes the capture and compression process of the CO_2, and not transportation and storage. The costs related to storing CO_2 are not evaluated here due to immature technical maturity of CO_2 storage in the North Sea. One can however assume that costs related to storage will increase the abatement cost significantly, thereby making the alternative less economically attractive.

10.3.6 Rating Table

Alternative	TRL	CO_2-Emission Reduction	Efficiency Improvement	Abatement Cost	Comments
Gas Turbines	9	0%	34.7%	765 NOK/ton	Base case
H_2	9	-7.6%	-25%	-2 669 NOK/ton	H_2 production from SMR, and NG/H_2 fuel blend for combustion
H_2 w/CC	9	15.1%	-30.8%	584 NOK/ton	Cost of transportation and storage excluded

11 Results and Discussion

11.1 Rating Table

A summary of TRL, CO_2-emission reduction, efficiency improvement and abatement cost for the 10 different options for power generation on offshore installations are shown below, in Table 11-1.

Table 11-1: Rating Table

Alternative	TRL	CO_2-Emission Reduction	Efficiency Improvement	Abatement Cost	Comments
Gas Turbines	9	0%	0%	765 NOK/ton	Base case
PFS	9	20.8%	34.5%	2 995 NOK/ton	Abatement cost from ConocoPhillips
FWT	9	20.8%	7.6%	1 156 NOK/ton	
Combined Cycle	9	7.8%	16.8%	-	Cost estimate for offshore combined cycle has not been found
HAT	5	6.8%	10.5%	-	Too low TRL for cost estimations
CHEOP	3	8.6%	15.2%	-	Too low TRL for cost estimations
CHEOP-CC	3	20.8%	13.4%	-	Too low TRL for cost estimations
EEM	9	5.5%	-	0.72 NOK/ton	
H_2	9	-7.6%	-25%	-2 669 NOK/ton	
H_2 w/CC	9	15.1%	-30.8%	584 NOK/ton	Cost of transportation and storage excluded

11.2 TRL

Most of the technologies discussed in this thesis is commercially available, however not all are currently suited for implementation on offshore installations due to space and weight limitations.

With TRL 9, PFS and combined cycle are already installed on several platforms, and the world's first FWTs dedicated for supplying power to offshore installations are scheduled to be operative by the end of 2020. Hydrogen production through SMR is however not installed on offshore installations yet. The size and weight of the equipment as well as efficiency decrease, increased gas consumption and CO_2-emissions makes the option a bad investment from all aspects. However, SMR enables efficient carbon capture, and when integrated, CO_2-emissions could be greatly reduced.

Of the low TRL alternatives, the HAT cycle proves valuable when commercialised, as it can reach efficiencies close to combined cycle with a lower net weight and volume. The CHEOP/CHEOP-CC systems based on fuel cells seems promising on all aspects reviewed in this thesis, given the development and commercialisation of the product is successful. The system can contribute to both higher efficiencies and reduced emissions as well as reduced noise pollutions and vibrations on the platform.

11.3 CO_2-Emission Reduction

Figure 11-1 shows the CO_2-Emission reduction in percentages compared to the simple cycle gas turbines and combined cycle operative on GEA today, in descending order.

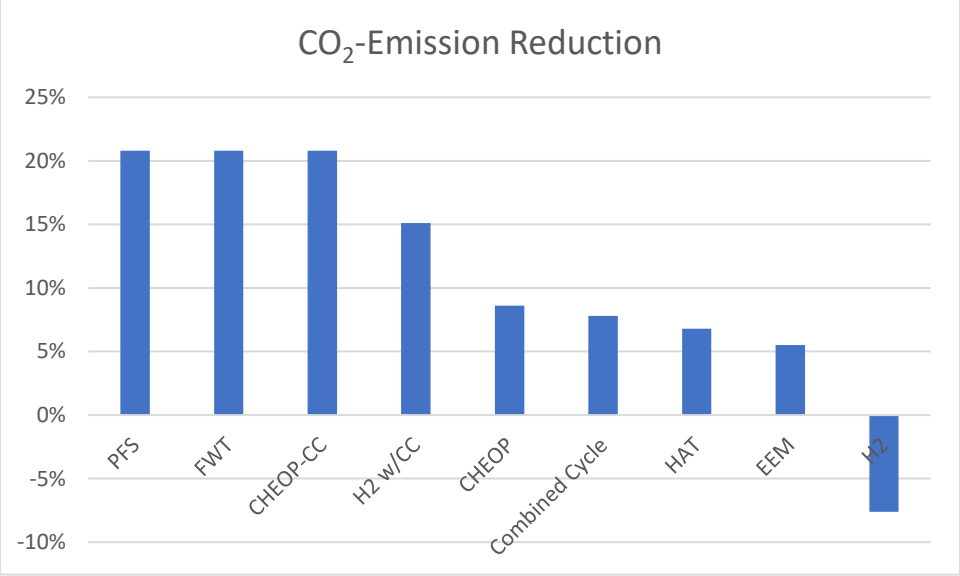

Figure 11-1: CO_2-emission reduction potential for the different alternatives in descending order

PFS, FWT and CHEOP-CC are the highest-ranked alternatives based purely on emission reduction with 20.8%, as all three solutions aims to remove the emissions from the gas turbines producing electricity completely. Of these three, PFS is the only alternative guaranteed to eliminate these emissions entirely. The solution with FWT would still require operation of gas turbines in periods when the correct wind conditions are not present, which will result in certain CO_2-emissions. CHEOP-CC would still leave small traces of CO_2-emission after the capture process.

CHEOP, Combined cycle and HAT all contribute to increasing the efficiency of the power generation, and thereby reduce CO_2-emissions with approximately 7% compared to 2018 level.

H_2-production through SMR without CC yields a negative emission reduction of -8% as more natural gas is consumed in the reforming process compared to the amount of natural gas being replaced by hydrogen in the gas turbines. However, combined with a CC unit, a net decrease in CO_2-emissions is found to be 15.1%, which is a significant decrease.

EEM offers the lowest decrease in CO_2-emissions of all alternatives studied, besides H_2 wo/CC. This is not surprising, as the alternative is based on the same gas turbines operating today, however with a different philosophy regarding energy efficiency. The decrease in CO_2-emissions are still very high considering the measures do not affect the productivity in any way, as they are only implemented when conditions allow for it. For example, using only one injection pump instead of two in certain periods.

11.4 Efficiency Improvement

Figure 11-4 shows the efficiency improvement offered by each alternative reviewed in this thesis, compared to today's solution.

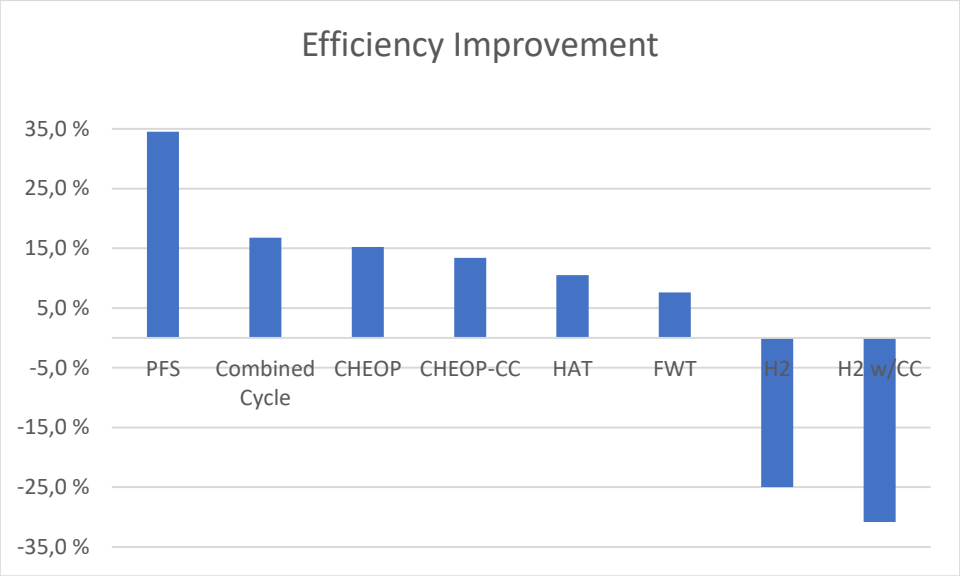

Figure 11-2: Efficiency improvement for the different alternatives, in descending order

On efficiency improvement, PFS offer the greatest results with an increase of nearly 35% compared to simple cycle gas turbines. This is mainly due to PFSs efficiency not being calculated from generation but rather power transmission, as the power will be supplied from shore.

The fuel-based options which generates energy on-deck range between 10-17% in increased efficiency. In practise these alternatives help to reduce CO_2-emissions by consuming less fuel for the same amount of power produced, and thereby emitting less CO_2.

From Table 11-1 FTW has the same emission reduction potential as PFS, but PFSs efficiency is significantly higher. The main reason for this is as stated above; PFS efficiency is calculated from the transmission of electricity, while FWTs efficiency is calculated from total production capacity compared to actual production which largely depend on wind conditions.

Finally, hydrogen production through SMR offers the lowest efficiency increase compared to simple cycle gas turbines. The chain conversion efficiency when treating the gas before utilization results in the substantial decrease. As neither of these processes are ideal, energy losses are expected in both the reforming- and combustion process, and when combined the losses are even bigger.

11.5 Abatement Cost

Of the four different rating factors, the abatement cost has been the most difficult to obtain and estimate. For four of the options a cost has not been estimated due to limited resources of the author. For the alternatives where cost is assessed, it is given with a high level of uncertainty and are only provided as a rough estimation and example for comparison. The costs estimations have been simplified and given without regards to discount rates and inflation. Taxes are also neglected except for a 78% tax on income from sales gas. Figure 11-3 shows the calculated abatement costs for the different alternatives, the green line indicates CO_2 break-even cost.

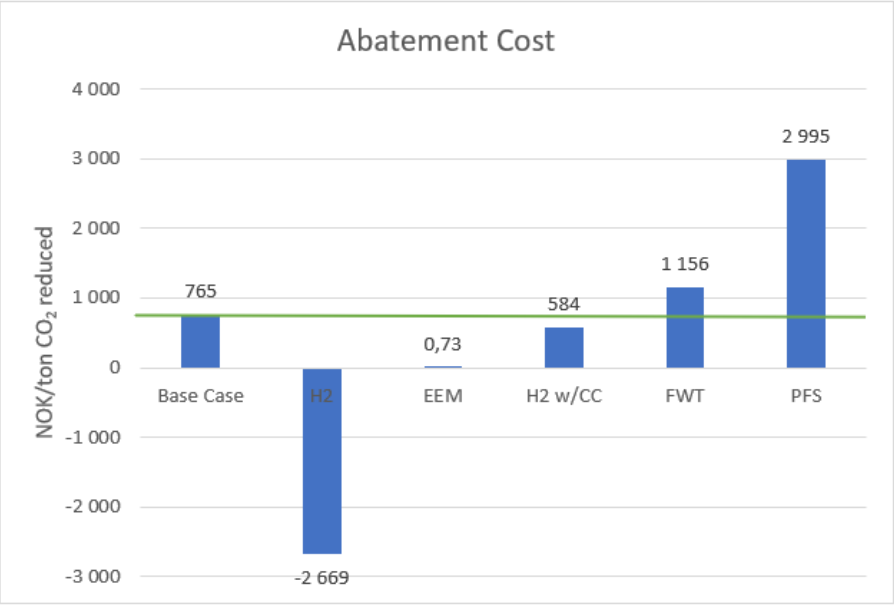

Figure 11-3: Abatement cost for the different alternatives

For the base case, the abatement cost is given as the cost of CO_2 today, namely 765 NOK/ton. Any abatement cost below the green line in the figure represent an economical profit.

For H_2 production by SMR the abatement cost is calculated to be – 2 669 NOK/ton. The cost is negative as more CO_2 is being emitted by choosing this solution compared to the base case. In practice it means the cost of the hydrogen plant is 2 669 NOK/ton CO_2 *increased*, which is a poor investment from both an economical and environmental point of view. By implementing carbon capture to the SMR plant, the CO_2-emissions reduce drastically, and the abatement cost amounts to 584 NOK/ton CO_2 reduced. The cost, however, only include capturing and compressing the CO_2. For the emissions to be avoided, the carbon needs to be transported and stored underground also. This will increase the cost significantly but has not been studied any further due to lack of evaluation and data regarding safe storage facilities in the North Sea.

The abatement cost for EEM is the lowest of all options, with 0.73NOK/ton CO_2 reduced. The cost was calculated with the high range numbers, meaning the cost of these measures most likely is lower than estimated here. The low cost is mainly due to change in energy philosophy rather than investing in new efficient equipment. The low cost proves how smart energy solutions has a positive effect on both expenditures and emission reductions.

Estimated abatement cost for FWT is calculated to be 1 156 NOK/ton and are based on general costs for floating wind turbines on a semi-sub foundation. The cost was originally given in Euro in 2015 figures and converted to NOK with the average exchange rate for the specific year. Inflation has not been accounted for, neither has taxes, except for a 78% tax on income from sales gas. Any modification-work necessary on the installations have also been overlooked. However, as FWT technology has matured during the last 5 years, a lower general cost of equipment and solutions can be expected. The final estimated cost of 1 156 NOK/ton can therefore be both higher or lower than estimated here.

PFS stands out as the most expensive option with an abatement cost of 2 995 NOK/ton CO_2 reduced. This estimate was originally given by ConocoPhillips in 2012, due to inflation and the amount of CO_2 emitted after their hypothetical installation period in 2017, the abatement cost for PFS will probably be higher today.

The abatement cost for the options of combined cycle, HAT and CHEOP/CHEOP-CC have not been estimated due to lack of data and low TRL rating. Therefore, it is difficult to say with certainty how much return one would get from the investment of these options. However, studies suggest the CHEOP system to be competitive to PFS financially.

11.6 Best Overall Alternative

Figure 11-4 shows the CO_2-Emission reduction in percentages in descending order, compared to the simple cycle gas turbines and combined cycle operative on GEA today. Applicable abatement cost for certain alternatives and CO_2 brake-even cost are also included for comparison.

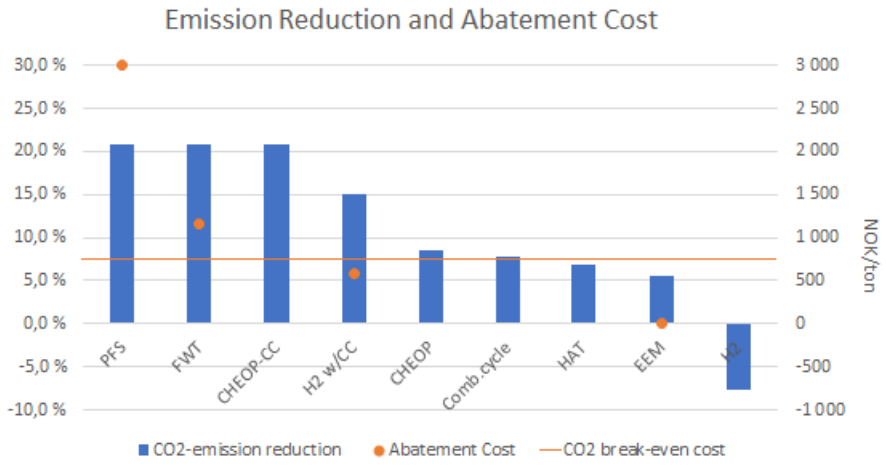

Figure 11-4: CO_2-emission reduction for the different alternatives in descending order, with relevant abatement costs

PFS offers the highest guaranteed emission reduction of 20.8%, however its abatement cost is the highest calculated among the alternatives and assumed to be too high for the investment to be attractive for an already operating field.

H_2 w/CC offers a 15% reduction in CO_2-emissions for an abatement cost lower than CO_2 break-even cost. However, total cost for the investment will increase as transportation and storage of the carbon has not been accounted for.

The lowest abatement cost is found for the energy efficiency measures alternative. A 5.5% decrease in the CO_2-emissons were accomplished with an abatement cost of 0.73 NOK/ton CO_2 reduced, which most likely is even lower than estimated. Despite the total CO_2-emission

decrease not being very high, this alternative offers a huge return on investment as the abatement cost is insignificant compared to current CO_2 cost of 765NOK/ton.

Of the nine alternatives studied in this thesis, Floating Wind Turbines stands out as the best alternative solution to the gas turbines producing power today. FWT offers a decent balance between cost and CO_2-emission reduction, with an abatement cost of only ~400NOK over todays CO_2 cost, and an emission reduction of over 20% compared to today's solution, assuming the correct wind conditions are present. This thesis has operated with a constant CO_2 cost of 765NOK/ton for the whole lifetime of the field, but in reality, this cost will increase with time as we strive to reach COPs goal to limit the average global temperature increase to below 2°C. A reasonable assumption would therefore be that the abatement cost for FWT would break even with the CO_2 cost in the future, thereby making the investment profitable.

To stabilize the energy profile over time, hydrogen production and storage through electrolysis could be applied to the FWT. This will eliminate the usage of the gas turbines producing electricity completely, as the excess power from periods with a lot of wind will be stored and used as a buffer for periods with less wind or increased energy demand. The costs associated with energy storage from FWT has however not been assessed in this thesis.

12 Conclusion

The EEM offers lowest cost per ton CO_2 reduced. The measures described and calculated in this thesis are already implemented on the fields and would not contribute to any further reduction. However, by continuing to explore other alternatives for EEM, further low-cost CO_2-emission reduction can be discovered.

The CHEOP/CHEOP-CC systems based on fuel cells seems promising on all aspects reviewed in this thesis. However, uncertainties revolving the technology is still high, as it is only rated with TRL 3. Although the abatement cost is suggested to be similar to PFS (and probably too high for an already existing field), the system could be valuable for new installations. Here the abatement cost would be greatly reduced, as no sunk costs and modification-work is included. The CHEOP system would leave a much smaller environmental footprint compared to PFS which requires kilometres of cables laid on the seabed. In addition, the expenditure of electricity applicable for PFS would be eliminated as CHEOP produces power from natural gas already available on the field.

Based on CO_2-emission reduction potential and estimated abatement cost, FWT stands out as the best alternative for power generation on GEA, if the fields were to reduce their CO_2-emissions towards a low carbon future. FWT would eliminate the use of gas turbines producing electricity most of the time, as wind conditions in the Ekofisk Area are strong enough to supply the fields with the necessary power on an average basis. Investing in FWT to supply the fields with electricity would cost 1 156 NOK/ton CO_2 reduced. The average annual decrease of CO_2-emissions would amount to 20.8% and the efficiency would increase by 7.8%. Given the fact that CO_2 costs experiences a gradually increase every year, a reasonable assumption would be for the abatement cost to break-even with CO_2 costs at some point, thereby making the investment economically profitable too, as well as environmentally beneficial.

References

[1] E. Britannica. "Greenhouse Gas." Encyclopædia Britannica, inc. https://www.britannica.com/science/greenhouse-gas (accessed 11.03.20).

[2] E. Britannica. "Global warming." https://www.britannica.com/science/global-warming (accessed 25.02.20).

[3] K. Olerud and S. Kallbekken, "Klimakonvensjonen," in *Store norske leksikon*, ed. SNL, 2019.

[4] UNFCCC. "What is the Kyoto Protocol?" https://unfccc.int/kyoto_protocol (accessed 25.02.20).

[5] I. U. Jakobsen and S. Kallbekken, "Parisavtalen," in *Store norske leksikon*, ed. SNL, 2020.

[6] Norsk Olje og Gass. "Klima og Miljø." https://www.norskoljeoggass.no/miljo/ (accessed 25.02.20).

[7] Finansdepartementet. "CO2-avgiften." https://www.regjeringen.no/no/tema/okonomi-og-budsjett/skatter-og-avgifter/veibruksavgift-pa-drivstoff/co2-avgiften/id2603484/ (accessed 25.02.20).

[8] Miljødirektoratet. "EUs system for klimakvoter." https://www.miljodirektoratet.no/ansvarsomrader/klima/klimakvoter/eus-klimakvotesystem/ (accessed 25.02.20).

[9] Miljødirektoratet. "Klimagassutslipp fra olje- og gassutvinning." https://miljostatus.miljodirektoratet.no/tema/klima/norske-utslipp-av-klimagasser/klimagassutslipp-fra-olje--og-gassutvinning/ (accessed 18.02.20).

[10] Oljedirektoratet, "Oversiktsskjema for NOx-avgiftspliktig utstyr," Oljedirektoratet, Unpublished work, 2019.

[11] ConocoPhillips. "Ekofisk." http://www.conocophillips.no/our-norway-operations/greater-ekofisk-area/ekofisk/ (accessed 16.03.20).

[12] Diskos. "Public Portal Production Data." https://portal.diskos.cgg.com/prod-report-module/ (accessed 25.02.20).

[13] Oljedirektoratet. "Embla." https://www.norskpetroleum.no/en/facts/field/embla/ (accessed 16.03.20).

[14] Oljedirektoratet. "Eldfisk." https://www.norskpetroleum.no/en/facts/field/eldfisk/ (accessed 16.03.20).

[15] ConocoPhillips, "Power From Shore to the Ekofisk Area," NOT. 14417800, 2012. [Online]. Available: https://energiogklima.no/wp-content/uploads/2012/08/Ekofisk-PFS-Report-Final-31-05-12.pdf

[16] Norwegian Petroleum Directorate, "Resource Report 2019," NPD, 2019. [Online]. Available: https://www.npd.no/globalassets/1-npd/publikasjoner/ressursrapport-2019/resource-report-2019.pdf

[17] ConocoPhillips, "UTSLIPPSRAPPORT 2017 for Ekofisk feltet," ConocoPhillips, 16686053-1, 13.06.2018; 2017. [Online]. Available: https://www.norskoljeoggass.no/globalassets/dokumenter/miljo/miljorapporter/feltspesifikke-utslippsrapporter-for-2017/ekofisk.pdf

[18] P. Styring, E. A. Quadrelli, and K. Armstrong, *Carbon dioxide utilisation: closing the carbon cycle*. Elsevier, 2014.

[19] EEX. "European Emission Allowance Auction (EUA) Primary Market." https://www.eex.com/en/market-data/environmental-markets/auction-market/european-emission-allowances-auction#!/2020/02/25 (accessed 25.02.20).

[20] *Endringer i CO2-avgiften*, 2019.

[21] C. Soares, *Gas turbines : a handbook of air, land and sea applications*, 2nd ed. Oxford, England ;,Waltham, Massachusetts: Butterworth-Heinemann, 2015.

[22] M. Assadi, *From Gas to Electricity - Course material for PET640*. University of Stavanger, 2018.

[23] B. Buecker, "Steam vs. Combined-Cycle vs. Cogeneration: Understanding the Basics," 18.08.2016. [Online]. Available: https://insights.globalspec.com/article/3119/steam-vs-combined-cycle-vs-cogeneration-understanding-the-basics

[24] D. G. AS, "TEKNOLOGIUTVIKLING OG KLIMAGASSUTSLIPP FRA PETROLEUMSVIRKSOMHETEN FRAM MOT 2030 OG ET LAVUTSLIPPSSAMFUNN I 2050," 1, Rev. 4, 2015. [Online]. Available: https://www.miljodirektoratet.no/globalassets/publikasjoner/m393/m393.pdf

[25] M. J. Mazzetti, "Offshore Energy Efficiency Technologies," 2013. [Online]. Available: https://www.sintef.no/globalassets/project/effort/effort-presentation-at-the-otc-conference-houston-may-6-2013.pdf

[26] Norsk olje og Gass, "Elkraft fra land til norsk sokkel," 2003. [Online]. Available: https://www.norskoljeoggass.no/contentassets/a515b22cdd514a00b02e01794484a9bc/elkraft-fra-land-til-norsk-sokkel-03.pdf

[27] (2016). *2, Klima - norsk sokkel i endring*. [Online] Available: http://konkraft.no/wp-content/uploads/2016/08/Konkraftrapport_komprimert_web.pdf

[28] S. W. Blume, *Electric power system basics : for the nonelectrical professional* (IEEE Press series on power engineering). Hoboken, N.J: Wiley-Interscience, 2007.

[29] J. Sandstad, "Vekselstrøm," in *Store norske leksikon*, ed. SNL, 2019.

[30] Oljedirektoratet, "Kraft fra land til norsk sokkel," TA - 2360, 2008. [Online]. Available: http://publikasjoner.nve.no/diverse/2008/kraftfralandtilnorsksokkel2008.pdf

[31] Nexans. "Submarine Cables." https://www.nexans.no/eservice/navigation/NavigationLocalGroup.nx?navigationId=342614#description (accessed 31.03.20.

[32] tyco Electronics. " What is a transformer and how does it work? ." http://www.cromptonusa.com/Potential%20Transformers.pdf (accessed 27.0320, 2020).

[33] T. E. Engineers. "Step up and step down transformers." https://www.top-ee.com/step-up-and-step-down-transformer/ (accessed 27.03.20, 2020).

[34] H. Abu-Rub, M. Malinowski, and K. Al-Haddad, *Power Electronics for Renewable Energy Systems, Transportation and Industrial Applications*. New York, UNITED KINGDOM: John Wiley & Sons, Incorporated, 2014.

[35] TranspowerNZ, "HVDC Concepts: section 3 - 6-pulse rectifier," ed, 09.10.13.

[36] N. Hörle, K. Erikkson, A. Maeland, and T. Nestli, "Electrical supply for offshore installations made possible by use of VSC technology," in *Cigré 2002 Confrene*, Paris, August 2002 2002. [Online]. Available: https://pdfs.semanticscholar.org/f1bd/0a2f590872681f7be32d84c78cb3af23f8e3.pdf?_ga=2.61863727.225240393.1585214038-1649210851.1585214038. [Online]. Available: https://pdfs.semanticscholar.org/f1bd/0a2f590872681f7be32d84c78cb3af23f8e3.pdf?_ga=2.61863727.225240393.1585214038-1649210851.1585214038

[37] J. Bauer, "Single-phase pulse width modulated rectifier," *Acta Polytechnica,* vol. 48, no. 3, 2008.

[38] HackTheWorld, "What is PWM?," ed, 01.09.17.

[39] ABB, "HVDC light - it's time to connect," ABB, Technical paper POW0038 REV. 09, 2017.

[40] (2015). *Først med kraft fra land*. [Online] Available: https://www.norskolje.museum.no/wp-content/uploads/2016/05/11-F%C3%B8rst-med-kraft-fra-land-fra-NOM-%C3%A5rbok-2015.pdf

[41] E. Pöyry, "Elektrifisering av Johan Castberg - tiltakskost og klimaanalyse," R-2016-002, 2016. [Online]. Available: https://www.equinor.com/content/dam/statoil/documents/impact-assessment/johan-castberg/statoil-elektrifisering-av-johan-castberg-tiltakskost-og-klimaanalyse.pdf

[42] ABB, "ABB tildelt kontrakt på kraft fra land til Johan Sverdrup," ed. online, 2015.

[43] M. Östling, "HVDC light," ABB - Head of Bid & Proposals, Grid Integration - HVDC, E-mail correspondence, 06.03.2020, 2020.

[44] G. Hadland and F. H. Sandberg. "Ny Valhall prosess- og boligplattform." https://www.kulturminne-valhall.no/Feltet/Nye-loesninger/Ny-Valhall-prosess-og-boligplattform#2 (accessed 05.04.20).

[45] Novatech, "Kostnadsestimater for ombygging av kraftløsning for eksisterende innretninger offshore," 2007. [Online]. Available: https://docplayer.me/9417943-Kostnadsestimater-for-ombygging-av-kraftlosning-for-eksisterende-innretninger-offshore.html

[46] Statista. "Average annual OPEC crude oil price from 1960 to 2020." https://www.statista.com/statistics/262858/change-in-opec-crude-oil-prices-since-1960/ (accessed 05.04.20).

[47] Ycharts. "European Union Natural Gas Import Price." https://ycharts.com/indicators/europe_natural_gas_price (accessed 01.04.20.

[48] Norsk Petroleum. "Petroleumsskatt." https://www.norskpetroleum.no/okonomi/petroleumsskatt/ (accessed 05.04.20).

[49] SSB. "Elektrisitetspriser." https://www.ssb.no/elkraftpris (accessed 02.04.20).

[50] E. Mælum, "Prisoppgang på Naturgass," 10.09.20. [Online]. Available: https://www.ssb.no/priser-og-prisindekser/artikler-og-publikasjoner/prisoppgang-pa-naturgass

[51] NVE. "Vindkraft." https://www.nve.no/energiforsyning/kraftproduksjon/vindkraft/?ref=mainmenu (accessed 04.04.20).

[52] WindEurope, "Offshore Wind in Europe - Key trends and statistics 2019," 01.02.20 2020. [Online]. Available: https://windeurope.org/wp-content/uploads/files/about-wind/statistics/WindEurope-Annual-Offshore-Statistics-2019.pdf

[53] Equinor. "Hywind Tampen." https://www.equinor.com/en/what-we-do/hywind-tampen.html (accessed 09.04.20).

[54] D. Roddier and J. Weinstein, "Floating Wind Turbines," *Mechanical Engineering,* vol. 132, no. 04, pp. 28-32, 2010, doi: 10.1115/1.2010-Apr-2.

[55] M. Guzzetti, "Floating Offshore Wind," 07.09.17. [Online]. Available: https://green-giraffe.eu/blog/floating-offshore-wind-coming-age

[56] D. Wood, "Introduction to Wind Turbine Technology," *Green Energy and Technology,* vol. 38, pp. 1-29, 2011, doi: 10.1007/978-1-84996-175-2_1.

[57] C. A. Badurek. "Wind Turbine." Encyclopædia Britannica, inc. https://www.britannica.com/technology/wind-turbine (accessed 09.04.20).

[58] DNV GL, "WIN WIN - Joint Industry Project: Wind-powered water injection ", 04.2016 2016. [Online]. Available: https://gateway2.presstogo.com/download/DownloadGateway.dll/GetHash?p_hash=BE1B38BB718539CC0261A5D09826B415BFE015002672C9C0D453E14B1A808FD08047553163B8736E718B8399429C6500A60C3C04192973AAA14C6E5DE9D4AFAEA99723870FCEF739B32A264DE149F6CC053F42C8725B30BD

[59] A. Durakovic. "WIN WIN Concept Prototype-Ready." https://www.offshorewind.biz/2019/05/09/win-win-concept-prototype-ready/S (accessed 10.04.20).

[60] StormGeo AS, "Kraftproduksjon og Vindforhold," 59-12, 2012. [Online]. Available: https://evalueringsportalen.no/evaluering/kraftproduksjon-og-vindforhold-fagrapport-til-strategisk-konsekvensutredning-av-fornybar-energiproduksjon-til-havs/Kraftproduksjon%20og%20vindforhold.pdf/@@inline

[61] NS Energy. "Kincardine Floating Offshore Wind Farm, Scotland." https://www.nsenergybusiness.com/projects/kincardine-floating-offshore-wind-farm-scotland/ (accessed 14.04.20).

[62] M. V. O. WIND. "The V164-10.0 MW™ Turbine." MHI Vestas Offshore Wind. https://www.mhivestasoffshore.com/innovations/ (accessed 14.04.20).

[63] Carbon Trust, "Floating Offshore Wind: Market and Technology Review " The Scottish Government, UK, 01.06.15 2015. [Online]. Available: https://prod-drupal-files.storage.googleapis.com/documents/resource/public/Floating%20Offshore%20Wind%20Market%20Technology%20Review%20-%20REPORT.pdf

[64] Tekniske Nyheter, "Hywind Tampen skal produsere 384 GWh." [Online]. Available: https://www.tekniskenyheter.no/forside/aktuelt/hywind-tampen-skal-produsere-384-gwh

[65] M. J. Coren. "Floating wind farms just became a serious business." Quartz. https://qz.com/1650433/hywind-scotland-makes-floating-wind-farms-a-serious-business/ (accessed 14.04.20).

[66] EolMed. "The Pilot Farm." EolMed. http://www.eolmed.fr/en/the-pilot-farm/ (accessed 14.04.20).

[67] Eoliennes Flottantes de Groix. "THE GROIX & BELLE-ILE PROJECT." http://eoliennes-groix-belle-ile.com/en/project/ (accessed 14.04.20).

[68] Ø. Flatebø, "Off-design Simulations of Offshore Combined Cycles," Master Master, Department of Energy and Process Engineering, NTNU, Trondheim, 2012.

[69] A. F. El-Sayed, *Aircraft propulsion and gas turbine engines*, Second edition. ed. Boca Raton ;,London ;,New York: CRC Press, Taylor & Francis Group, 2017.

[70] L. Nord and O. Bolland, "Steam bottoming cycles offshore -- Challenges and possibilities," *Journal of Power Technologies,* vol. 92, pp. 201-207, 01/01 2012. [Online]. Available: https://www.researchgate.net/profile/Lars_Nord2/publication/259840669_Steam_bottoming_cycles_offshore_--_Challenges_and_possibilities/links/5707a1df08ae8883a1f7e47c/Steam-bottoming-cycles-offshore--Challenges-and-possibilities.pdf.

[71] G. Power. "HA technology now available at industry-first 64 percent efficiency." GE Power. https://www.genewsroom.com/press-releases/ha-technology-now-available-industry-first-64-percent-efficiency (accessed 30.04.20).

[72] P. Kloster, "Energy Optimization on Offshore Installations with Emphasis on Offshore Combined Cycle Plants," presented at the SPE Offshore Europe Oil and Gas Conference and Exhibition, Aberdeen, United Kingdom, 1999/1/1/, 1999. [Online]. Available: https://doi.org/10.2118/56964-MS.

[73] Norsk Olje og Gass. "Upgrade of combined cycle system." https://energiledelse.norskoljeoggass.no/en/Tiltaksliste/Articles/Tiltak58 (accessed 21.04.20.

[74] U.S. Energy Information Administration. "Average Construction Cost." Eia. https://www.eia.gov/electricity/generatorcosts/ (accessed 11.06.20), 2020).

[75] P. M. Rosén, "Evaporative Cycles - in Theory and in Practise," Doctorate, Department of Heat and Power Engineering, Lund University, Lund, Sweden, 2000.

[76] Thermoptim. "Humid Air Gas Turbine." https://direns.mines-paristech.fr/Sites/Thopt/en/co/cycle-hat.html (accessed 23.04.20.

[77] B. Nyberg and M. Thern, "Thermodynamic studies of a HAT cycle and its components," *Applied Energy,* vol. 89, no. 1, pp. 315-321, 2012/01/01/ 2012, doi: https://doi.org/10.1016/j.apenergy.2011.07.036.

[78] M. E. Diego, M. Akram, J. M. Bellas, K. N. Finney, and M. Pourkashanian, "Making gas-CCS a commercial reality: The challenges of scaling up," *Greenhouse Gases: Science and Technology,* Article vol. 7, no. 5, pp. 778-801, 2017, doi: 10.1002/ghg.1695.

[79] M. Mosayebnezhad, A. Saberi Mehr, A. Lanzini, D. Misul, and M. Santarelli, "Technology review and thermodynamic performance study of a biogas-fed micro humid air turbine," *Renewable Energy,* vol. 140, 03/15 2019, doi: 10.1016/j.renene.2019.03.064.

[80] T. Lindquist, "Evaluation, Experience and Potential of Gas Turbine Based Cycles with Humidification," Doctorate, Department of Heat and Power Engineering, Lund University, Lund, Sweden, 2002.

[81] M. Yagi, H. Araki, H. Tagawa, T. Koganezawa, C. Myoren, and T. Takeda, "Progress of the 40 MW-class advanced humid air turbine tests," *Journal of Engineering for Gas Turbines and Power,* Article vol. 135, no. 11, 2013, Art no. 112002, doi: 10.1115/1.4025037.

[82] T. Takeda, H. Araki, Y. Iwai, T. Morisaki, and K. Sato, "Test Results of 40MW-Class Advanced Humid Air Turbine and Exhaust Gas Water Recovery System," in *ASME Turbo Expo 2014: Turbine Technical Conference and Exposition*, 2014, vol. Volume 3A: Coal, Biomass and Alternative Fuels; Cycle Innovations; Electric Power; Industrial and Cogeneration, V03AT07A037, doi: 10.1115/gt2014-27281. [Online]. Available: https://doi.org/10.1115/GT2014-27281

[83] Y. Hu, H. Li, and J. Yan, "Techno-economic evaluation of the evaporative gas turbine cycle with different CO2 capture options," *Applied Energy,* vol. 89, no. 1, pp. 303-314, 2012/01/01/ 2012, doi: https://doi.org/10.1016/j.apenergy.2011.07.034.

[84] K.-A. Adamson, *Stationary fuel cells : an overview*, Oxford: Elsevier Science, 2007.

[85] M. C. Péra, D. Hissel, H. Gualous, and C. Turpin, "Fuel Cells." Hoboken, NJ USA: Hoboken, NJ USA: John Wiley & Sons, Inc., 2013, pp. 151-207.

[86] Prototech AS. "Clean Highly Efficient Offshore Power (CHEOP)." Prototech. https://www.prototech.no/projects/10454/clean-highly-efficient-offshore-power-cheop/ (accessed 19.05.20).

[87] S. Dharmalingam, V. Kugarajah, and M. Sugumar, "Chapter 1.7 - Membranes for Microbial Fuel Cells," in *Microbial Electrochemical Technology*, S. V. Mohan, S. Varjani, and A. Pandey Eds.: Elsevier, 2019, pp. 143-194.

[88] The Research Council of Norway, "Raising energy efficiency and reducing greenhouse gas emissions," 2018. [Online]. Available: https://www.forskningsradet.no/contentassets/a01a2a8dee99419ba422d4063d5fbf57/nfr_energy-efficiency_20181214.pdf

[89] Stormfjord Oil & Gas, "Prototech CHEOP V2," ed, 12.10.2015.

[90] GASSNOVA. "Clean Highly Efficient Offshore Power with CO2 Capture (CHEOP-CC)." https://climit.no/project/616060-clean-highly-efficient-offshore-power-with-co2-capture-cheop-cc/ (accessed 20.05.20).

[91] T. M. Svendsen, "CHEOP-CC," E-mail correspondence, 24.05, 2020.

[92] Norsk olje og Gass. "Modification of oil export pump." https://energiledelse.norskoljeoggass.no/en/Tiltaksliste/Articles/Tiltak62 (accessed 29.05.20).

[93] Norsk Olje og Gass. "Operations optimisation of gas compressor to pipeline." https://energiledelse.norskoljeoggass.no/en/Tiltaksliste/Articles/Tiltak63 (accessed 29.05.20).

[94] ConocoPhillips, "Utslippsrapport 2014 for Ekofisk feltet," 15918907-1, 03.03.15 2015. [Online]. Available: https://www.norskoljeoggass.no/contentassets/d8ab4fbb4565487cac88ba5b9f813e34/ekofisk-2014.pdf

[95] Norsk Olje og Gass. "Operations optimisation of Waste Heat Recovery Unit (WHRU)." https://energiledelse.norskoljeoggass.no/en/Tiltaksliste/Articles/Tiltak60 (accessed 29.05.20).

[96] S. Sunita. "Hydrogen: A Clean, Flexible Energy Carrier." Office of Energy Efficiency & Renewable Energy. https://www.energy.gov/eere/articles/hydrogen-clean-flexible-energy-carrier (accessed 07.05.20).

[97] J. Z. Zhang, *Hydrogen generation, storage, and utilization*, Hoboken, New Jersey: Wiley : ScienceWise Publishing, 2014.

[98] The Linde Group. *Hydrogen Recovery by Pressure Swing Adsorption*. (2020). Linde Group. [Online]. Available: https://www.linde-engineering.com/en/images/HA_H_1_1_e_09_150dpi_NB_tcm19-6130.pdf

[99] M. Sankir, *Hydrogen Production Technologies* (Advances in Hydrogen Production and Storage (AHPS) Ser). Somerset: John Wiley & Sons, Incorporated, 2017.

[100] A. Godula-Jopek, *Hydrogen Production: By Electrolysis*, 1st ed.. ed. Berlin: John Wiley & Sons, Incorporated, 2015.

[101] D. J. Goldmeer, "Power to Gas: Hydrogen for Power Generation," GEA33861, 2019. [Online]. Available: https://www.ge.com/content/dam/gepower/global/en_US/documents/fuel-flexibility/GEA33861%20Power%20to%20Gas%20-%20Hydrogen%20for%20Power%20Generation.pdf

[102] GE Power. "Hydrogen Fueled Gas Turbines " GE Power. https://www.ge.com/power/gas/fuel-capability/hydrogen-fueled-gas-turbines (accessed 13.05.20).

[103] N. Lindstrand. "This Swedish scientist works towards fulfilling Siemens' 2030 hydrogen pledge." Siemens. https://new.siemens.com/global/en/company/stories/energy/hydrogen-capable-gas-turbine.html (accessed 13.05.20).

[104] D. J. Goldmeer, A. Sanz, M. Adhikari, and A. Hundal, "GAS TO POWER: THE ART OF THE POSSIBLE

The Fuel Flexibility of GE Power's Aeroderivative Gas Turbines," GE Power, GEA34108, 2018. [Online]. Available: https://www.ge.com/content/dam/gepower-pw/global/en_US/documents/GasPower/gasturbines/GEA34108_Aero_Fuel_Flexibility_Whitepaper_Final.pdf

[105] R. Tarkowski, "Underground hydrogen storage: Characteristics and prospects," *Renewable and Sustainable Energy Reviews,* vol. 105, pp. 86-94, 2019/05/01/ 2019, doi: https://doi.org/10.1016/j.rser.2019.01.051.

[106] V. Spallina, D. Pandolfo, A. Battistella, M. C. Romano, M. Van Sint Annaland, and F. Gallucci, "Techno-economic assessment of membrane assisted fluidized bed reactors for pure H2 production with CO2 capture," *Energy Conversion and Management,* vol. 120, pp. 257-273, 2016/07/15/ 2016, doi: https://doi.org/10.1016/j.enconman.2016.04.073.

[107] Oljedirektoratet. "Conversion." https://www.norskpetroleum.no/en/calculator/about-energy-calculator/ (accessed 16.05.20).

[108] Equinor. "Sleipner Field." Equinor. https://www.equinor.com/no/what-we-do/norwegian-continental-shelf-platforms/sleipner.html (accessed 30.04.20).

[109] E. Halland, W. T. Johansen, and F. Riis, "CO2 storage atlas: Norwegian north sea," *Norwegian Petroleum Directorate, PO Box,* vol. 600, 2011.

[110] Carbon Capture & Storage Association. "Capture." CCSa. http://www.ccsassociation.org/what-is-ccs/capture/ (accessed 04.05.20).

[111] S. A. Rackley, *Carbon Capture and Storage*. Oxford, UNITED STATES: Elsevier Science & Technology, 2017.

[112] B. Rai, "CO2 dehydration after CO2 capture," Master, Department of Process, Energy and Environmental Technology, University College of Southeast Norway, Porsgrunn, 2016. [Online]. Available: https://openarchive.usn.no/usn-xmlui/bitstream/handle/11250/2479825/MasterRai2016.pdf?sequence=1&isAllowed=y

[113] A. Witkowski, M. Majkut, and S. Rulik, "Analysis of pipeline transportation systems for carbon dioxide sequestration," *Archives of Thermodynamics,* vol. 35, pp. s. 117-140, 03/01 2014, doi: 10.2478/aoter-2014-0008.

[114] J. Geske, N. Berghout, and M. van den Broek, "Cost-effective balance between CO2 vessel and pipeline transport. Part I – Impact of optimally sized vessels and fleets," *International Journal of Greenhouse Gas Control,* vol. 36, pp. 175-188, 2015/05/01/ 2015, doi: https://doi.org/10.1016/j.ijggc.2015.01.026.

Appendix

Table 0-1: Cost Estimate of PFS solution ref. 2019

Description	Unit	Production Stop [days]		
		11	90	180
Equipment & Installation	NOK	2 392 217 460	2 392 217 460	2 392 217 460
+ Project Management	NOK	239 221 746	239 221 746	239 221 746
+ Operating Cost PFS	NOK	232 800 000	232 800 000	232 800 000
+ Production stop	NOK	3 833 614 472	31 365 936 586	62 731 873 172
+ Energy Cost PFS	NOK	2 857 586 746	2 857 586 746	2 857 586 746
Total Cost PFS	NOK	9 555 440 424	37 087 762 538	68 453 699 124
- Operating Cost GT	NOK	- 585 800 000	- 585 800 000	- 585 800 000
- Gas Surplus	NOK	- 711 957 294	- 711 957 294	- 711 957 294
- CO_2 emission cost	NOK	- 3 659 371 380	- 3 659 371 380	- 3 659 371 380
Total Investment Cost	NOK	4 598 311 750	32 130 633 864	63 496 570 450
CO_2-emission reduction	ton	4 783 492	4 783 492	4 783 492
Abatement cost		961	6 717	13 274

Table 0-2: Cost Estimate of PFS solution ref. 2020

Description	Unit	Production Stop [days]		
		11	90	180
Equipment & Installation	NOK	2 392 217 460	2 392 217 460	2 392 217 460
+ Project Management	NOK	239 221 746	239 221 746	239 221 746
+ Operating Cost PFS	NOK	232 800 000	232 800 000	232 800 000
+ Production stop	NOK	3 833 614 472	31 365 936 586	62 731 873 172
+ Energy Cost PFS	NOK	2 822 088 774	2 822 088 774	2 822 088 774
Total Cost PFS	NOK	9 519 942 452	37 052 264 566	68 418 201 152
- Operating Cost GT	NOK	- 585 800 000	- 585 800 000	- 585 800 000
- Gas Surplus	NOK	- 15 698 316	- 15 698 316	- 15 698 316
- CO_2 emission cost	NOK	- 3 659 371 380	- 3 659 371 380	- 3 659 371 380
Total Investment Cost	NOK	5 259 072 755	32 791 394 870	64 157 331 456
CO_2-emission reduction	ton	4 783 492	4 783 492	4 783 492
Abatement cost		1 099	6 855	13 412